Diss. ETH No. 16035

Microheterogeneity of Soil Organic Matter investigated by C-1s NEXAFS Spectroscopy and X-ray Microscopy

Marc Schumacher

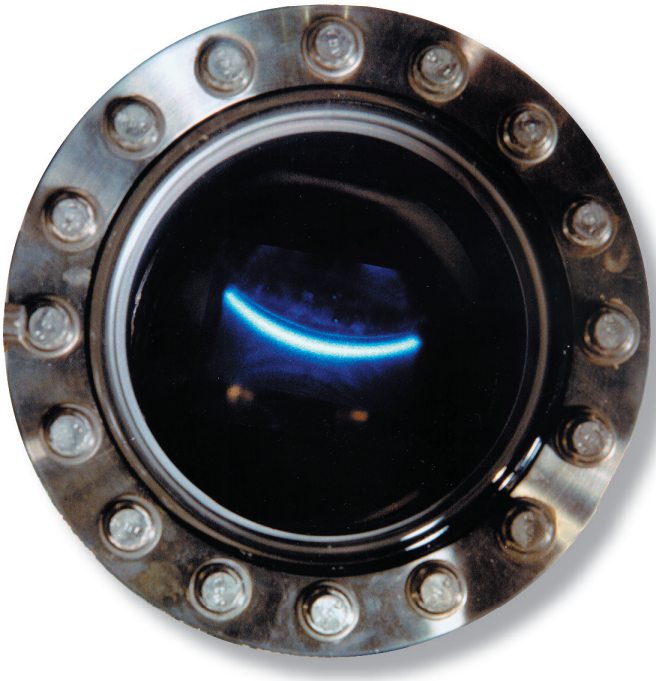

Zurich 2005

Diss. ETH No. 16035

Microheterogeneity of Soil Organic Matter investigated by C-1s NEXAFS Spectroscopy and X-ray Microscopy

A dissertation submitted to the
Swiss Federal Institute of Technology Zurich

for the degree of
Doctor of Natural Sciences

presented by
Marc Schumacher
Dipl. phil. nat., University of Berne
born March 30, 1976
from Sennwald, SG

accepted on the recommendation of

Prof. Dr. Ruben Kretzschmar, examiner
Prof. Dr. Chris Jacobsen, co-examiner
Dr. Andreas Scheinost, co-examiner
Dr. Iso Christl, co-examiner

Zurich 2005

Table of contents

Summary

The presence of natural organic matter (NOM) in soils and freshwaters has a profound influence on many chemical reactions that occur in these terrestrial and aquatic ecosystems. Adsorbed NOM on mobile mineral particles can either enhance or decrease the transport behavior of nutrients or contaminants within soils and affects their chemical properties to a large extent. Organic matter adsorption to mineral phases depends first and foremost on the chemical characteristics of the particular carbon functional groups present in the organic structure. Depending on its origin, the chemical properties and the microbial activity of its environment, the chemistry of NOM may change significantly and at various scales.

Organic matter in soils and freshwaters exists as dissolved molecules, colloids and particles. It is appropriate to regard these distinctions as dynamic, however, because organic matter can be interconverted readily between these forms. Carbon in natural systems is classified as either inorganic or organic carbon, and organic carbon is further classified on the basis of particle size and solubility. Depending on the particular combination of filtration, acidification, purging and oxidation steps leading to an analytical measurement, a wide variety of fractions of organic carbon can be distinguished. The total amount of organic carbon within soil and surface waters is commonly referred to as natural organic matter (NOM), whereas the term DOM (dissolved organic matter) is used for the fraction of organic matter, which passes through a 0.45 µm filter. The group of humic substances refers to the fraction of natural organic matter, which is defined upon their solubility in acid and base. This fraction can be further divided into humic acids, fulvic acids and humins. This work focused on the investigation of the chemical heterogeneity occuring in natural organic matter and humic substances using synchrotron-based carbon-1s near-edge X-ray absorption fine structure (NEXAFS) spectroscopy and scanning transmission X-ray microscopy (STXM). The major goals of this dissertation were to improve the qualitative and quantitative interpretation of C-1s NEXAFS spectra of natural organic matter samples of soil and aquatic origin.

Well characterized reference humic substances were analyzed in order to gain a deeper knowledge about the collection and interpretation of C-1s spectra of natural organic matter samples. A comparison of different spectral deconvolution schemes on spectra of reference humic substances was applied in the first part of this project in order to quantify the spectral features present in C-1s NEXAFS spectra of humic substances. The data was compared and correlated with results derived from published quantification schemes. The resulting data was further correlated with quantitative data derived from solid-state cross-polarization magic angle spinning (CP-MAS) ^{13}C-nuclear magnetic resonance (NMR) spectroscopy. Statistical analysis showed that the spectral quantification applied in this study provides positive correlations for five carbon groups. A further application of calculated linear regression equations between C-1s NEXAFS and ^{13}C-NMR data resulted in absolute quantifications which are in good agreement with data reported in the literature. These equations were used within the analytical chapters of this work in order to correct and calibrate the raw peak areas of C-1s NEXAFS spectra.

The variability of DOM of aquatic origin with regard to seasonal variations was investigated by analyzing samples from five different locations in Scandinavia, taken in fall (September to October) and spring (April to May), respectively. The samples were analyzed by Fourier-Transform infrared (FT-IR), CP-MAS ^{13}C-NMR and C-1s NEXAFS spectroscopy. Seasonal variations between the samples taken in spring and fall in terms of functional group distribution could not be detected. The samples turned out to be very similar in terms of elemental composition and exhibited a remarkably high spectral uniformity. Determinations of radiocarbon age showed that median ages for both spring and fall samples were less than 50 years. These findings suggest that the samples are generated from recent litter and biomass decomposition within relatively short timescales and are therefore not influenced by seasonal variations.

The mobile, colloidal fraction of NOM derived from fresh soil material was investigated by analyzing the organic carbon content of water-dispersible soil colloids extracted from three soils along a toposequence in northern Switzerland. Analysis was carried out at three different scales: First, variations within regions of distinct particles were investigated. Second, an analysis of differences between particles from the same soil horizons was carried out. In a third scale, variations between particles extracted from different soil types were analyzed and compared statistically. Spectral analysis was carried out by means of principal component and cluster analysis. The results demonstrated that NOM as-

sociated with soil colloids is chemically heterogeneous at the micrometer scale, especially in contents of aromatic and carboxyl carbon. However, differences in NEXAFS spectra between regions of single particles were much smaller than differences between averaged spectra of different particles isolated from the same horizon. Moreover, it could be shown that variations between particles derived from different soil types were smaller than the observed inter-particular variations within single soil horizons.

In conclusion, this work demonstrated that C-1s NEXAFS spectroscopy can be used to quantify specific carbon groups present in NOM and humic substances. It could be shown that heterogeneity within NOM samples of terrestrial and aquatic origin occurs at various scales. The use of STXM and C-1s NEXAFS spectroscopy allowed the direct examination of aggregate structures of NOM as well as its association with minerals and permitted to resolve these variations in functional group chemistry at high spatial resolution. Both techniques contributed to the understanding of the complex chemistry of NOM and its important role in the environment.

Zusammenfassung

Die Präsenz von natürlicher organischer Substanz (engl.: NOM) in terrestrischen und aquatischen Ökosystemen übt einen tief greifenden Einfluss auf zahlreiche chemische Reaktionen aus, die an diesen Orten auftreten. Natürliche organische Substanz, adsorbiert an mobilen Mineralpartikeln, kann das Transportverhalten von sowohl Nähr- als auch von Schadstoffen in Böden signifikant beeinflussen und einen starken Einfluss auf ihr weiteres chemisches Verhalten in der Umwelt ausüben. Die Sorption von NOM an Mineralphasen hängt in erster Linie von den chemischen Eigenschaften der zahlreichen Kohlenstoffgruppen ab, welche ihre chemische Struktur prägen. Abhängig davon, wie die vorherrschenden chemischen und mikrobiellen Bedingungen im Umfeld der organischen Substanz sind und wo diese ursprünglich gebildet worden ist, können sich ihre chemischen Eigenschaften innerhalb unterschiedlicher Grössenordnungen markant verändern. Organische Substanz in Böden und Gewässern existiert in Form von gelösten Molekülen, kolloidalen Partikeln oder als NOM-Mineral-Komplexe. Diese Unterscheidung sollte jedoch als dynamisch erachtet werden, da natürliche organische Substanz fliessende Übergänge zu allen dieser drei Formen bilden kann. Kohlenstoff, der chemische Grundbaustein von NOM, kann in die Gruppen des organischen und anorganischen Kohlenstoffs unterteilt werden, wobei die Gruppe des organischen Kohlenstoffs aufgrund von Parametern wie Partikelgrösse oder Löslichkeit weiter aufgetrennt werden kann: Mittels Kombinationen verschiedener Auftrennungsschritte wie der Filtration, Ansäuerung, Ausgasung oder der Oxidation werden zahlreiche Untergruppen von organischem Kohlenstoff unterschieden. Die Gesamtmenge an organischem Kohlenstoff welche sich in Boden- und Wasserproben befindet, wird üblicherweise natürliche organische Substanz genannt, wogegen der Begriff des gelösten, organischen Kohlenstoffs (engl.: DOM) für die Fraktion benutzt wird, die als Filtrat durch einen Filter mit einer Porengrösse von 0.45 µm vorliegt. Die Gruppe der Huminstoffe gehört zu dem Teil der natürlichen organischen Substanz, die aufgrund ihrer Löslichkeit in Säure und Base chemisch weiter fraktioniert werden kann. Es werden Huminsäuren, Fulvosäuren und Humine unterschieden.

Diese Arbeit konzentrierte sich auf die Erforschung der chemischen Heterogenität von natürlicher organischer Substanz und Huminstoffen terrestrischen und aquatischen Ursprungs. Für diese Zwecke wurde synchrotron-basierende C-1s near-edge Röntgen-absorptions Spektroskopie (NEXAFS) und Röntgenmikroskopie eingesetzt. Die Ziele dieser Dissertation waren die Verbesserung der sowohl qualitativen wie auch der quantitativen Interpretation von C-1s NEXAFS Daten von NOM-Proben aquatischen und terrestrischen Ursprungs. Um einen besseren Einblick in die Aufnahme und Auswertung der C-1s Spektren von Huminstoffen zu gewinnen, wurden chemisch gut charakterisierte Referenz-Huminstoffe mittels NEXAFS Spektroskopie untersucht. In einem ersten Teil dieses Projekts wandte man verschiedene Quantifizierungsmethoden an, um die Quantifizierbarkeit von C-1s NEXAFS Daten näher zu studieren. Die Daten wurden anschließend mit Angaben aus anderen Studien verglichen und statistisch korreliert. Zusätzlich konnten die Daten mit Ergebnissen aus ^{13}C-NMR (nukleare Magnetresonanz) verglichen und anschliessend kalibriert werden. Eine statistische Analyse der Resultate führte zu positiven Korrelationen für fünf funktionelle Kohlenstoffgruppen. Eine Regressionsanalyse zwischen C-1s NEXAFS und ^{13}C-NMR Daten zeigte, dass die errechneten, absoluten Quantifizierungen der einzelnen funktionellen Gruppen gut mit Daten übereinstimmen, wie sie in der Literatur beschrieben werden. Die Ergebnisse dieser Analyse wurden in den weiteren Kapiteln dieser Arbeit benutzt, um die Rohdaten der C-1s NEXAFS Resultate nachträglich auf absolute Werte nachzukalibrieren.

Um die chemische Variabilität und den Einfluss von saisonalen Unterschieden auf die Chemie von DOM genauer zu verstehen, wurden zehn Proben aus fünf Lokalitäten in Skandinavien untersucht. Die Proben sind aquatischen Ursprungs und konnten im Herbst, zwischen September und Oktober, sowie im Frühling, zwischen April und Mai entnommen werden. Die Proben wurden mittels Fourier-Transform Infrarot Spektroskopie (FT-IR), nuklearer Magnetresonanz (^{13}C-NMR) und C-1s NEXAFS Spektroskopie untersucht. Es zeigte sich, dass saisonale Schwankungen im Bezug auf die quantitative Verteilung von spezifischen funktionellen Kohlenstoffgruppen innerhalb der Proben eine marginale Rolle spielten. Ferner konnte für ihre Elementarverteilung sowie für ihre Spektren eine bemerkenswerte Ähnlichkeit zwischen den Frühlings- und Herbstproben nachgewiesen werden. Eine Altersbestimmung aller Proben mittels der Radiocarbon-(^{14}C)-Methode zeigte, dass die gemittelten Alter sowohl der Frühlings- als auch der Herbst-Proben jünger als 50 Jahre waren. Dies lässt den Schluss zu, dass diese organischen Proben aus der Zersetzung von rezenter Biomasse stam-

men und innerhalb kürzester Zeiträume gebildet werden müssen. Aus demselben Grund sind keine saisonalen Schwankungen in der Verteilung der einzelnen Kohlenstoffgruppen nachweisbar.

Die mobile Fraktion von NOM, wie sie in frischem Bodenmaterial in Form von kolloidalen Partikeln zu finden ist, wurde anhand von Proben untersucht, welche aus drei unterschiedlichen Bodentypen und je zwei Horizonten extrahiert worden sind. Die Analyse erfolgte innerhalb drei verschiedener Skalen. Zuerst wurden die chemischen Unterschiede innerhalb einzelner Bodenpartikel untersucht (Intra-partikuläre Heterogenität). In einem nächst-grösseren Massstab wurde eine Analyse von Unterschieden zwischen einzelnen Partikeln vom selben Horizont durchgeführt (Inter-partikuläre Heterogenität). Zuletzt wurden die Unterschiede von Partikeln, welche aus unterschiedlichen Bodentypen extrahiert worden sind, analysiert und statistisch miteinander verglichen. Zur Analyse der Spektren wurden spezifische Programme benutzt, welche auf statistischer Hauptkomponenten- und Clusteranalyse beruhen. Die Ergebnisse zeigten, dass natürliche organische Substanz Heterogenitäten im Bereich von wenigen Mikrometer aufweist, insbesondere im Bezug auf Anteile an aromatischem und carboxyl-Kohlenstoff. Des Weiteren konnte beobachtet werden, dass die Variationen zwischen einzelnen Partikeln aus unterschiedlichen Bodentypen kleiner sind als die beobachteten Variationen zwischen Partikeln von verschiedenen Horizonten vom selben Bodentyp.

Zusammenfassend beschreibt diese Arbeit den Gebrauch von C-1s NEXAFS Spektroskopie und Röntgenmikroskopie zur Identifikation and Quantifizierung von reaktiven funktionellen Gruppen in organischen Boden- und Gewässerproben. Es wird gezeigt, dass Heterogenitäten innerhalb dieser Proben in verschiedenen räumlichen Ausdehnungen auftreten und einen starken Einfluss auf ihr chemisches Verhalten in der Umwelt ausüben. Der Gebrauch von Röntgenmikroskopie und C-1s NEXAFS Spektroskopie erlaubt die in-situ Analyse dieser Heterogenitäten in sowohl aggregierten Strukturen von natürlicher organischer Substanz wie auch in ihrer Assoziation mit Mineralpartikeln und ermöglicht es, die Variationen reaktiver funktioneller Gruppen innerhalb dieser Partikel mit hoher räumlicher Auflösung zu visualisieren und zu quantifizieren. Der Gebrauch dieser neuartigen Techniken trägt zum Verständnis der komplexen chemischen Reaktionen bei, wie sie in natürlicher organischer Substanz im Bereich weniger Mikrometer vorkommen und helfen mit, ihre überaus wichtige Rolle in natürlichen Ökosystemen besser zu verstehen und erklären zu können.

1 Introduction

1.1 Natural organic matter in the environment

The role of natural organic matter (NOM) in soil and aquatic systems is of major concern in environmental sciences. The presence of NOM in soils, groundwater and surface waters strongly affects the chemical behavior of metals, nutrients and potential pollutants due to various sorption and complexation reactions that may occur within these ecosystems (Sparks, 1995). NOM can form strong complexes with metal ions like aluminum or iron and several trace elements like copper or lead, leading to either enhanced or decreased mobility of these metals (Sparks, 1995). Their behavior in natural environments is controlled mainly by the distribution of NOM between immobile solid phases, mobile colloidal particles and dissolved species (Kretzschmar *et al.*, 1999). After adsorption to stable colloidal phases, the metals can be transported over large distances and may infiltrate and contaminate groundwater resources over wide areas (McCarthy & Zachara, 1989).

Natural organic matter in soils, ground and surface waters exists as dissolved molecules (< 1 nm), colloids (< 1 µm) and particles (> 10 µm). These distinctions should to be regarded as dynamic because NOM can be converted readily between these forms by dissolution and precipitation as well as by sorption and aggregation processes (Sparks, 1995; Swift, 1996). Organic carbon in natural environments can be divided on the basis of particle size and solubility. The total amount of organic carbon is commonly referred to as natural organic matter (NOM). Depending on the particular combination of filtration, acidification, purging and oxidation steps, a wide variety of fractions of carbon can be distinguished. The classification of NOM into non-humic substances and humic substances such as humic acids (HA), fulvic acids (FA) and humins, defined upon their solubility in acid and base, is the most referred one.

Plant litter and the microbial biomass are the major parent materials for the formation of NOM in terrestrial environments, where polysaccharides, lignin, aliphatic biopolymers and tannins are the major chemical constituents of the organic structure of NOM (Schwarzenbach *et al.*, 1993). The composition and relative abundance of these components may vary widely among plant species and tissue type, which is reflected by the large chemical heterogeneity of NOM (Spielvogel *et al.*, 2004). Oades (1989) demonstrated that a number of factors are decisive for controlling the humification processes in soils and therefore for the formation of NOM. These factors are the amount of litter input, the proportion and distribution of plant parts, as well as the relative proportion of the different plant tissues and their initial chemical composition. As NOM is a mixture of different molecules with sizes varying between 0.5 to 400 nm and a molecular weight ranging from 200 to > 10^5 g mol^{-1}, it is not easy to attribute a particular size to it (Clapp & Hayes, 1999). By calculation of acid-base titration data, de Wit et al. (1993) stated that the diameter of high molecular weight humic molecules present in NOM can generally be estimated to be around 5 nm, whereas Kim et al. (1992) found NOM aggregates with diameters up to 400 nm in saline aquifer systems. Schulten et al. (2000) proposed a NOM model with a molecular weight of 7760.16 g mol^{-1} and an average elemental composition of $C_{349}H_{401}N_{26}O_{173}S$, corresponding to an elemental analysis of 54.02 % C, 5.21 % H, 4.69 % N, 35.67 % O and 0.41 % S.

For the characterization of the chemical composition of natural organic matter, several approaches using modern analytical techniques are available. The use of chemolytic techniques such as hydrolysis (Kögel-Knabner, 1995), solvent extraction (Dinel *et al.*, 1990) or CuO oxidation (Goni & Hedges, 1990) have been described extensively to isolate amino acids, carbohydrates and lipids from soil material. However, only a part of the soil organic matter present in specific structures can be identified with these techniques. Another method for assessing the chemical composition of natural organic matter is the use of analytical pyrolysis as applied by Leinweber et al. (1998) and Saiz-Jimenez (1994). A disadvantage of this method is the fact, that the interpretation of pyrolysis data requires detailed knowledge of the pyrolysis behavior of the compounds under study (Schnitzer & Schulten, 1995). Furthermore, thermal secondary reactions can cause considerable modifications of the original compound (Schmiers *et al.*, 1999). Alternative techniques for the chemical examination of NOM are non-destructive spectroscopic methods, which include infra-red (IR) spectroscopy, electron spin resonance (ESR) spectroscopy and nuclear magnetic resonance (NMR)

spectroscopy, although all these methods require extraction and purification steps, which may influence the chemical properties of the sample under study as well. IR spectroscopy provides rapid and reliable information on the bulk chemical composition of NOM as described by Haberhauer et al. (1998), but the method suffers limitations in the quantification of particular carbon groups. The method of ESR spectroscopy gives information on species that contain unpaired electrons as in the case for free radicals within NOM as described by Cheshire et al. (1998). However, both methods are relatively insensitive and reveal low resolution, where specific organic compounds cannot be identified unambiguously. The use of cross-polarization magic angle spinning (CP-MAS) ^{13}C-NMR spectroscopy has greatly increased in the past decade and the technique has become a standard tool for the structural investigation of NOM and humic substances (Cody & Saghi-Szabo, 1999). A wide variety of researchers applied ^{13}C-NMR spectroscopy for the determination of the various carbon functional groups present in environmental samples (Almendros *et al.*, 2000; Malcolm, 1989). Mahieu et al. (1999) conducted a statistical survey of the ^{13}C-NMR spectra of several hundred whole soils and soil size fractions. The review by Perdue and Ritchie (2003) provided a statistical summary of more than 82 reintegrated ^{13}C-NMR spectra of humic substances and NOM samples derived from freshwaters. For the NOM samples, the mean percentages of 5 % carbonyl, 19 % carboxyl, 27 % aromatic, 25 % O-alkyl and 24 % alkyl, respectively. These results are in good agreement with data published by Mahieu et al. for soil NOM samples, although in the review of Perdue and Ritchie, aromatic and O-alkyl carbon groups showed slightly higher standard deviations (sd < 8%) than the data presented by Mahieu et al.. However, Mao et al. (2000) reported that CP-MAS ^{13}C-NMR spectroscopy techniques overestimate sp^3-hybridized carbon in alkyl and O-alkyl groups and underestimate sp^2-hybridized carbon in aromatic, carboxyl and carbonyl functional groups. Furthermore, the number of structural subunits and the chemical shift regions of each subunit may vary from one study to another (Cody & Saghi-Szabo, 1999; Mahieu *et al.*, 1999).

As mentioned earlier in this chapter, the presence of NOM in natural systems affects the chemical behavior of nutrients and potential contaminants to a large extent. Radionuclides and heavy metals have been found to be associated with anionic organic molecules comprising of both hydrophilic and hydrophobic acid fractions of natural organic matter (Champ *et al.*, 1984). Kukkonen et al. (1990) showed that hydrophobic organic contaminants like polychlorinated biphenyl and benzo(a)pyrene bind preferentially to hydrophobic NOM.

Whether contaminant transport is enhanced (Dunnivant *et al.*, 1992) or retarded (Totsche *et al.*, 1997) depends on the mobility of the natural organic matter that acts as a carrier. The mobility of NOM in natural porous media is governed by its reactivity with the solid matrix and is further complicated by flocculation and precipitation reactions (Römkens & Dolfing, 1998). These reactions occur at low pH and with high concentrations of polyvalent and potentially bridging ions such as calcium, aluminum or iron. In soil and aquatic systems, the main components for adsorption of natural organic matter are iron and aluminum hydroxides as well as clay minerals (Sposito, 1984).

It is obvious, that functional group chemistry on one hand and macro-molecular structure on the other governs the behavior of NOM in the environment, whereas both properties are strongly interrelated and one influences the other (Schmidt *et al.*, 1999). For instance, most studies suggest that the chemical composition varies with the size of the particular NOM fraction and that differences between size fractions may have a strong influence on the environmental behavior of these molecules (Christl *et al.*, 2000; Kukkonen *et al.*, 1990). However, it is still unclear at which scale the occurring heterogeneity of natural organic matter becomes relevant and to which extent the chemical properties of possible contaminants within water and soil environments may be affected. Other studies have shown that the summarized chemical characteristics of organic-mineral particles have direct effects on properties such as soil aggregation and the resulting physical behavior of soil material. It was clearly shown that organic matter is the decising factor for physicochemical reactions at organic-mineral surfaces (Christl & Kretzschmar, 2001; Kretzschmar *et al.*, 1997). Despite these studies, the role of NOM in environmental ecosystems and its heterogeneity down from the micrometer up to the particle scale is still controversial and needs to be investigated at these respective levels.

While conventional laboratory spectroscopy and microscopy techniques suffer from lack of sensitivity, element-specific X-ray absorption spectroscopy and spectromicroscopy methods using synchrotron radiation can allow the microscopic examination of NOM at the micrometer scale. The use of soft X-rays with wavelengths between the K-absorption edges of oxygen and carbon (543 eV/2.3 nm and 284e V/4.4 nm) is of particular interest for studies with environmental samples, because within this energy range water is highly transparent to X-rays compared to other substances. This “water-window” contrast arises from a difference in absorptivity for water and carbonaceous (or other dense inorganic) material (Kirz *et al.*, 1991). The samples can easily

be examined in a hydrated state, at atmospheric conditions and without any pre-treatment such as the removal of iron or oxygen (Jacobsen & Neuhäusler, 1999). Recent developments in soft zone plate optics and instrumental design have enabled 30 nm imaging of hydrated specimen (Medenwaldt & Uggerhoj, 1998). An addition to these techniques is synchrotron-based scanning transmission X-ray microscopy (STXM), where the distribution of elements like carbon or oxygen can be mapped versus that of other, heavier elements. The addition of a tunable monochromator at energies from 280 to 320 eV allows the collection of X-ray absorption spectra close to the carbon 1s-absorption edge (C-1s NEXAFS). In the past decade, several studies were conducted on the research of coal samples (Cody *et al.*, 1995), the investigation of biopolymers like peptides or amino acids (Boese *et al.*, 1997) or the carbon chemistry of interplanetary dust particles (Chapman *et al.*, 1995) by applying STXM and C-1s NEXAFS spectroscopy. More recently, Scheinost et al. (2001) investigated the distribution of carbon within selected IHSS reference fulvic acids, humic acids and NOM, whereas Jokic et al. (2003) and Schäfer et al. (2003) conducted X-ray absorption spectroscopy experiments on non-living organic matter in soils. Only little research has been done focusing on the chemical heterogeneities of humic substances and aqueous NOM samples at the particle scale. Rothe et al. (2000) investigated interactions of humic acid with clay colloids whereas Thieme et al. (2003) mapped calcareous precipitates within soil samples of a few microns in scale. However, the use of STXM and C-1s NEXAFS spectroscopy as a tool for the investigation of environmental samples opens up the possibility to speciate and quantify the major carbon groups present in naturally derived NOM and its chemistry in a hydrated state. Moreover, the method permits the in-situ analysis of nanoscale heterogeneity present in NOM with high spatial resolution and is able to provide direct data from organic-mineral reaction interfaces.

1.2 Objectives of this study

The research objectives adressed in this thesis were the investigation of NOM and humic substances by means of C-1s NEXAFS spectroscopy and scanning transmission X-ray microscopy. The detection and quantification possibilities of C-1s NEXAFS spectroscopy were investigated on well characterized humic substances reference samples. The relative carbon contents of the reactive carbon groups present in the organic structure of the samples were determined by spectral analysis and calibrated against ^{13}C-NMR data. The quantification scheme applied for these reference samples was then applied to DOM samples and colloidal particles of unknown chemical composition, where the chemical heterogeneity of these samples was analyzed and quantified at different scales. The fundamentals of C-1s NEXAFS spectroscopy and STXM are described in Chapter 2. In order to study the quantification possibilities of C-1s NEXAFS spectroscopy for specific carbon functional groups, standardized reference humic substances were investigated with STXM and solid-state CP-MAS ^{13}C-NMR spectroscopy (Chapter 3). The particular objective of this study was to determine, wether C-1s NEXAFS spectroscopy is able to provide quantitative information about contents of reactive carbon groups present in humic substances. An adapted spectral deconvolution scheme after Scheinost et al. (2001) was applied on the spectral data of the samples and compared with other deconvolution schemes. The results were correlated with data obtained from CP-MAS ^{13}C-NMR spectroscopy by calculation of linear regressions for each carbon group and used for further quantifications. The chemical variability of ten DOM samples of aquatic origin was investigated by FT-IR, CP-MAS ^{13}C-NMR and C-1s NEXAFS spectroscopy (Chapter 4) and analyzed with respect to seasonal and geographic differences. Radiocarbon (^{14}C) ages were determined in order to provide information about the mean turnover times of DOM samples from boreal freshwater catchments. In Chapter 5, water-dispersible colloidal particles extracted from three soils along a toposequence in northern Switzerland were analyzed by C-1s NEXAFS spectroscopy and STXM. The aim of this study was to show, wether colloidal particles exhibit changes in carbon functional group chemistry at the scale of single particles, horizons or soil types. The spectral deconvolution, quantification and calibration with CP-MAS ^{13}C-NMR data applied on these water dispersible colloids was based on results presented in Chapter 3 and provided for the first time a detailed chemical analysis and quantification of reactive carbon functional groups of aqueous, environmental samples.

Literature cited

Almendros, G., Dorado, J., Gonzalez-Vila, F.J., Blanco, M.J. & Lankes, U. 2000. ^{13}C NMR assessment of decomposition patterns during composting of forest and shrub biomass. *Soil Biol. Biochem.* **32**: 793-804.

Boese, J., Osanna, A., Jacobsen, C. & Kirz, J. 1997. X-Ray absorption near-edge structure of amino acids and peptides. *J. Electron Spectrosc.* **85**: 9-15.

Champ, D.R., Young, J.L., Robertson, D.E. & Abel, K.H. 1984. Chemical speciation of long-lived radionuclides in a shallow groundwater flow system. *Water Pollut. Res. J. Can.* **19**: 35-54.

Chapman, H.N., Bajt, S., Flynn, G. & Keller, L.P. 1995. Carbon mapping and Carbon-XANES measurements on an interplanetary dust particle using a Scanning-Transmission X-ray Microsocope. *Meteoritics*. **30**: 496-497.

Cheshire, M.V. & Senesi, N. 1998. In: *Structure and Surface Reactions of Soil Particles* (P.M. Huang, N. Senesi *et al.* eds.) John Wiley & Sons, Chichester. p. 325-376.

Christl, I., Knicker, H., Kögel-Knabner, I. & Kretzschmar, R. 2000. Chemical heterogeneity of humic substances: Characterization of size fractions obtained by hollow-fibre ultrafiltration. *Eur. J. Soil Sci.* **51**: 617-625.

Christl, I. & Kretzschmar, R. 2001. Relating ion binding by fulvic and humic acids to chemical composition and molecular size. I. Proton binding. *Environ. Sci. Technol.* **35**: 2505 -2511.

Clapp, C.E. & Hayes, M.B.H. 1999. Sizes and shapes of humic substances. *Soil Sci.* **164**: 777-789.

Cody, G.D., Botto, R.E., Ade, H., Behal, S., Disko, M. & Wirick, S. 1995. Inner-shell spectroscopy and imaging of a subbituminous coal: In-situ analysis of organic and inorganic microstructure using C(1s)-, Ca(2p)-, and Cl(2s)-NEXAFS. *Energ. Fuel*. **9**: 525-533.

Cody, G.D. & Saghi-Szabo, G. 1999. Calculation of the ^{13}C NMR chemical shift of ether linkages in lignin derived geopolymers: Constraints on the preservation of lignin primary structure with diagenesis. *Geochim. Cosmochim. Acta*. **63**: 193-205.

de Wit, J.C.M., van Riemsdijk, W.H. & Koopal, L.K. 1993. Proton Binding to Humic Substances. 1. Electrostatic Effects. *Environ. Sci. Technol.* **27**: 2005-2014.

Dinel, H., Schnitzer, M. & Mehuys, G.R. 1990. In: *Soil Biochemistry* (J.-M. Bollag & G. Stotzky eds.) Vol. 6, M. Dekker, New York. p. 397-429.

Dunnivant, F.M., Jardine, P.M., Taylor, D.L. & McCarthy, J.F. 1992. Cotransport of cadmium and hexachlorobiphenyl by dissolved organic carbon through columns containing aquifer material. *Environ. Sci. Technol.* **26**: 360-368.

Goni, M.A. & Hedges, J.I. 1990. Potential applications of cutin-derived CuO reaction products for discriminating vascular plant sources in natural environments. *Geochim. Cosmochim. Acta*. **54**: 3073-3081.

Haberhauer, G., Rafferty, B., Strebl, F. & Gerzabek, M.H. 1998. Comparison of the composition of forest soil litter derived from three different sites at various decompositional stages using FTIR spectroscopy. *Geoderma*. **83**: 331-342.

Jacobsen, C. & Neuhäusler, U. 1999. *Soft X-ray optics and spectromicroscopy: Potential for soil science specimens*, NSLS annual report. Brookhaven National Laboratory (BNL), Upton.

Jokic, A., Cutler, J.N., Ponomarenko, E., van der Kamp, G. & Anderson, D.W. 2003. Organic carbon and sulphur compounds in wetland soils: Insights on structure and transformation processes using K-edge XANES and NMR spectroscopy. *Geochim. Cosmochim. Acta*. **67**: 2585-2597.

Kim, J.I., Delakowitz, B., Zeh, P., Probst, T., Lin, X., Ehrlicher, U. & Schauer, C. 1992. *Colloid migration in groundwaters: geochemical interactions of radionuclides with natural colloids*, 2nd progress report. Technische Universität München, München.

Kirz, J., Ade, H., Jacobsen, C., Ko, C.H., Lindaas, S., McNulty, I., Sayre, D., Williams, S., Zhang, X. & Howells, M. 1991. Soft x-ray microscopy with coherent x-rays. *Rev. Sci. Instrum.* **63**: 557-563.

Kögel-Knabner, I. 1995. In: *Methods in Applied Soil Microbiology and Biochemistry* (P. Nannipieri & K. Alef eds.) Academic Press, London. p. 66-78.

Kretzschmar, R., Borkovec, M., Grolimund, D. & Elimelech, M. 1999. Mobile subsurface colloids and their role in contaminant transport. *Adv. Agron.* **66**: 121-194.

Kretzschmar, R., Hesterberg, D. & Sticher, H. 1997. Influence of adsorbed humic acid on surface charge and flocculation of kaolinite. *Soil Sci. Soc. Am. J.* **61**: 101-108.

Kukkonen, J., McCarthy, J.F. & Oikari, A. 1990. Effects of XAD-8 fractions of dissolved organic carbon on the sorption and bioavailability of organic micropollutants. *Arch. Environ. Contam. Toxicol.* **19**: 551-557.

Leinweber, P. & Schulten, H.R. 1998. Advances in analytical pyrolysis of soil organic matter. *J. Anal. Appl. Pyrol.* **47**: 165-189.

Mahieu, N., Powlson, D.S. & Randall, E.W. 1999. Statistical analysis of published carbon-13 CP-MAS NMR spectra of soil organic matter. *Soil Sci. Soc. Am. J.* **63**: 307-319.

Malcolm, R.L. 1989. In: *Humic Substances II: In Search of Structure* (M.B.H. Hayes, P. McCarthy *et al.* eds.) John Wiley & Sons, New York. p. 339-372.

Mao, J.-D., Hu, W.-G., Schmidt-Rohr, K., Davies, G., Ghabbour, E.A. & Xing, B. 2000. Quantitative characterization of humic substances by solid-state carbon-13 nuclear magnetic resonance. *Soil Sci. Soc. Am. J.* **64**: 873-884.

McCarthy, J.F. & Zachara, J.M. 1989. Subsurface transport of contaminants. *Environ. Sci. Technol.* **23**: 496-502.

Medenwaldt, R. & Uggerhoj, E. 1998. Description of an x-ray microscope with 30 nm resolution. *Rev. Sci. Instrum.* **69**: 2974-2977.

Oades, J.M. 1989. In: *Minerals in Soil Environments* (J.B. Dixon & S.B. Weed eds.) Soil Science Society of America, Madison. p. 89-159.

Perdue, E.M. & Ritchie, J.D. 2003. In: *Treatise on Geochemistry* (H.D. Holland & K.K. Turekian eds.) Vol. 5, Elsevier, p. 273-318.

Römkens, P.F. & Dolfing, J. 1998. Effect of Ca on the solubility and molecular size distribution of DOC and Cu binding in soil solution samples. *Environ. Sci. Technol.* **32**: 363-369.

Rothe, J., Denecke, M.A. & Dardenne, K. 2000. Soft X-Ray spectromicroscopy investigation of the interaction of aquatic humic acid and clay colloids. *J. Colloid Interf. Sci.* **231**: 91 -97.

Saiz-Jimenez, C. 1994. *Application of pyrolysis-gas chromatography/mass spectrometry to soil chemistry*. In: Transactions 15th International Congress of Soil Science, Acapulco.

Schäfer, T., Hertkorn, N., Artinger, R., Claret, F. & Bauer, A. 2003. Functional group analysis of natural organic colloids and clay association kinetics using C(1s) spectromicroscopy. *J. Phys. IV*. **104**: 409-412.

Scheinost, A.C., Kretzschmar, R., Christl, I. & Jacobsen, C. 2001. In: *Humic Substances: Structures, Models and Functions* (E.A. Ghabbour & G. Davies eds.) Royal Society of Chemistry, Cambridge. p. 37 -40.

Schmidt, C., Thieme, J., Neuhäusler, U., Schulte-Ebbert, U., Abbt-Braun, G., Specht, C. & Jacobsen, C. 1999. *Association of particles and structures in the presence of organic matter*. In: 6th international conference on X-ray Microscopy, Berkeley.

Schmiers, H., Friebel, J., Streubel, P., Hesse, R. & Köpsel, R. 1999. Change of chemical bonding of nitrogen of polymeric n-heterocyclic compounds during pyrolysis. *Carbon*. **37**: 1965-1978.

Schnitzer, M. & Schulten, H.R. 1995. Analysis of organic matter in soil extracts an whole soils by pyrolysis-mass spectrometry. *Adv. Agron.* **55**: 167-217.

Schulten, H.R. & Leinweber, P. 2000. New insights into organic-mineral particles: Composition, properties and models of molecular structure. *Biol. Fertil. Soils*. **30**: 399-432.

Schwarzenbach, R.P., Gschwend, P.M. & Imboden, D.M. 1993. *Environmental Organic Chemistry*. John Wiley & Sons, New York.

Sparks, D.L. 1995. *Environmental Soil Chemistry*. Academic press, San Diego.

Spielvogel, S., Knicker, H. & Kögel-Knabner, I. 2004. Soil organic matter composition and soil lightness. *J. Plant Nutr. Soil Sci.* **167**: 545-555.

Sposito, G. 1984. *The Surface Chemistry of Soils*. Oxford University Press, New York.

Swift, R.S. 1996. In: *Methods of Soil Analysis: Chemical methods* (D.L. Sparks ed.) Soil Science Society of America, Madison. p. 1018-1020.

Thieme, J., Schneider, G. & Knöchel, C. 2003. X-ray tomography of a microhabitat of bacteria and other soil colloids with sub-100nm resolution. *Micron*. **34**: 339-344.

Totsche, K.U., Danzer, J. & Kögel-Knabner, I. 1997. Dissolved organic matter-enchanced retention of polycyclic aromatic hydrocarbons in soil miscible displacement experiments. *J. Environ. Qual.* **26**: 1090-1100.

2 Fundamentals of C-1s NEXAFS spectroscopy

2.1 X-ray spectroscopy

2.1.1 Theoretical background

Electrons provide vital information about the bonding environment of the specific element they belong to. Near-edge X-ray absorption fine structure (NEXAFS) spectroscopy methods can provide vital information on the status of these electrons in the molecules (Teo, 1986). These electron energy levels and their respective electronic spectra can be well understood by first examining the electronic states and spectra of simple mono- and diatomic molecules, as shown in Figure 2.1 (Stöhr, 1996).

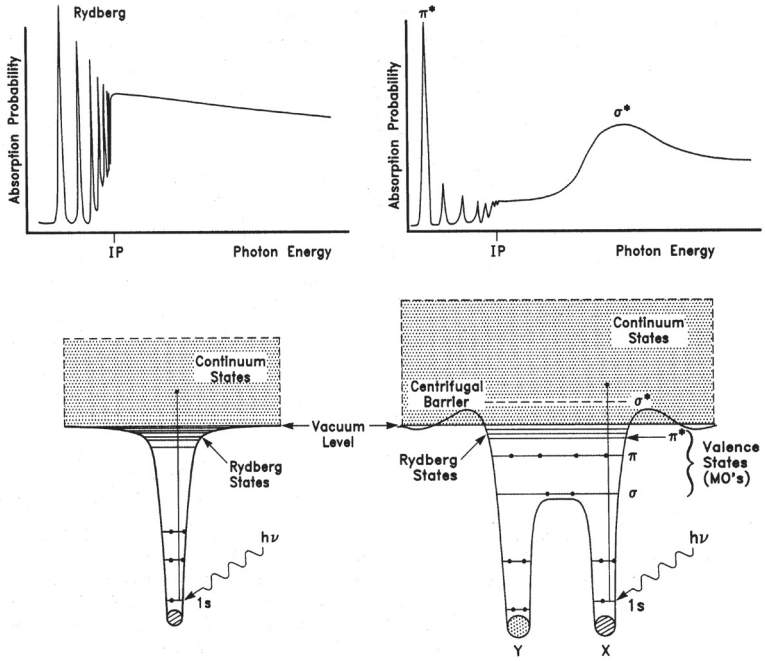

Figure 2.1:
Schematic potentials and K-shell spectra of single atoms (left) and diatomic molecules (right). From Stöhr, with permission (1996).

In the case of single atoms, as shown on the left side of Figure 2.1, energy states of electrons can be determined from the Coulomb potential of the nucleus. Some of these states are empty (Rydberg states) and differences in their energy states become smaller with distance away from the nucleus. Finally, they converge to the vacuum level or continuum states (grey), which correspond to the energy region above the ionization potential (IP) and have no relation to the atom. When electrons in single atoms are excited, they make transitions from occupied atomic orbitals to empty Rydberg orbitals. Such transitions occur when the incident energy is equal to the difference between the energy states of these orbitals. The electronic spectra show distinct, well developed peaks that correspond to the electronic transitions of these discrete levels. The right side of Figure 2.1 depicts the situation where two atoms (X and Y) are brought closer together, as in the case of diatomic molecules such as O_2 or N_2. Significant overlaps resulting from the atomic orbitals of these two atoms form molecular orbitals (MO) with several valence states. Electrons from these two atoms become delocalized and move into these respective molecular orbitals (Stöhr, 1996). These linear combinations of atomic orbitals result in the formation of both bonding (π, σ) and antibonding (π^*, σ^*) molecular orbitals, which are below and above the energy levels of the atomic orbitals of the individual atoms, shown as solid and dashed lines, respectively. The energy levels of both bonding and antibonding orbitals as well as their energy differences are affected by the intensity of the overlap of the atomic orbitals. In addition, changes in the type of atom and its energy states also modify the energy levels of the particular MO's. The electronic spectra of these molecules provide information on orbital energy levels and therefore the strength of interactions between the atoms. Since the innermost (1s) electrons are localized and are not affected significantly by the overlap of the outermost (valence) orbitals, the transition of these 1s electrons can be used as a ruler to measure the bonding interactions between the different atoms (Stöhr *et al.*, 1984).

The same approach can be used to understand the chemical bonding in polyatomic molecules and polymers. The electronic spectrum of a polymer can be described as the sum of the spectra of individual diatomic components (Morra *et al.*, 1996). Since the orbital composition and energy states of an atom of interest in a molecule are modified primarily by the energy states of its neighbors, this so-called building-block approach is valid for describing the electronic structure of polymers (Morra *et al.*, 1996). However, not only do interactions of diatomic molecules and their respective orbitals contribute to the overall spectrum of

this central atom, but also the complete local coordination around the atom as well as its hybridized orbitals should be considered (Stöhr, 1996). In the case of molecules which exhibit delocalized electrons such as those with conjugated π-systems, the coordination environment beyond the first neighbors should be taken into account as well (Bianconi *et al.*, 1988).

2.1.2 C-1s NEXAFS spectroscopy

A typical X-ray absorption spectrum of a molecule exhibits intense peaks that correspond to the bound state transitions at low energies, followed by the scattering-related features a few eV above these transitions. The part of the X-ray absorption spectrum that corresponds to the bound state transitions is referred to as X-ray absorption near-edge structure (XANES) or near-edge X-ray absorption fine structure (NEXAFS), whereas the spectrum well above the bound state transitions is called extended X-ray absorption fine structure (EXAFS) (Teo, 1986). Since the electronic transitions are sensitive to the local coordination environment, electronic spectra can be used to identify the functional groups of molecules and their local bonding environment. Therefore, X-ray absorption spectroscopy is described as an element specific spectroscopy (Stöhr, 1996).

When an element absorbs X-rays, electrons jump from a level in the atomic core, as discussed previously. First, they make transitions to the lowest-lying unoccupied molecular orbitals and then to higher energies up to the continuum, finally resulting in an ionization of the element. Such quantum jumps from core atomic levels to the empty orbitals require energies that are characteristic for each element (Stöhr, 1996; Teo, 1986). Quantum mechanical considerations, called selection rules, limit the type of allowed electron transitions, whereas each type of transition represents a different edge designation and energy. The position of this ionization edge, meaning the energy difference between the initial electronic level and the continuum, is a direct expression of the ionization energy of the element in its chemical bonding environment. That energy strongly depends on the valence (oxidation state) of the element. It becomes increasingly difficult to ionize an element as its oxidation state changes from negative to neutral and then to positive values (Stöhr, 1996). The actual position of this absorption threshold depends first on the element absorbing the X-rays and second on its oxidation state. All X-ray absorption edges have fine structure at the edge, indicating allowed transitions into vacant electronic levels lying just below the continuum.

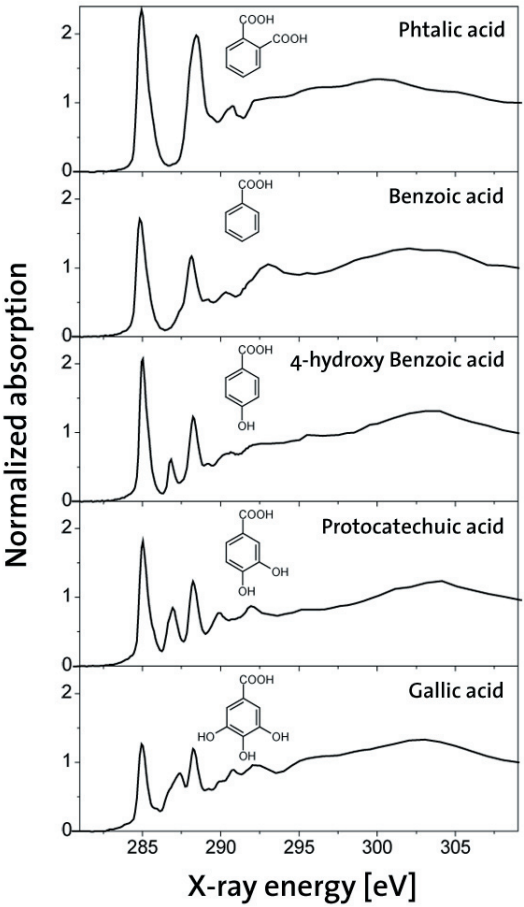

Figure 2.2:
C-1s NEXAFS spectra of simple organic acids. Adapted from Plaschke et al., with permission (2004).

These low-lying vacant states include anti-bonding orbitals, whose energy and symmetry provide information about the chemical environment of the sample. In this study, the focus was on the spectral features of carbon, referred to as C-1s NEXAFS spectroscopy. Molecules containing π-orbitals generally have their lowest energy inner-shell transition to the first incompletely occupied or antibonding π^*-molecular orbital (MO) (Stöhr, 1996). This transition is typically observed as a sharp and well pronounced absorption band several eV below the ionization threshold for the specific molecule. Depending on the molecule, there are several numbers of π^* states observable. As the X-ray energy is increased, the energy of the incident photon exceeds the ionization potential (IP) of the core electron. Typically, IP's for carbon range from 290-296 eV, where low values correspond to aliphatic and aromatic carbon and highest values to carboxylic bound carbon (Kaznacheyev *et al.*, 2002). In addition to antibonding π-orbitals (π^*), there are also antibonding σ molecular orbitals (σ^*). The 1s-σ^* transitions to these molecular orbitals are found several electron volts above the ionization threshold. The more delocalized nature of the electron in the σ^* state coupled with the multiplicity of several 1s-σ^* transitions leads to a high overlap and makes peak designations within this region of the NEXAFS spectrum rather dif-

ficult. In order to illustrate the multiple features contributing to a C-1s NEXAFS spectrum, absorption spectra of simple organic acids are presented in Figure 2.2. The C-1s spectra for phtalic and benzoic acid are dominated by spectral features, which are typical for molecules containing unsaturated functional groups such as phenyl rings and double bonds (Stöhr, 1996). The spectra exhibit low-energy $1s \rightarrow \pi^*$ transitions around 285 eV, characteristic for aromatic carbon bonds. The shape of these bands varies with the chemical and electronic structure of these polymers, as can be observed in the spectrum of e.g. gallic acid (Hitchcock *et al.*, 1986; Urquhart *et al.*, 2000). The peak at 286.5 eV, most pronounced in the spectrum of protocatechuic acid and 4-hydroxy benzoic acid, corresponds to transitions that are due to electron-withdrawing bound atoms to the carbon structure, as in the case for phenols or aryl ether (Stöhr, 1996; Yang *et al.*, 1995). Each phenolic group attached to the aromatic ring contributes to the feature at 286.5 eV and makes the signal intensity directly proportional to the amount of phenolic groups present in the sample. Moreover, all five spectra exhibit transitions at 288.5 eV, characteristic for carboxyl functional groups (Cody *et al.*, 1998), whereas the spectrum of phtalic acid exhibits the most pronounced signal due to two carboxyl carbon groups attached to the ring structure. In addition to these pronounced absorption bands, several more spectral features can be observed in C-1s NEXAFS spectra such as signals for O-alkyl carbon groups at 289.4 eV (Scheinost *et al.*, 2001) and spectral features that are characteristic for carbonyl carbon groups at X-ray energies of 290.5 eV (Urquhart & Ade, 2002). The technique is therefore able to unambiguously detect at least five major reactive functional groups and provide qualitative as well as quantitative information about the local carbon chemistry of the particular sample under study.

2.1.3 X-ray microscopy

Soft X-ray microscopy makes use of X-rays with an energy of 100 to 1000 eV or wavelengths of 1 to 10 nm. These wavelengths are much smaller than those of visible light, giving the potential for high spatial resolution imaging. In scanning transmission X-ray microscopy, the beam is focused on the sample and the transmitted flux is collected using a photodiode or a proportional counter. An illustration of such an image scan is shown in Figure 2.3. For imaging with X-rays, the beam needs to be focused on a small spot using either zone plates, compound refractive lenses, Kirkpatrick-Baez mirrors, or tapered capillaries (Attwood, 2000).

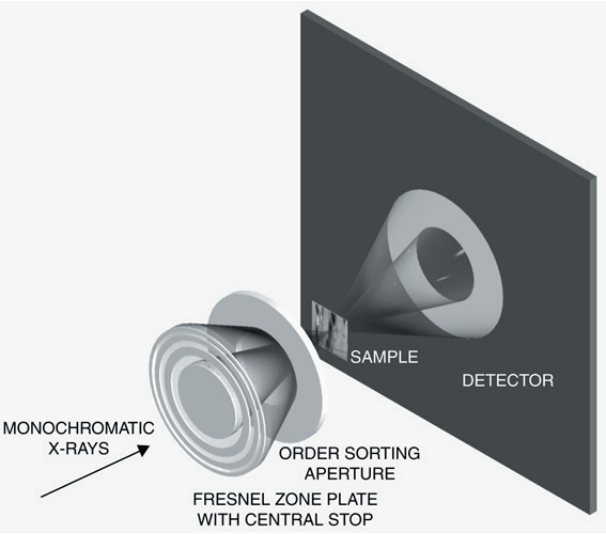

Figure 2.3:
Illustration of an image scan. The first order focus of the zone plate is isolated from unwanted, higher diffraction orders by the combination of a central stop on the zone plate and an order sorting aperture (pinhole). The sample is scanned through the X-ray focus and an X-ray detector measures the transmitted X-ray flux for every sample position. From Feser, with permission (2002).

Except for photoemission electron microscopes, all soft X-ray microscopes are based on focusing with zone plates and use sample transmission to collect high resolution images (Ade *et al.*, 1997). The spatial resolution of the incoming X-ray beam depends on the outer zone width of the zone plate. Up to now, a spatial resolution of 30 nm can be acquired (Feser, 2002). For data acquisition, a two-dimensional image is collected by scanning the sample stage at fixed photon energy, set by the grating and by keeping the zone plate at the appropriate focal distance from the sample. Absorption spectra at one specific point within the image or a sequence of images at different energies can be collected by changing the photon energy and by moving the zone plate accordingly. This stack of images provides the absorption contrast and a NEXAFS spectrum in the third dimension at any selected location on the image. The combination of X-ray imaging of samples with the collection of NEXAFS is typically referred to as microspectroscopy.

2.2 The Stony Brook Scanning Transmission X-ray Microscope

All X-ray absorption experiments presented in this thesis were conducted at beamline X-1A at the National Synchrotron Light Source in Upton, N.Y., using the scanning transmission X-ray microscope (STXM) developed by the group of J. Kirz and C. Jacobsen from the State University of New York (SUNY) in Stony Brook.

2.2.1 Instrumentation

A schematic setup of the X-1A beamline and the STXM is presented in Figure 2.4. In scanning transmission X-ray microscopy, spatial coherence is crucially needed in order to get the highest possible spatial resolution, limited only by diffraction (Wang & Jacobsen, 1997). To obtain high coherent flux, a bright source can be spatially filtered and monochromatized. The X-1 undulator serves as a tunable, bright soft X-ray source based on 35 periods of $SmCo_5$ hybrid magnets, shown on the right side of the figure. The undulator can be tuned to photon energies between 250 to 800 eV, covering absorption thresholds for elements such as carbon, oxygen or chlorine (Henke *et al.*, 1993).

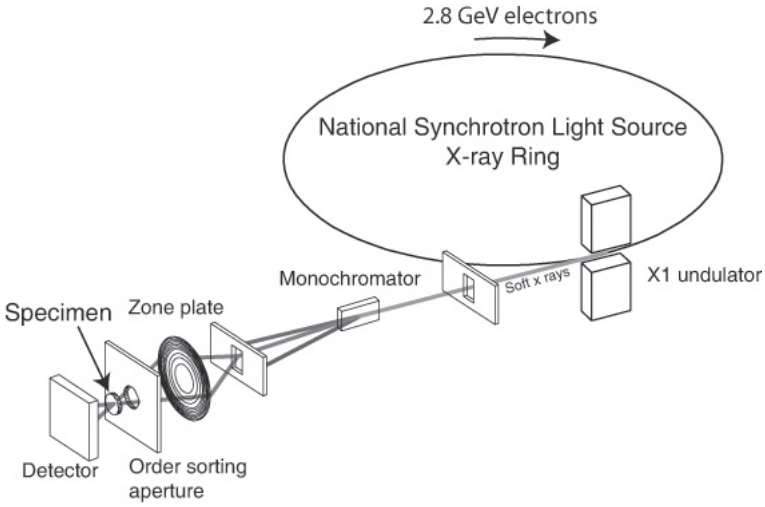

Figure 2.4:
Schematic setup overview of the X-1A beamline and the Scanning Transmission X-ray Microscope. Adapted from Wang (1998).

A toroidal mirror deflects and focuses the generated synchrotron radiation from the undulator onto the monochromator entrance slit in the horizontal plane, and onto the exit slits in the vertical plane. The monochromator, shown in the middle of Figure 2.4, consists of a spherical grating with 900 lines per mm. The energy resolution is determined by the entrance slit size. The exit slit coming afterwards determines the spatial coherence of the X-ray beam. After having passed all beamline optics, the beam reaches the actual microscope setup as shown on the left of Figure 2.4. The X-rays exit the beamline vacuum and illuminate the zone plate. The order sorting aperture (OSA), located between zone plate and the sample, prevents unwanted diffraction orders (except for the first order used for imaging) from entering the microscope. The OSA must be precisely aligned to the center stop of the zone plate, so that no other light from higher diffraction orders can reach the sample. A photograph of the microscope is presented in Figure 2.5.

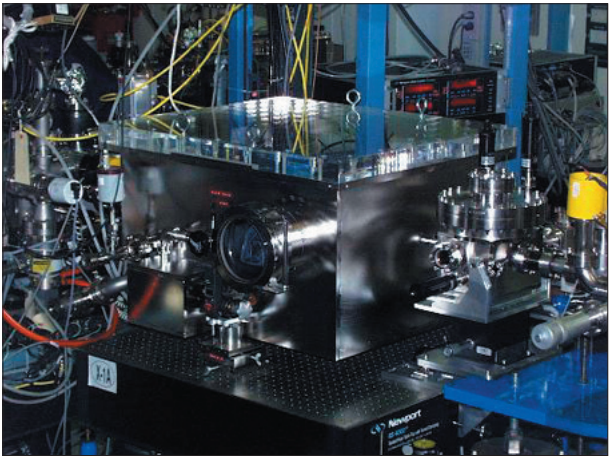

Figure 2.5:
Photograph of the STXM. The X-ray beam enters the microscope from the right. Adapted from Feser (2002).

The sample can be moved perpendicular to the beam both in x- and y-direction, using either stepper motors with step sizes typically between 10 to 50 µm for coarse, large image steps up to several mm, or piezoelectric actuators for high resolution scans of smaller image fields of 1 to 10 µm. The dwell time per image pixel ranges between 1 ms for quick overview scans to 120 ms for images with good photon statistics. The distance between exit window and counter

can be up to 1 cm. A constant helium flow in the detector and sample region ensures high transmission. During experiments, the microscope is covered with a plexiglass top in order to provide constant, undisturbed conditions. The radiation transmitted through the sample is detected by an improved multi-wire proportional counter, counting with low noise and linearly up to 1 Mhz count rate (Feser *et al.*, 2001). An extensive discussion on the microscope and its specifications is presented by Kirz et al. (1995).

2.2.2 Sample preparation

Dry films

For C-1s NEXAFS measurements of freeze-dried sample material, thin films with 50 to 200 nm of thickness have to be prepared and deposited afterwards onto 100 nm thick Si_3N_4 windows (Silson Ltd., Northampton, UK) and air-dried. The high absorption coefficient of carbon at these wavelengths, $\mu = 10^4$ cm^2 g^{-1} requires the sample thickness to be less than 800 nm for imaging purposes and less than 400 nm for quantitative spectroscopy (Henke *et al.*, 1982). Absorption spectra of samples thinner than 50 nm often show a poor signal-to-noise ratio, whereas the spectra of samples thicker than 200 nm can be distorted by absorption saturation (Urquhart *et al.*, 1999). Typically, sections of ~ 100 nm in thickness are ideal for X-ray microscopy and C-1s NEXAFS spectroscopy purposes.

Hydrated samples

In order to investigate colloidal particles in aqueous solutions, the sample mount has to be changed from a simple sample holder to a wet specimen chamber or wet cell. Figure 2.6 shows photographs of a mounted wet specimen chamber. The wet cell is a double-sample mount with two opposite silicon nitride windows, whereas a thin water layer is formed between the surfaces within those windows. An O-ring seal is made between the metal parts of the chamber in order to retain the water and avoid evaporation. The thickness of the water layer is controlled by three screws that press the two parts together. Further details on the wet specimen chamber are presented by Neuhäusler et al. (2000).

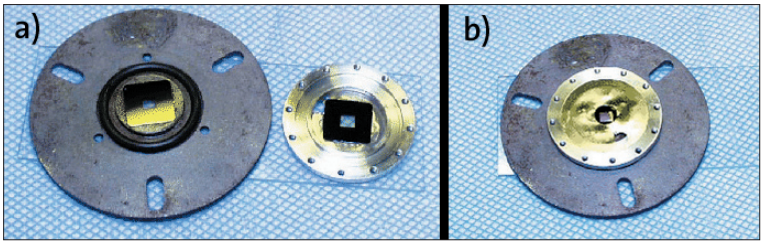

Figure 2.6:
Photographs of the wet specimen chamber. Adapted from Feser (2002).

a) The two halves of the wet specimen chamber, each with a silicon nitride membrane. After placing a droplet of sample material on one half of the sample holder, both parts are screwed together and adjusted in pressure with screws (backside).

b) After the adjustment of the pressure within both silicon nitride windows and sealed the cell with tape in order to prevent the sample from drying out, the wet cell is ready for insertion into the microscope.

2.2.3 Measuring modes

The STXM can be operated in two spectroscopic modes. The first mode is the conventional spectroscopy mode, typically used for the collection of C-1s NEXAFS spectra of dry films. The second operation mode is the microspectroscopy mode, which is commonly used for the collection of NEXAFS spectra of hydrated samples using the wet specimen chamber.

Conventional spectroscopy mode

In conventional spectroscopy mode, the sample is positioned in a way that the X-ray focus spot hits the region of interest within the sample. While the sample stays in place, absorption data are taken by changing the photon energy, refocusing the zone plate accordingly and detecting the signal in transmission. A common absorption spectrum consists of 512 data points and covers an energy range of about 30 eV in order to cover pre- and post-edge signals. A normalization spectrum I_o without sample material has to be taken in order to take into account the spectral variations resulting from non-constant output of the undulator, the beamline and the zone plate optics (Jacobsen & Kirz, 1998).

Microspectroscopy mode

The second possibility of collecting X-ray absorption data is the microspectroscopy mode or alternatively the "image-stack" acquisition mode as implemented by Jacobsen et al. (2000). An automated routine takes a data set of images at

closely spaced photon energies within a defined range of energies. The set of images obtained can be aligned afterwards using an autocorrelation routine, whereas variations in X-ray intensity or offsets of the sample can be eliminated. The region from which a spectrum is obtained is limited by the microscope resolution, allowing the collection of spectral information from very small sample regions that would otherwise not be accessible when using the conventional spectroscopy technique. Special attention has to be paid in considering regions in the image without sample material (I_o) for spectra normalization. These regions have to be in practice at least sample regions that do not contain the particular absorption edge element. For these specific compounds, the X-ray absorption can be assumed to be constant over a small energy interval (Engstrom *et al.*, 1991; Winn *et al.*, 2000). A disadvantage of this measuring mode is that it is very time-consuming. Even if one chooses to acquire modest quality images, the acquisition of a stack data set takes between 3 and 6 hours. The advantage of such a set is that it contains spectra of all image points within the investigated sample. Some sample regions might not attract the attention of the user during the experiment, but might turn out to be interesting when analyzing the data set, for example with principal component or cluster analysis (Lerotic *et al.*, 2004). Further details on the collection and the analysis of image stacks are given in Jacobsen et al. (2000).

Literature cited

Ade, H., Smith, A.P., Zhang, H., Zhuang, G.R., Kirz, J., Rightor, E.G. & Hitchcock, A.P. 1997. X-ray spectromicroscopy of polymers and tribological surfaces at beamline X1-A at the NSLS. *J. Electron Spectrosc.* **84**: 53-72.

Attwood, D.T. 2000. *Soft X-rays and Extreme Ultraviolet Radiation: Principles and Applications*. Cambridge University Press, New York.

Bianconi, A., Garcia, J. & Benfatto, M. 1988. XANES in condensed systems. *Top. Curr. Chem.* **145**: 29 - 67.

Cody, G.D., Ade, H., Wirick, S., Mitchell, G.D. & Davis, A. 1998. Determination of chemical-structural changes in vitrinite accompanying luminscence alteration using C-NEXAFS analysis. *Org. Geochem.* **28**: 441-455.

Engstrom, P., Larsson, S., Rindby, A., Buttkewitz, A., Garbe, S., Gaul, G., Knochel, A. & Lechtenberg, F. 1991. A Submicron Synchrotron X-Ray-Beam Generated by Capillary Optics. *Nucl. Instrum. Meth. A*. **302**: 547-552.

Feser, M. 2002. *Scanning Transmission X-ray Microscopy with a Segmented Detector*. Doctoral dissertation, Department of Physics and Astronomy, State University New York (SUNY), Stony Brook.

Feser, M., Jacobsen, C., Rehak, P., DeGeronimo, G., Holl, P. & Strüder, L. 2001. In: *X-ray Micro- and Nano-Focusing: Applications and Techniques II* (I. McNulty ed.) Vol. 4499, Society of Photo-Optical Instrumentation Engineers (SPIE), Bellingham. p. 117-125.

Henke, B.L., Gullikson, E.M. & Davis, J.C. 1993. X-ray interactions: Photoabsorption, scattering, transmission and reflection at E=50-30'000 eV, Z=1-92. *Atomic Data and Nuclear Data Tables*. **54**: 181-342.

Henke, B.L., Lee, P., Tanaka, T.J., Shimabukuro, R.L. & Fujikawa, B.K. 1982. Low-energy X-ray interaction coefficients: Photoabsorption, scattering and reflection. *Atomic Data and Nuclear Data Tables*. **27**: 1-144.

Hitchcock, A.P., Newbury, D.C., Ishii, I., Stöhr, J., Horsley, J.A., Redwing, R.D., Johnson, A.L. & Sette, F. 1986. Carbon K-shell excitation of gaseous and condensed cyclic hydrocarbons: C_3H_6, C_4H_8, CH_8, C_5H_{10}, C_6H_{10}, C_6H_{12} and C_8H_8. *J. Chem. Phys.* **85**: 4849-4862.

Jacobsen, C. & Kirz, J. 1998. X-ray microscopy with synchrotron radiation. *Nat. Struct. Biol.* **5**: 650-653.

Jacobsen, C., Wirick, S., Flynn, G. & Zimba, C. 2000. Soft x-ray spectroscopy from image sequences with sub-100nm spatial resolution. *J. Microsc.* **197**: 173-184.

Kaznacheyev, K., Osanna, A., Jacobsen, C., Plashkevych, O., Vahtras, O., Agren, H., Carravetta, V. & Hitchcock, A.P. 2002. Innershell absorption spectroscopy of amino acids. *J. Phys. Chem. A.* **106**: 3153-3168.

Kirz, J., Jacobsen, C. & Howells, M. 1995. Soft X-Ray microscopes and their biological applications. *Q. Rev. Biophys.* **28**: 33 -130.

Lerotic, M., Jacobsen, C., Schäfer, T. & Vogt, S. 2004. Cluster analysis of soft X-ray spectromicroscopy data. *Ultramicroscopy*. **100**: 35-57.

Morra, M.J., Fendorf, S.E. & Brown, P.D. 1996. Speciation of sulphur in humic and fulvic acids using X-ray absorption near-edge structure (XANES) spectroscopy. *Geochim. Cosmochim. Acta*. **61**: 683-688.

Neuhäusler, U., Jacobsen, C., Schulze, D.G., Scott, D. & Abend, S. 2000. A specimen chamber for soft X-Ray spectromicroscopy on aqueous and liquid samples. *J. Synchrotron Radiat*. **7**: 110 -112.

Plaschke, M., Rothe, J., Denecke, M.A. & Fanghanel, T. 2004. Soft X-ray spectromicroscopy of humic acid europium(III) complexation by comparison to model substances. *J. Electron Spectrosc.* **135**: 53-62.

Scheinost, A.C., Kretzschmar, R., Christl, I. & Jacobsen, C. 2001. In: *Humic Substances: Structures, Models and Functions* (E.A. Ghabbour & G. Davies eds.) Royal Society of Chemistry, Cambridge. p. 37 -40.

Stöhr, J. 1996. *NEXAFS spectroscopy*. Springer, Berlin.

Stöhr, J., Gland, J.L., Kollin, E.B., Koestner, R.J., Johnson, A.L., Muetterties, E.L. & Sette, F. 1984. Desulfurization and structural transformation of thiophene on the Pt(111) surface. *Phys. Rev. Lett.* **53**: 2161-2164.

Teo, B.K. 1986. *EXAFS: Basic principles and data analysis*. Springer, Berlin.

Urquhart, S.G. & Ade, H. 2002. Trends in the carbonyl core (C 1s, O 1s) - π^* C=O transition in the near-edge X-ray absorption fine structure spectra of organic molecules. *J. Phys. Chem. B.* **106**: 8531-8538.

Urquhart, S.G., Ade, H., Rafailovich, M., Sokolov, J.S. & Zhang, Y. 2000. Chemical and vibronic effects in the high-resolution near-edge X-ray absorption fine structure spectra of polystyrene isotopomers. *Chem. Phys. Lett.* **322**: 412 -418.

Urquhart, S.G., Hitchcock, A.P., Smith, A.P., Ade, H., Lidy, W., Rightor, E.G. & Mitchell, G.E. 1999. NEXAFS spectromicroscopy of polymers: overview and quantitative analysis of polyurethane polymers. *J. Electron Spectrosc.* **100**: 119-135.

Wang, Y. 1998. *Three-dimensional Imaging in Soft X-ray Microscopy*. Doctoral dissertation, Department of Physics and Astronomy, State University New York (SUNY), Stony Brook.

Wang, Y. & Jacobsen, C. 1997. A numerical study of resolution and contrast in soft X-ray contact microscopy. *J. Microsc.* **191**: 159-169.

Winn, B., Ade, H., Buckley, C., Feser, M., Howells, M., Hulbert, S., Jacobsen, C., Kaznacheyev, K., Kirz, J., Osanna, A., Maser, J., McNulty, I., Miao, J., Oversluizen, T., Spector, S.J., Sullivan, B., Wang, Y., Wirick, S. & Zhang, H. 2000. Illumination for coherent soft X-Ray applications: The new X1-A beamline at the NSLS. *J. Synchrotron Radiat.* **7**: 395 -404.

Yang, M.X., Xi, M., Bent, B.E., Stevens, P. & White, J.M. 1995. NEXAFS studies of halobenzenes and phenyl groups on Cu (111). *Surf. Sci.* **341**: 9-18.

3 Can C-1s NEXAFS spectroscopy be used to quantify functional carbon groups in humic substances?

M. Schumacher, A.C. Scheinost, I. Christl, C. Jacobsen & R. Kretzschmar
Submitted for publication in the European Journal of Soil Science

Summary

Synchrotron-based C-1s near-edge X-ray absorption fine structure (NEXAFS) spectroscopy combined with scanning transmission X-ray microscopy (STXM) is increasingly used to study the C group chemistry of humic substances with spatial resolution, while information on the reliability of the C group quantification by this method is restricted. We therefore investigated 11 well characterized humic acid, fulvic acid and natural organic matter samples originating from soil, peat, coal, and freshwater, with both solid-state CP-MAS ^{13}C-NMR and C-1s NEXAFS spectroscopies. Using different deconvolution methods, the highest correlation was obtained for aromatic C (R^2 = 0.82), followed by O-alkyl (R^2 = 60), carbonyl (R^2 = 53), phenol (R^2 = 51) and carboxyl C (R^2 = 44). Alkyl-C was not predictable. While the choice of the deconvolution method had an influence on the correlations, the main error source is the detailed chemical information hidden in the NEXAFS spectra. Especially the oscillator strengths of phenolic, carboxyl and carbonyl bands, which are influenced by the specific chemical environment of these groups, counteract simple deconvolution approaches. More sophisticated deconvolution methods based on ab-initio quantum chemical approaches are required to further develop this technique as a promising and substantial investigation tool for environmental samples. In spite of their restricted predictive power, the established regression equations should be useful for the semi-quantification of specific functional groups by C-1s NEXAFS spectroscopy, because of the wide range of origin and chemical properties of the employed humic samples.

3.1 Introduction

Soil organic matter is a fundamental component in the global carbon cycle (Sparks, 1995). Soil organic matter is a heterogeneous mixture of naturally occurring compounds of plant and microbial origin in various stages of decomposition (Stevenson, 1982). These biomass residues can be transformed by degradation reactions into different groups of complex organic compounds (Oades, 1989). The chemical composition of these compounds consists of carbohydrates (10 %), lipids (10 %), nitrogen-compounds (10 %) and humic substances (70 %) (Schnitzer, 1991), but may differ considerably in varying environments. As a major portion of the total organic carbon pool in soils, humic substances (HS) play an important role in many biogeochemical and environmental processes due to their protolyzing or complexing characteristics (McCarthy & Zachara, 1989; Schlesinger, 1991). Based upon their solubility in acid and base, HS can be chemically fractionated into fulvic acids, humic acids and humins (Clapp & Hayes, 1999), containing highly variable amounts of reactive carbon functional groups. This heterogeneity within various scales has made the structural and functional characterization of HS extremely challenging. Synchrotron-based Scanning Transmission X-ray microscopy (STXM) combined with near-edge X-ray absorption fine structure (NEXAFS) spectroscopy has been shown to be a powerful method to investigate the carbon chemistry of humic substances at high spatial resolution (Myneni *et al.,* 2002; Plaschke *et al.,* 2001; Schäfer *et al.,* 2003). The application of X-ray microscopy probes the local bonding environment of carbon in the presence of water without substantial attenuation of the sample material (Jacobsen, 1999). The imaging possibilities of STXM provide further insight into the functional group chemistry of carbon-rich areas within the scale of less than one micrometer (Jacobsen *et al.,* 2000).

In the past, C-1s NEXAFS spectroscopy has been employed to study coal samples (Cody *et al.,* 1995; Cody *et al.,* 1996), humic substances (Rothe *et al.,* 2000; Scheinost *et al.,* 2001) and biopolymers (Ade & Urquhart, 2000; Kikuma & Tonner, 1996). In these studies, the carbon functional group chemistry of samples with unknown composition has been inferred from spectra of reference samples by comparing band heights and shapes. Other studies have demonstrated the potential of this technique for characterizing single colloidal particles in soils (Jokic *et al.,* 2003). While C-1s NEXAFS spectroscopy has shown its usefulness for the identification of chemical C groups and their heterogeneity on spatial scales, the method still suffers limitations in terms of the quantification of different carbon groups.

Few studies have investigated correlations between ^{13}C-NMR derived C group quantities and the areas of corresponding NEXAFS bands. Scheinost et al. (2001) investigated one fulvic acid (FA) sample and five humic acid (HA) size fractions and found R^2-values of 0.79 for aromatic C, 0.83 for phenolic C and 0.50 for carboxyl C. Schäfer et al. (2003) investigated four groundwater FA samples from organic rich clay (Gorleben, Germany), and reported R^2-values of 0.90 for aromatic C, 0.98 for phenol C, 0.99 for aliphatic C and 0.95 for carbonyl C, while no significant correlation was found for carboxyl C. Solomon et al. (2005) investigated 12 humic samples extracted from clay and silt fractions of soils, which were collected under different land uses in Ethiopia. They found R^2-values of 0.41 for aromatic C, 0.55 for phenolic C, 0.38 for carboxylic C and 0.62 for O-alkyl C. These studies show a remarkable variability of correlations for C groups, which may be explained by the different variability in C group composition and origin of the samples. The intention of our present study was therefore to investigate the correlations between ^{13}C-NMR and C-1s NEXAFS derived C group compositions using well characterized reference samples, which should be as representative as possible for a wide variety of humic samples. The information obtained should improve the quantitative interpretation of C-1s NEXAFS spectra of a broader range of specimen and establish a consistent quantification scheme for environmental samples.

3.2 Materials and methods

3.2.1 Humic samples

A total of 11 samples was selected, five humic acids (HA), four fulvic acids (FA) and two natural organic matter (NOM) samples (Table 3.1). Sample collection, extraction and purification is described by McCarthy and Malcolm (1978) for the standard samples of the International Humic Substances Society (IHSS), by Christl et al. (2000) for the two samples from Switzerland and by Vogt et al. (2001) for the Birkenes NOM sample from Norway.

Table 3.1:
Humic samples with corresponding descriptions.

Label	Description
Humic acids (HA)	
SR HA	Suwannee river humic acid, IHSS (1S101H)
Soil HA	Elliott soil humic acid, IHSS (1S102H)
Peat HA	Pahokee peat humic acid, IHSS (1S103H)
PUHA	Humic acid from a humic Gleysol in Northern Switzerland (Christl *et al.,* 2000)
Leon HA	Leonardite humic acid, IHSS (1S104H)
Fulvic acids (FA)	
SR FA	Suwannee river fulvic acid, IHSS (1S101F)
Soil FA	Elliott soil fulvic acid, IHSS (1S102F)
Peat FA	Pahokee peat fulvic acid, IHSS (1S103F)
PUFA	Fulvic acid from a humic Gleysol in Northern Switzerland (Christl *et al.,* 2000)
Natural organic matter (NOM)	
SR NOM	Suwannee river natural organic matter (SR-NOM; 1R101N)
Birk NOM	Freshwater sample from Birkenes, Norway, collected during fall 1999 (Vogt *et al.,* 2001)

3.2.2 Solid-state CP-MAS ^{13}C-NMR spectroscopy

All samples were analyzed by solid-state cross-polarization magic-angle spinning ^{13}C-nuclear magnetic resonance (CP-MAS ^{13}C-NMR) spectroscopy (Figure 3.1, Table 3.2). Although the IHSS samples have been characterized by solution-state ^{13}C-NMR and ^{1}H-NMR spectroscopy in 1989, we decided to re-analyze

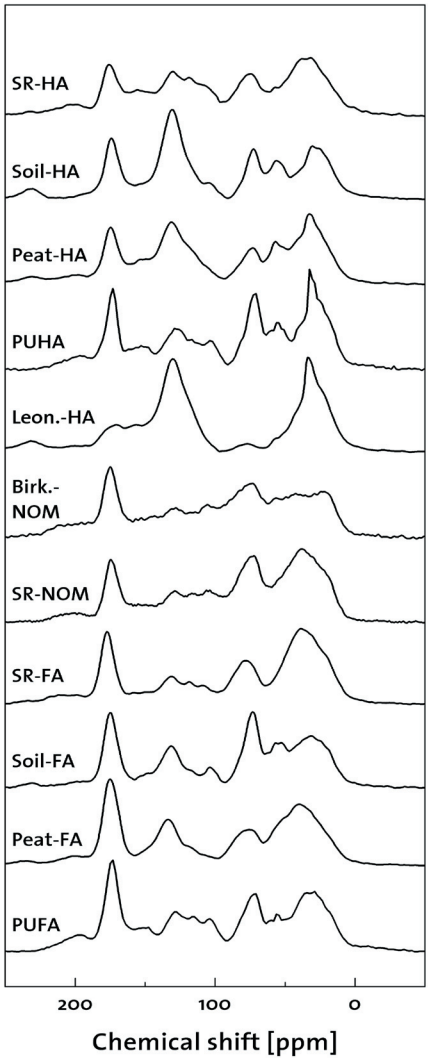

Figure 3.1:
Solid-state CP-MAS ^{13}C-NMR spectra of fulvic acid (FA), humic acid (HA), and natural organic matter (NOM) reference samples (see Table 3.1 for sample details).

all samples with solid-state ^{13}C-NMR spectroscopy. Solid-state ^{13}C-NMR spectroscopy provides a better signal-to-noise ratio as well as a higher spectral resolution, resulting in lower detection limits and spectra of higher quality (Malcolm, 1989; Peersen *et al.*, 1993). Freeze-dried samples were analyzed on a NMR spectrometer (DSX 200, Bruker, Germany) at a resonance frequency of 50.3 MHz. A magic-angle spinning speed of 6.8 kHz was used, with a contact time of 1 ms and a pulse delay of 400 ms. In order to avoid spin modulation of Hartmann-Hahn conditions, a ramped ^{1}H pulse decreasing was used (Peersen *et al.*, 1993). 18'000 to 20'000 single scans were collected for each sample. Line broadening between 50 and 150 Hz was applied prior to Fourier transformation. The chemical shift was referenced to tetramethylsilane (0 ppm) and adjusted using glycine (176.04 ppm) as an external standard. For data analysis, all spectra were divided into chemical shift regions assigned to the chemical group classes alkyl C (0-45 ppm), O-alkyl C (45-110 ppm), aromatic C (110-160 ppm), phenolic C (140-160 ppm), carboxyl C (160-185 ppm) and carbonyl C (185-220 ppm). For quantification, chemical shift regions were integrated and normalized against the integrated total area.

Further details on the investigation of soil and environmental samples by CP-MAS ^{13}C-NMR spectroscopy and their quantification are given in Kögel-Knabner et al. (1988). Comparison of the newly measured solid-state NMR data of IHSS standards with those conducted by Thorn et al. (1989) using solution-state CP-MAS ^{13}C-NMR differ by less than 10 % for all C groups, after accounting for the slightly different characteristic NMR regions used in both studies.

Table 3.2:
Relative distribution of organic C functional groups identified by solid-state CP-MAS ^{13}C-NMR spectroscopy.

Sample	Percentage distribution of carbon within indicated regions [ppm]					
	Alkyl	**O-Alkyl**	**Aromatic ***	**Phenolic**	**Carboxyl**	**Carbonyl**
	0-45	*45-110*	*110-140*	*140-160*	*160-185*	*185-220*
SR HA	26	30	17	8	14	5
Soil HA	23	26	27	7	14	3
Peat HA	27	25	22	8	14	4
PUHA	28	31	16	6	15	5
Leon. HA	34	11	31	10	10	4
Birk. NOM	23	37	11	6	15	8
SR NOM	29	39	11	5	12	4
SR FA	33	31	11	4	15	6
Soil FA	25	36	13	5	17	4
Peat FA	26	29	14	6	20	5
PUFA	24	29	17	6	18	6

** without phenolic C*

3.2.3 Collection of C-1s NEXAFS spectra

Thin films were prepared from the humic samples for C-1s NEXAFS spectroscopy as follows. 2 mg of freeze dried material was dissolved in 0.5 mL of high purity deionized water at room temperature. A 1-2 µL droplet of the solution was deposited onto a 100 nm thick Si_3N_4 window (Silson Ltd., Northampton, UK) and air-dried. The thickness of the dried film normally varied with radial distance from the centre of the droplet, allowing the selection of regions with appropriate thickness for absorption measurements in transmission mode (Figure 3.2). C-1s NEXAFS spectra were collected at the scanning transmission X-ray microscope (STXM) on beamline X-1A at the National Synchrotron Light Source (NSLS)

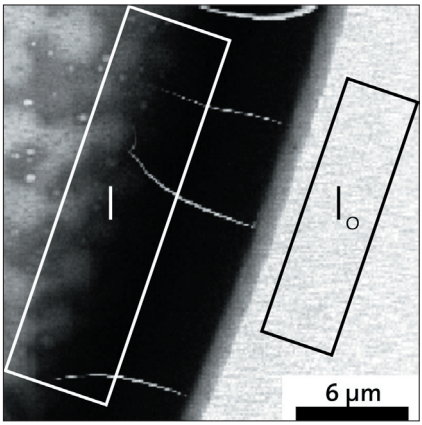

Figure 3.2:
STXM image of the sample PUFA acquired at a photon energy of 290 eV. Variable absorption is due to variations in thickness, with the outer rim of the sample corresponding to the thickest part. Cracks formed on the outer rim during drying. Sample spectra were recorded at 25 different spots within the film (I), and set to ratio against energy scans recorded at four spots outside of the film (I_o).

in Upton, N.Y.. The STXM was operated inside a He-purged enclosure at room temperature and atmospheric pressure. The monochromator was calibrated with CO_2 by assigning the C-1s→3s transition to 292.8 eV. Details on the instrument specifications have been reported elsewhere (Jacobsen *et al.,* 1991). After mounting the sample on the sample holder, the X-ray beam was focused on the sample surface by selecting the edge of a humic film and running a line scan normal to this edge at different focal distances. An image with high spatial resolution (40 nm steps) and high C contrast (energy of 290 eV) was collected by scanning the sample normal to the beam with capacitance-controlled piezo-transducers. Based on such high-resolution images (see an example in Figure 3.2), homogeneous regions with appropriate film thickness were selected for NEXAFS spectroscopy, whereas regions with airborne fibres or cracks in the film were discarded.

For the collection of C-1s NEXAFS spectra, the samples were moved out of focus by 50 µm to sample a larger film area. The photon energy was then scanned across the C-1s edge, while simultaneously maintaining the sample at the pre-selected, energy-depending focal distance. The intensity of the transmitted beam was monitored by a proportional counter. Spectra were collected at energies from 280 eV to 315 eV in energy steps of 0.1 eV with dwell times of 120 ms. Sample spectra, I(E) were collected at 25 different spots within the films. Since it is not possible due to space limitations to measure the incoming beam before the sample, reference spectra $I_o(E)$ were collected at four spots outside of the film, but through the same Si_3N_4 window as the film. Sample and reference spectra were averaged and absorption spectra were calculated using $A = \ln(I/I_o)$. In order to allow quantitative comparisons, all collected spectra were normalized by setting the pre-edge region to zero and the region from 309 to 311 eV to the value of one (Stöhr, 1996). Single absorption spectra were discarded, if the sample thickness was too thin or too thick, as evaluated by the difference in absorption between the pre-edge region (280 eV) and the region with highest absorption (either the carboxyl band at 288.5 eV or the broad post-edge maximum at around 295 eV). Spectra with absorption less than 0.3 suffered from high noise due to small signal-to-noise ratio, whereas spectra with absorption above 2 were distorted by absorption saturation, often resulting in truncated carboxyl bands.

3.2.4 Deconvolution of C-1s NEXAFS spectra

In order to compare the chemistry of the different samples quantitatively, two different least-squares fitting schemes were applied to the normalized NEXAFS spectra in the energy range of 280 to 310 eV. The first scheme based on seven Gaussians (labelled "G-7") follows the procedure suggested by Scheinost et al. (2001) except for an additional band accounting for carbonyl C. Figure 3.3 shows two examples for this fitting scheme, with seven Gaussians for electronic transitions and one arctangent function for modelling the ionization step. Five Gaussians represented the following chemical groups with mean band energies: aromatic C at 285.0 eV, phenolic C at 286.6 eV, carboxyl C at 288.5 eV, O-alkyl C at 289.5 eV and carbonyl C at 290.5 eV. The full width at half maximum (FWHM) of these bands was fixed at 1.0 eV, while the height was floating during the fit. Except for the carbonyl C band, which was fixed at 290.5 eV, all band energies could be reliably fitted without constraints. Only the spectrum of the Birkenes NOM had a clear spectral feature in the carbonyl region, in line with its relatively high carbonyl C content of 5.6 % (Table 3.4), which allowed a free fit of the cor-

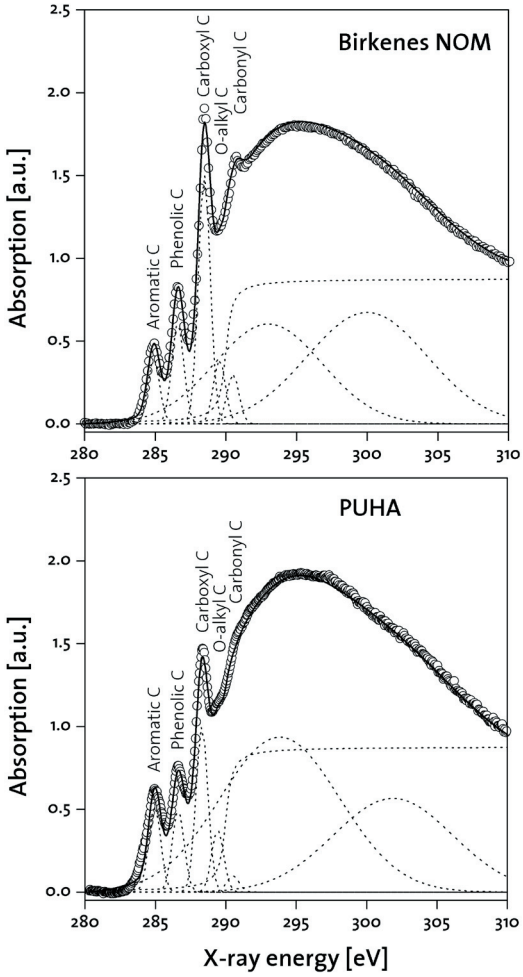

Figure 3.3:
Deconvolution of two representative C-1s NEXAFS spectra using the G-7 scheme (7 Gaussians and one arctangent).

responding band position (290.6 eV). The position of the arctangent function was fixed at 290.0 eV, with a FWHM of 1.0 eV. A value of 1 was used as initial guess of height, but then floated during the fit. Note that in the case where a number of chemically different bound carbon atoms are present, several ionization steps should be present. In practice, however, one cannot accurately simulate the intensity and positions of the continuum steps without detailed knowledge of the carbon chemistry. The simplest approach is then to use an arctangent or step-error function (Lenardi *et al.,* 1999; Stöhr, 1996). In addition to the five diagnostic bands, two broad Gaussians were used to model the sum of post-edge σ*-transitions. Their band energies varied from 293.0 to 296.3 eV and from 300.0 to 303.8 eV, respectively. No constraints were imposed on their fits. The second scheme follows a procedure suggested by Solomon et al. (2005), and includes two additional bands accounting for quinone and aliphatic C groups, which is therefore labelled "G-9" (Figure 3.4). The seven diagnostic bands were fitted with Gaussians at 284.3 eV (quinone C, fixed during fit), 285.1 eV (aromatic C), 286.5 eV (phenolic C), 287.3 eV (aliphatic C, fixed during fit), 288.5 eV (carboxyl C), 289.5 eV (O-alkyl C) and 290.5 eV (carbonyl C).

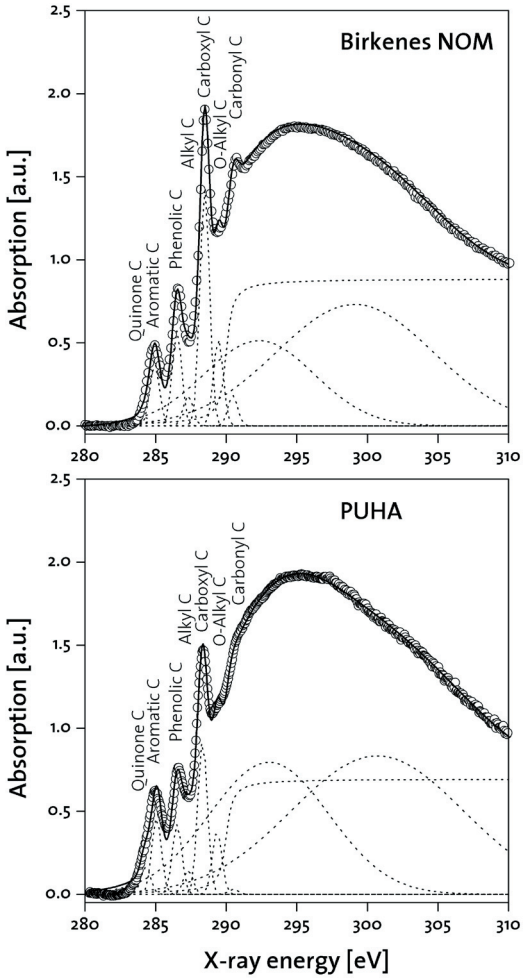

Figure 3.4:
Deconvolution of two representative C-1s NEXAFS spectra using the G-9 scheme (9 Gaussians and one arctangent).

The FWHM of these bands was fixed at 0.8 eV (Note that Solomon et al. refer to a FWHM of 0.4 eV, which is obviously only half of the FWHM as can be seen from Fig. 1 in their paper). Furthermore, band positions of aromatic, phenolic, carboxyl and O-alkyl C groups were freely fitted, which improved the fit of the edge structure. To allow for a better comparison between the two methods, the arctangent function and the two σ* Gaussians were fitted according to the G-7 scheme. This deviation from the original scheme slightly changed the absolute areas of the diagnostic bands, but did not influence tendencies of the relative band areas. Relative band areas were calculated referring to the total area of the diagnostic Gaussian line shapes, i.e. using the area of the first five bands for the G-7 scheme, and of the first seven bands for the G-9 scheme. An alternative approach, the calculation of relative band areas referred to the total area of the spectra up to 310 eV, reduced the correlations between NMR and NEXAFS groups substantially and is therefore not presented here.

3.3 Results

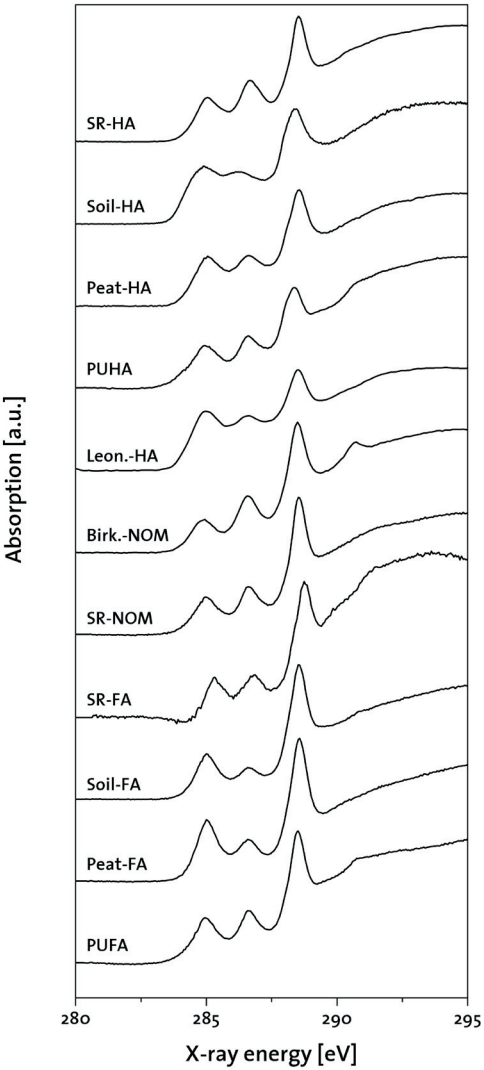

Figure 3.5:
C-1s NEXAFS spectra of fulvic acid (FA), humic acid (HA) and natural organic matter (NOM) reference samples (see Table 3.1 for sample details).

The selected reference samples represent a variety of sources of humic substances, including soil, peat, coal (Leonardite NOM), and fresh water of North America and Europe (Table 3.1). Table 3.2 shows the wide variation in carbon group composition as determined by solid-state CP-MAS ^{13}C-NMR spectroscopy: Alkyl C varies from 23 to 34 %, O-alkyl C from 11 to 39 %, aromatic C from 15 to 41 %, phenolic C from 4 to 10, carboxyl C from 10 to 20 %, and carbonyl C from 3 to 8 %. The distribution of functional groups between HA, FA and NOM follows previously observed trends (Mahieu *et al.,* 1999; Malcolm, 1989; Thorn *et al.,* 1989): HA samples have relatively high amounts of aromatic and phenolic carbon groups, whereas the FA have relatively high amounts of carboxyl and O-alkyl groups. The NOM samples are similar to FA samples, but have the highest amount of O-alkyl C of all samples.

The Leonardite HA sample derived from coal is separated from other HA samples by its very high amount of aromatic and phenolic C and the very low amount of aliphatic and O-alkyl C. A detailed chemical characterization of the Leonardite HA sample was recently reported by Olivella et al. (2002). Due to the variation of sample sources, the large variation of functional C groups, and their pattern typical for HA, FA and NOM, the samples are well suited to investigate the potential of C-1s NEXAFS for the quantification of C groups in humic samples. Figure 3.5 shows the C-1s NEXAFS spectra of the selected reference samples. All 11 spectra show the same triplet structure of three clearly resolved bands at 285.0, 286.6, and 288.5 eV, which correspond to the π^*-transitions of aromatic, phenol and carboxylic C, respectively. While band positions appear to be constant, band intensities vary considerably. The spectra of three samples, PUHA, Birkenes NOM and PUFA, have a small, but still discernible band at 290.5 eV, which can be assigned to carbonyl C. Besides this band, the σ^*-dominated post-edge regions (> 290 eV) are relatively featureless, with some variation in the slope (compare the relatively steep slope of SR-FA with the flat slope of Soil-FA).

Table 3.3:
Integrated and normalized C-1s NEXAFS band areas derived from deconvolution scheme G-7. In addition, means and standard deviations of band positions are given. Note that the positions of quinone and alkyl C bands were not fitted.

Sample	Integrated peak areas within indicated regions [eV]				
	Aromatic	**Phenolic**	**Carboxyl**	**O-Alkyl**	**Carbonyl**
	285.0 ± 0.2	*286.6 ± 0.2*	*288.5 ± 0.2*	*289.5 ± 0.2*	*290.5 ± 0.1*
SR HA	18.2	23.2	43.9	13.1	1.6
Soil HA	25.3	18.1	39.9	14.9	1.8
Peat HA	22.7	20.1	42.5	12.9	1.8
PUHA	20.8	19.9	40.2	15.1	4.0
Leon HA	36.4	23.3	36.4	3.9	0.0
Birk NOM	13.3	21.0	45.7	14.8	5.2
SR NOM	15.4	19.6	47.3	14.7	3.0
SR FA	15.3	15.4	46.7	19.2	3.3
Soil FA	18.5	12.2	52.0	15.8	1.5
Peat FA	21.9	14.8	49.7	12.3	1.3
PUFA	17.2	18.0	45.5	16.3	3.1

Table 3.4:
Integrated and normalized C-1s NEXAFS band areas derived from deconvolution scheme G-9. In addition, means and standard deviations of band positions are given. Note that the positions of quinone and alkyl C bands were not fitted.

Sample	Integrated peak areas within indicated regions [eV]						
	Quinone	Aromatic	Phenolic	Alkyl	Carboxyl	O-Alkyl	Carbonyl
	284.3 ± 0.0	*285.1 ± 0.05*	*286.5 ± 0.2*	*287.3 ± 0.0*	*288.5 ± 0.2*	*289.5 ± 0.2*	*290.5 ± 0.1*
SR HA	1.6	17.5	19.5	7.4	41.2	12.8	0.0
Soil HA	11.6	21.3	16.9	6.4	33.0	10.9	0.0
Peat HA	3.6	21.0	15.9	8.3	39.3	11.9	0.0
PUHA	6.5	18.1	16.7	5.6	36.7	14.9	1.4
Leon HA	7.9	25.2	17.7	11.4	29.5	8.3	0.0
Birk NOM	1.4	11.3	17.3	5.6	43.0	15.8	5.6
SR NOM	2.2	14.3	13.9	4.1	47.4	16.6	1.5
SR FA	0.0	17.9	13.0	0.0	50.2	18.8	0.0
Soil FA	1.3	19.6	7.9	2.1	51.8	14.6	2.5
Peat FA	1.1	24.1	11.5	2.6	48.9	10.0	1.9
PUFA	2.9	16.2	14.0	4.0	42.4	15.8	4.7

Especially in comparison with synthetic polymers (see e.g., Urquhart & Ade, 2002), the spectra appear very homogenous, which indicates similar chemical environments of carbon in all samples. The spectra are similar to NEXAFS spectra of other soil humic fractionates (Scheinost *et al.,* 2001; Solomon *et al.,* 2005), unfractionated soil samples (Jokic *et al.,* 2003), groundwater colloids (Schäfer *et al.,* 2003), Aldrich humic acid (Plaschke *et al.,* 2001; Rothe *et al.,* 2000) and the organic fraction of interplanetary dust particles (Flynn *et al.,* 2003b). A compilation of normalized NEXAFS band areas and positions determined by fit methods G-7 and G-9 is given in Tables 3.3 and 3.4, respectively. Both fits confirm the visual observation of the small variations in band positions within C groups, and achieve identical (within the error of analysis) mean band positions of the C groups. Furthermore, both methods attain similar ranges of band areas within C groups. The band areas of the two additional bands, representing quinone and alkyl C, are comparably small and therefore do not strongly influence the band areas of neighboring bands.

Table 3.5 compiles the results of the regression analysis between C-1s NEXAFS and ^{13}C-NMR band areas for both fit methods. Note that areas of the NEXAFS aromatic band were regressed against the NMR areas 110-140 ppm, i.e. excluding the phenol regions 140-160 ppm, and NEXAFS areas of quinone and aromatic C were combined (G-9). Independent of the fit method, the highest correlation is observed for aromatic C, followed by O-alkyl, carbonyl, phenolic and carboxyl carbon with R^2-values decreasing in this order. The lowest correlation was observed for alkyl C (only G-9). Accounting for the two additional quinone and alkyl bands (G-9) decreased the correlations of all C groups in comparison to the simpler G-7 approach. The observed correlation coefficients are similar to the ones observed for size fractions of sample PUHA with a similar variation of C group composition (except for aromatic C, where it was smaller) (Scheinost *et al.,* 2001) and similar to the coefficients reported for humic substances extracted from Ethiopian soils (Solomon *et al.,* 2005).

Table 3.5:
Correlations between C-1s NEXAFS band areas and percent C in the corresponding functional groups (derived from ^{13}C-NMR). Results for deconvolution scheme G-7 are shown on top, those for G-9 at the bottom. Regressions are calculated with NEXAFS areas as dependent variable and ^{13}C-NMR areas as independent variable. Slopes and intercepts are given with standard deviations.

Groups G-7	**R^2**	**Intercept**	**Slope**
Aromatic C	0.82	6 ± 2	0.9 ± 0.1
Phenolic C	0.51	9 ± 3	1.5 ± 0.5
Carboxyl C	0.44	28 ± 6	1.1 ± 0.4
O-Alkyl C	0.60	2 ± 3	0.4 ± 0.1
Carbonyl C	0.53	-1 ± 1	0.8 ± 0.2
Groups G-9	**R^2**	**Intercept**	**Slope**
Aromatic & Quinone C	0.77	8 ± 3	0.8 ± 0.2
Phenolic C	0.41	7 ± 3	1.2 ± 0.5
Aliphatic C	0.02	2 ± 8	0.1 ± 0.3
Carboxyl C	0.34	19 ± 11	1.5 ± 0.7
O-Alkyl C	0.55	4 ± 3	0.3 ± 0.1
Carbonyl C	0.49	-3 ± 2	1.0 ± 0.3

The correlation coefficients are, however, much smaller than the values reported for aromatic (R^2 = 0.90), phenol (R^2 = 0.98), alkyl (R^2 = 0.99) and carbonyl (R^2 = 0.95) C of four groundwater fulvic acids (Schäfer *et al.,* 2003). Due to a very small variation of carboxyl C, however, no significant correlation was found by Schäfer et al. for these samples.

In Figure 3.6, the normalized NEXAFS band areas of fit method G-7 are plotted against the normalized NMR band areas. Only for aromatic and for carbonyl C, both NMR and NEXAFS result in similar band areas, as can be seen from the summarizing plot in the lower right corner of Figure 3.6, where the data points of these two groups scatter around the 1:1 line. NEXAFS band areas for O-alkyl are always smaller in comparison to NMR, and those of phenol and carbonyl C are always larger. This observation is in line with the NEXAFS study on colloids extracted from Gorleben, Germany (Schäfer *et al.,* 2003). The extreme C group composition of the Leonardite HA sample improves the correlations for aromatic, carboxyl and O-alkyl C.

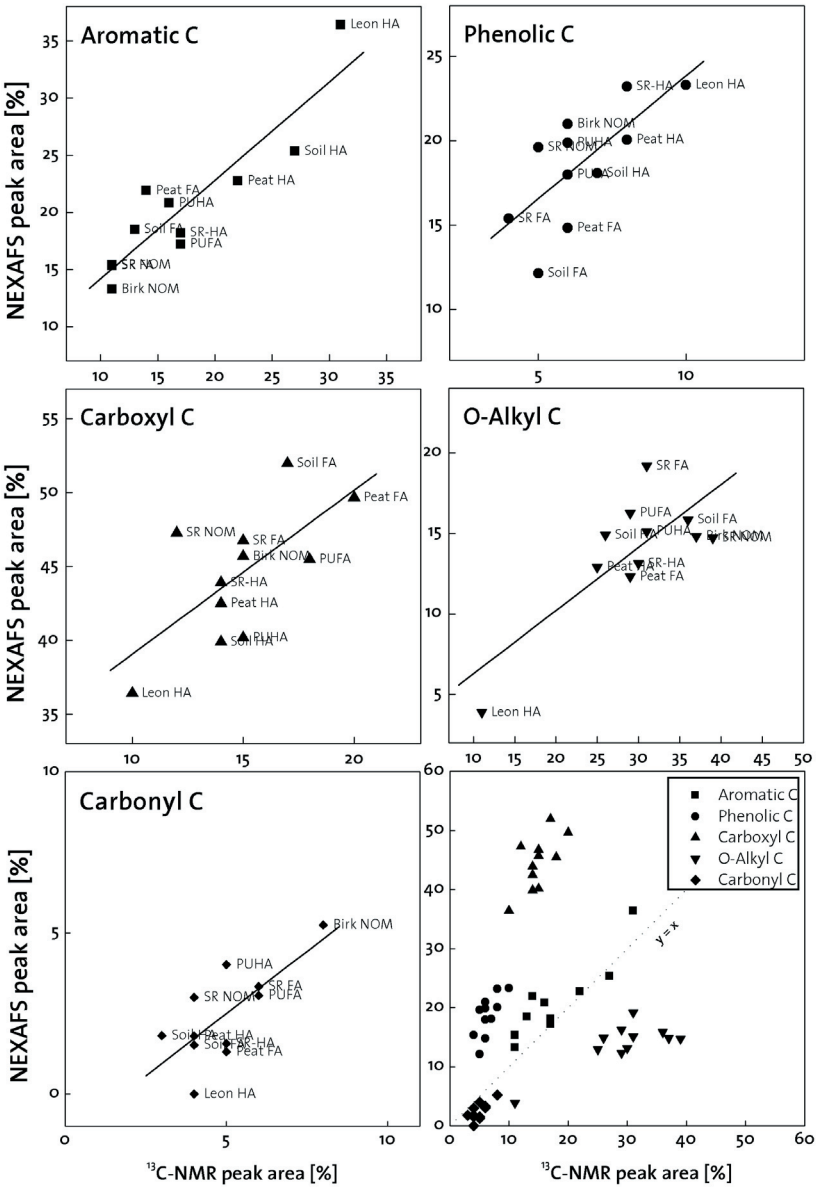

Figure 3.6:
Correlation plots between normalized ^{13}C-NMR and C-1s NEXAFS peak areas. NEXAFS peaks were fitted according to the G-7 scheme.

3.4 Discussion

The large range of correlations, from R^2 of 0.82 for aromatic C to 0.02 for alkyl C, may have several reasons: (i) misinterpretation of the observed band structure, and consequently accounting for too many or not enough bands during the fit, and a possible wrong assignment of the bands to chemical groups, hence a general failure of the building block approach; (ii) fit problems related to poorly resolved, overlapping bands and consequently an over-parameterization of the non-linear fit model; (iii) limitation of the building block approach with regard to the quantification of C groups; (iv) a failure of CP-MAS ^{13}C-NMR spectroscopy employed as reference method for the quantification of C groups. These possible causes will be discussed in the following.

3.4.1 Building block approach for qualitative analysis

The building block has shown its validity for the qualitative interpretation of NEXAFS spectra during more than two decades (Stöhr, 1996). It has been applied to a large variety of synthetic and natural organic samples in the last decade, and peak assignments seem to be reliable (Cody *et al.,* 1995; Hitchcock & Mancini, 1994; Plaschke *et al.,* 2004; Scheinost *et al.,* 2001; Urquhart & Ade, 2002). The peak near 285 eV is unequivocally assigned to double carbon-carbon bonds without hetero-atoms as nearest neighbors (Stöhr, 1996). This well pronounced peak is followed by a transition taking place at an energy of 286.5 eV and is related to permitted transitions C(1s)→π*, induced by the presence of oxygen or other electron withdrawing substituents. This spectral feature is assigned to resonances of the aromatic carbon bonded to oxygen, as in the case of phenol or aryl ether (Ishii & Hitchcock, 1988; Thieme *et al.,* 2000). The third peak at 288.5 eV can be assigned to the second C(1s)→π* transition, also referred to as a C(1s)→2π* transition, present in carboxyl carbon (Urquhart *et al.,* 1999). Note that the ~3 eV increase in energy in the respective transition is due to the electron withdrawing nature of oxygen. A feature present, but in this array of samples not readily observable except (for Birkenes NOM), is the transition taking place around 290.5 eV. This peak is assigned to the C(1s)→π* transition, present in carbonyl carbon (Urquhart & Ade, 2002). These peak positions have been confirmed for humic substances and relevant reference phases by Scheinost et al. (2001) and Plaschke et al. (2004). In conclusion, a failure of the building block approach for qualitative interpretation of spectra seems to be very unlikely.

3.4.2 Model over-parameterization

In spite of the obvious consensus on the interpretation of spectra, fitting models applied to the spectra of organic matter of similar composition vary with regard to the number of bands fitted and in other fitting details (Jokic *et al.,* 2003; Schäfer *et al.,* 2003; Scheinost *et al.,* 2001; Solomon *et al.,* 2005). The two fitting approaches used in this work demonstrated that fit results critically depend on the choice of initial parameters as well as on constraints imposed during the fit. This problem further increased when the number of Gaussian bands was increased from seven to nine (models G-7 and G-9) and had to be counteracted by a rising number of fixed parameters. The fit of the spectra was not significantly improved by adding more bands, while the correlations between NEXAFS and NMR data decreased. Hence, over-parameterization of the fit models is a severe problem for the reliable determination of band areas. However, if such fit problems would be solely responsible for the variation of correlations, one would expect correlations for the well resolved bands of aromatic, phenolic and carboxyl C to be closer than those of the unresolved bands for O-alkyl and carbonyl. Since this tendency was not observed, an additional factor must be responsible for the variation of correlations.

3.4.3 Building block approach for quantitative analysis

While the influence of structural variations on band positions of smaller chemical molecules and synthetic polymers has been extensively investigated by Hitchcock and co-workers (Hitchcock & Mancini, 1994) and more recently by Kaznacheyev et al. (2002), systematic investigations on structures relevant for humic matter are scarce. Nevertheless, some conclusions on the correlations of specific groups can be drawn. The intensity of the aromatic band intensity increases with increasing number of unsubstituted C atoms in the ring, and is reduced by an increasing number of substituted C atoms (Plaschke *et al.,* 2004). Furthermore, little variation of the aromatic band position has been observed for model compounds (Plaschke *et al.,* 2004; Scheinost *et al.,* 2001). Both features, the linear dependence of band area on aromatic unsubstituted C groups as well as the invariance of band width and position, explain the high correlation between NEXAFS and NMR data ($R^2 = 0.82$). In contrast, the correlation is much smaller for phenolic C groups ($R^2 = 0.51$). This can be explained with the observation that an increasing number of phenolic groups does not lead to an increase of the phenol band intensity, but to a pronounced splitting of the phenol band at 286.5 eV. For instance, an increase of OH-substitution causes a pronounced splitting

and shift towards higher energies of the phenol band (Plaschke *et al.,* 2004). Hence the relatively small correlation between NEXAFS and NMR data for this specific C group may be due to this behavior, suggesting a substantial variation in the local structure of phenolic C groups in humic substances. However, only the NEXAFS spectrum of Soil HA shows a significant shift of the phenol band to lower energy, while its position in spectra of other samples remains very much constant.

Similarly, the carboxyl band shifts to higher energy when the number of neighboring carboxyl groups on an aromatic ring increases (Plaschke *et al.,* 2004). A carboxyl band position of 288.5 eV is in line with corresponding spectral features of phtalic acid, while benzoic acid shows a lower band energy. Hence the observed band position of 288.5 eV indicates that in humic substances carboxyl structures similar to phtalic acid prevail, i.e. structures with two carboxyl groups in neighboring (para) positions. Such band shifts influence the oscillator strength of the carboxyl band and may therefore be responsible for the relatively poor correlation (R^2 = 0.44) between NEXAFS and NMR data Urquhart et al. (2002) observed a large shift of the carbonyl band position from 286.5 eV to ~290.5 eV in C-1s NEXAFS spectra of synthetic polymers. Since the corresponding band was poorly resolved for all humic samples except for Birkenes NOM (Figures 3.3, 3.4 and 3.5), its position could not be freely fitted, but had to be fixed at 290.5 eV. Consequently, the poor correlation for this group may be attributed to the fixed and possibly wrong position, but also to the relatively small content (< 10 %) in the samples.

The O-alkyl band could be freely fitted since it is squeezed in between the strong carboxyl band and the arctangent function modelling the ionization step at 290 eV (Figures 3.3 and 3.4). However, the band position is not resolved and may be biased. Moreover, due to the mixed-valence/Rydberg-like character of this band, its oscillator strength is weak in comparison to that of other bands (Figure 3.6). Nevertheless, the correlation between NEXAFS and NMR data is relatively close (R^2 = 0.60), mostly because of the significant O-alkyl group variation introduced by the Leonardite HA sample. A similar correlation has been found by Solomon et al. (2005), confirming the good predictability of this group. Alkyl bands were fitted with the G-9 method. The band position had to be kept fixed during the fit due to its unresolved position between the phenol and the carboxyl bands. Its inclusion in the deconvolution did not improve the fit of the spectra and decreased the NMR/NEXAFS correlations for other C groups.

In analogy to the O-alkyl band, its band area was much smaller than expected from the NMR results, confirming the weak oscillator strength of mixed-valence/Rydberg transitions. Consequently, no statistically meaningful correlation between the NMR and NEXAFS data was found, in line with the findings of Solomon et al. (2005), but contradictory to the findings of Schäfer et al. (2003).

3.4.4 Reliability of reference NMR method

Finally, it is likely that the quantification of C groups by CP-MAS ^{13}C-NMR is responsible for parts of the data scattering. The use of cross-polarization magic angle spinning (CP-MAS) ^{13}C-NMR spectroscopy has greatly increased in the past decade and the technique has become a standard tool for the structural investigation of NOM and humic substances (Cody & Saghi-Szabo, 1999). A wide variety of researchers applied ^{13}C-NMR spectroscopy for the determination of the various carbon functional groups present in environmental samples (Christl *et al.,* 2000; Kögel-Knabner, 2002; Spielvogel *et al.,* 2004). However, several possible problems of quantitative NMR spectroscopy of humic substances have been described (Malcolm, 1989; Mao *et al.,* 2000; Peersen *et al.,* 1993). Mao et al. (2000) stated that CP-MAS ^{13}C-NMR spectroscopy techniques overestimate sp^3-hybridized carbon in alkyl and O-alkyl groups and underestimate sp^2-hybridized carbon in aromatic, carboxyl and carbonyl functional groups. Furthermore, the number of structural subunits and the chemical shift regions of each subunit may vary widely from one study to another. Conclusions regarding the quantitative interpretation of NMR data of NOM samples have therefore to be drawn with caution. On the other hand, functional groups determined by CP-MAS ^{13}C-NMR spectroscopy have been found to be in close agreement with those determined by independent methods (Christl & Kretzschmar, 2001; Christl *et al.,* 2001). Hence, it seems to be unlikely that the poor correlations for some of the C groups are strongly influenced by the employed reference method.

3.5 Conclusions

Our results demonstrate that for a wide range of humic matter, a relatively simple deconvolution scheme of C-1s NEXAFS spectra only allows to predict the content of aromatic C with satisfying reliability (R^2 = 0.82). For O-alkyl (R^2 = 60), carbonyl (R^2 = 53), phenol (R^2 = 51) and carboxyl C (R^2 = 44), statistically significant correlations between ^{13}C-NMR and C-1s NEXAFS were observed. It has to be assumed that the sensitivity and reliability of NMR for the quantification of functional C group is much higher. While general fitting problems, the choice of the deconvolution model and some noise in the reference data may be responsible for part of the poor correlations, the main error source is the detailed chemical information that is hidden in the NEXAFS spectra and counteracts simple deconvolution methods. Hence, more sophisticated fitting approaches based on ab-initio quantum chemical approaches are needed to improve the quantification of C groups. Nevertheless, because of the wide chemical range of humic reference samples used in our study, the regression equations obtained in this study should be useful for the semi-quantification of specific functional groups obtained by C-1s NEXAFS spectroscopy. This is especially true for those cases, where NEXAFS due to its combination with sub-micron spatial resolution scanning transmission X-ray microscopy is the method of choice (Flynn *et al.,* 2003a; Myneni *et al.,* 2002; Plaschke *et al.,* 2001; Rothe *et al.,* 2000; Schäfer *et al.,* 2003; Schumacher *et al.,* 2005). However, a further development of the data evaluation method is required to further develop this technique as a promising and substantial investigation tool for environmental samples.

Acknowledgements

This project has been financially supported by the Swiss Federal Institute of Technology Zurich (Grant No. 01753). All NEXAFS analyses were performed at beamline X-1A at the National Synchrotron Light Source at the Brookhaven National Laboratory in Upton, N.Y., which is supported by the Department of Energy. Operation of the Stony Brook STXM is supported by National Science Foundation grants CHE-0221934 and OCE-0221029. The NMR analyses were kindly performed by Dr. H. Knicker at the Technical University Munich. Furthermore, the authors would like to gratefully acknowledge S. Wirick of the Department of Physics, SUNY Stony Brook and K. Barmettler from ETH Zurich for their contribution and support to this work.

Literature cited

Ade, H. & Urquhart, S.G. 2000. In: *Chemical Applications of Synchrotron Radiation* (T.K. Sham ed.) World Scientific Publishing Co. Ltd., Singapore.

Christl, I., Knicker, H., Kögel-Knabner, I. & Kretzschmar, R. 2000. Chemical heterogeneity of humic substances: Characterization of size fractions obtained by hollow-fibre ultrafiltration. *Eur. J. Soil Sci.* **51**: 617-625.

Christl, I. & Kretzschmar, R. 2001. Relating ion binding by fulvic and humic acids to chemical composition and molecular size. I. Proton binding. *Environ. Sci. Technol.* **35**: 2505 -2511.

Christl, I., Milne, C.J., Kinniburgh, D.G. & Kretzschmar, R. 2001. Relating ion binding by fulvic and humic acids to chemical composition and molecular size. II. Metal binding. *Environ. Sci. Technol.* **35**: 2512 -2517.

Clapp, C.E. & Hayes, M.B.H. 1999. Sizes and shapes of humic substances. *Soil Sci.* **164**: 777-789.

Cody, G.D., Botto, R.E., Ade, H., Behal, S., Disko, M. & Wirick, S. 1995. Inner-shell spectroscopy and imaging of a subbituminous coal: In-situ analysis of organic and inorganic microstructure using C(1s)-, Ca(2p)-, and Cl(2s)-NEXAFS. *Energ. Fuel.* **9**: 525-533.

Cody, G.D., Botto, R.E., Ade, H. & Wirick, S. 1996. The application of soft X-ray microscopy to the in-situ analysis of sporinite in coal. *Int. J. Coal Geol.* **32**: 69-86.

Cody, G.D. & Saghi-Szabo, G. 1999. Calculation of the ^{13}C NMR chemical shift of ether linkages in lignin derived geopolymers: Constraints on the preservation of lignin primary structure with diagenesis. *Geochim. Cosmochim. Acta*. **63**: 193-205.

Flynn, G., Keller, L.P., Feser, M., Wirick, S. & Jacobsen, C. 2003a. The origin of organic matter in the solar system: Evidence from the interplanetary dust particles. *Geochim. Cosmochim. Acta*. **67**: 4791-4806.

Flynn, G., Keller, L.P., Wirick, S., Jacobsen, C. & Sutton, S.R. 2003b. Analysis of interplanetary dust particles by soft and hard X-ray microscopy. *J. Phys. IV*. **104**: 367-372.

Hitchcock, A.P. & Mancini, D.C. 1994. Bibliography and database of inner-shell excitation-spectra of gas-phase atoms and molecules. *Journal of Electron Spectroscopy and Related Phenomena*. **67**: 1-132.

Ishii, I. & Hitchcock, A.P. 1988. The oscillator strengths for C1s and O1s excitation of some saturated and unsaturated organic alcohols, acids and esters. *J. Electron Spectrosc.* **46**: 55-84.

Jacobsen, C. 1999. Soft x-ray microscopy. *Trends in Cell Ciology*. **9**: 44-47.

Jacobsen, C., Williams, S., Anderson, E., Browne, M.T., Buckley, C., Kern, D., Kirz, J., M., R. & Zhang, X. 1991. Diffraction-limited imaging in a scanning transmission x-ray microscope. *Opt. Commun.* **86**: 351-364.

Jacobsen, C., Wirick, S., Flynn, G. & Zimba, C. 2000. Soft x-ray spectroscopy from image sequences with sub-100nm spatial resolution. *J. Microsc.* **197**: 173-184.

Jokic, A., Cutler, J.N., Ponomarenko, E., van der Kamp, G. & Anderson, D.W. 2003. Organic carbon and sulphur compounds in wetland soils: Insights on structure and transformation processes using K-edge XANES and NMR spectroscopy. *Geochim. Cosmochim. Acta*. **67**: 2585-2597.

Kaznacheyev, K., Osanna, A., Jacobsen, C., Plashkevych, O., Vahtras, O., Agren, H., Carravetta, V. & Hitchcock, A.P. 2002. Innershell absorption spectroscopy of amino acids. *J. Phys. Chem. A*. **106**: 3153-3168.

Kikuma, J. & Tonner, B.P. 1996. XANES spectra of a variety of widely used organic polymers at the C K-edge. *J. Electron Spectrosc.* **82**: 53-60.

Kögel-Knabner, I. 2002. The macromolecular organic composition of plant and microbial residues as inputs to soil organic matter. *Soil Biol. Biochem.* **34**: 139-162.

Kögel-Knabner, I., Zech, W. & Hatcher, P. 1988. Chemical composition of the organic matter in forest soils: The humus layer. *Z. Pflanzenern. Bodenkunde*. **151**: 331-340.

Lenardi, C., Piseri, P., Briois, V., Bottani, C.E., Li Bassi, A. & Milani, P. 1999. Near-edge x-ray absorption fine structure and Raman characterization of amorphous and nanostructured carbon films. *J. Appl. Phys. A*. **85**: 7159-7167.

Mahieu, N., Powlson, D.S. & Randall, E.W. 1999. Statistical analysis of published carbon-13 CP-MAS NMR spectra of soil organic matter. *Soil Sci. Soc. Am. J.* **63**: 307-319.

Malcolm, R.L. 1989. In: *Humic Substances II: In Search of Structure* (M.B.H. Hayes, P. McCarthy *et al.* eds.) John Wiley & Sons, New York. p. 339-372.

Mao, J.-D., Hu, W.-G., Schmidt-Rohr, K., Davies, G., Ghabbour, E.A. & Xing, B. 2000. Quantitative characterization of humic substances by solid-state carbon-13 nuclear magnetic resonance. *Soil Sci. Soc. Am. J.* **64**: 873-884.

McCarthy, J.F. & Zachara, J.M. 1989. Subsurface transport of contaminants. *Environ. Sci. Technol.* **23**: 496-502.

McCarthy, P. & Malcolm, R.L. 1978. *The need to establish a reference collection of humic substances*. In: 9th Materials Research Symposium, National Bureau of Standards, Gaithersburg.

Myneni, S.C.B., Warwick, T., Martinez, G.A. & Meigs, G. 2002. *C-Functional group chemistry of humic substances and their spatial variation in soils*.

Oades, J.M. 1989. In: *Minerals in Soil Environments* (J.B. Dixon & S.B. Weed eds.) Soil Science Society of America, Madison. p. 89-159.

Olivella, M.A., del Rio, J.C., Palacios, J., Vairavamurthy, M.A. & de las Heras, F.X.C. 2002. Characterization of humic acid from leonardite coal: an integrated study of PY-GC-MS, XPS and XANES techniques. *J. Anal. Appl. Pyrol.* **63**: 59-68.

Peersen, O.B., Wu, X., Kustanovich, I. & Smith, S.O. 1993. Variable-amplitude cross-polarization MAS-NMR. *J. Magn. Reson. Ser. A*. **104**: 334-339.

Plaschke, M., Rothe, J., Denecke, M.A. & Fanghanel, T. 2004. Soft X-ray spectromicroscopy of humic acid europium(III) complexation by comparison to model substances. *J. Electron Spectrosc.* **135**: 53-62.

Plaschke, M., Rothe, J., Schäfer, T., Denecke, M.A., Dardenne, K., Pompe, S. & Heise, K.H. 2001. Combined AFM and STXM in situ study of the influence of Eu(III) on the agglomeration of humic acid. *Colloid Surface A*. **197**: 245 -256.

Rothe, J., Denecke, M.A. & Dardenne, K. 2000. Soft X-Ray spectromicroscopy investigation of the interaction of aquatic humic acid and clay colloids. *J. Colloid Interf. Sci.* **231**: 91 -97.

Schäfer, T., Hertkorn, N., Artinger, R., Claret, F. & Bauer, A. 2003. Functional group analysis of natural organic colloids and clay association kinetics using C(1s) spectromicroscopy. *J. Phys. IV*. **104**: 409-412.

Scheinost, A.C., Kretzschmar, R., Christl, I. & Jacobsen, C. 2001. In: *Humic Substances: Structures, Models and Functions* (E.A. Ghabbour & G. Davies eds.) Royal Society of Chemistry, Cambridge. p. 37 -40.

Schlesinger, W.H. 1991. *Biogeochemistry: An analysis of global change*. Academic press, San Diego.

Schnitzer, M. 1991. Soil organic matter: The next 75 years. *Soil Sci.* **151**: 41-58.

Schumacher, M., Christl, I., Scheinost, A.C., Jacobsen, C. & Kretzschmar, R. 2005. Heterogeneity of water-dispersible soil colloids investigated by Scanning Transmission X-ray Microscopy and C-1s XANES micro-spectroscopy. *Environmental Science & Technology*. in review.

Solomon, D., Lehmann, J., Kinyangi, J., Liang, B. & Schäfer, T. 2005. Carbon K-edge NEXAFS and FTIR-ATR spectroscopic investigation of organic carbon speciation in soils. *Soil Sci. Soc. Am. J.* **69**: 107-119.

Sparks, D.L. 1995. *Environmental Soil Chemistry*. Academic press, San Diego.

Spielvogel, S., Knicker, H. & Kögel-Knabner, I. 2004. Soil organic matter composition and soil lightness. *J. Plant Nutr. Soil Sci.* **167**: 545-555.

Stevenson, F.J. 1982. *Humus chemistry: Genesis, Composition, Reactions*. John Wiley & Sons, New York.

Stöhr, J. 1996. *NEXAFS spectroscopy*. Springer, Berlin.

Thieme, J., Schmidt, C., Abbt-Braun, G., Specht, C. & Frimmel, F.H. 2000. In: *Refractory Organic Substances in the Environment* (F.H. Frimmel & G. Abbt-Braun eds.) John Wiley & Sons, New York.

Thorn, K.A., Folan, D.W. & McCarthy, P. 1989. *Characterization of the International Humic Substances Society Standard and Reference Fulvic and Humic Acids by Solution State Carbon-13 (^{13}C) and Hydrogen-1 (^{1}H) Nuclear Magnetic Resonance Spectrometry*, Water-Ressources Investigations Report. USGS, Denver.

Urquhart, S.G. & Ade, H. 2002. Trends in the carbonyl core (C 1s, O 1s) - π^* C=O transition in the near-edge X-ray absorption fine structure spectra of organic molecules. *J. Phys. Chem. B.* **106**: 8531-8538.

Urquhart, S.G., Hitchcock, A.P., Smith, A.P., Ade, H., Lidy, W., Rightor, E.G. & Mitchell, G.E. 1999. NEXAFS spectromicroscopy of polymers: overview and quantitative analysis of polyurethane polymers. *J. Electron Spectrosc.* **100**: 119-135.

Vogt, R.D., Gjessing, E., Andersen, D.O., Clarke, N., Gadmar, T., Bishop, K., Lundström, U. & Starr, M. 2001. *Natural Organic Matter in the Nordic countries*, NT Technical report. NORDTEST, Espoo.

4 Seasonal variation of the chemical composition of aquatic dissolved organic matter in boreal forest catchments

M. Schumacher, I. Christl, K. Barmettler, C. Jacobsen & R. Kretzschmar
Submitted for publication in Biogeochemistry

Summary

Ten samples of aquatic dissolved organic matter (DOM) derived from five boreal forest catchments in Scandinavia were investigated by elemental analysis, FT-IR, solid-state CP-MAS ^{13}C-NMR and C-1s NEXAFS spectroscopy. The samples were extracted by reverse osmosis during the spring and fall seasons and analyzed with regard to seasonal variations in the elemental composition and the carbon functional group distribution. All analyses revealed that the samples did not exhibit significant seasonal differences. The differences observed for three FT-IR spectra were shown to be due to contributions of inorganic compounds such as sulphates and silicates rather than due to differences in the organic structures. The results from solid-state ^{13}C-NMR and C-1s NEXAFS spectroscopy indicated that the all DOM samples were highly hydrophilic materials, which are rich in O-alkyl carbon, but poor in aromatic and phenolic carbon. The differences between DOM samples from different catchments were remarkably small. Radiocarbon dating of the samples resulted in an average ^{14}C-age of $\leq$ 50 years before present time for the total sample set, suggesting that the DOM samples rather consisted of recent organic matter than of refractory organic compounds. Therefore, we conclude that the freshwater DOM mainly represents fresh litter material which is chemically altered to organic matter of a relatively uniform chemical composition.

4.1 Introduction

Natural organic matter (NOM) occurs in nearly all aquatic environments including lakes, rivers, oceans, soil water and groundwater (Schnitzer, 1991). In rivers and lakes, NOM is mainly present as dissolved organic matter (DOM), but it can also be associated with colloidal particles. Because of practical reasons, DOM is usually defined as the NOM fraction which passed through as 0.45 µm filter. Average concentrations of DOM, expressed as dissolved organic carbon (DOC), range from about 0.1 mg L^{-1} in groundwater to 33 mg L^{-1} in peat bogs (Perdue & Ritchie, 2003). Transport of NOM in rivers is an important flux component within the global carbon cycle. Furthermore, it plays an important role in the biogeochemical cycling and bioavailability of metals (e.g., Al, Fe, Cu), which can form stable complexes with organic functional groups of NOM (Buffle *et al.,* 1987; Tipping *et al.,* 2002). The composition of DOM in freshwater environments has been studied thoroughly and has recently been reviewed by Perdue and Ritchie (2003). On average, freshwater DOM has an elemental mass composition of 49.5 ± 3.3 % C, 5.0 ± 1.0 % H, 43.0 ± 4.1 % O, 1.7 ± 1.0 % N, and 2.0 ± 1.3 % S. The reported average molecular weight varies considerably, with typical values ranging from less than 1 kDa to more than 100 kDa (Leenheer & Croue, 2003). This large range in reported molecular weights may partly be explained by the use of different techniques applied for size measurements. Using size exclusion chromatography, Perdue and Ritchie (2003) report a median value of 1.7 kDa for the weight-averaged molecular weight of 37 DOM samples. On average, more than 80 % of aquatic DOM can be isolated by resins either as hydrophobic or hydrophilic acid fractions, which are often present in a ratio of about 2:1 (Perdue & Ritchie, 2003). The hydrophobic acid fraction typically consists of fulvic acids and smaller amounts of humic acids. Less than 20 % of DOM consists of hydrophilic bases and neutral compounds. Amounts of identifiable biomolecules of terrestrial or aquatic origin, such as amino acids (~1.8 %), sugars (~3.0 %) and lignin-derived phenols (~0.6 %) are typically small (Perdue & Ritchie, 2003).
Surface waters in the subarctic and cold continental climatic zones in the northern hemisphere are often particularly rich in DOM. Under boreal forest and bog vegetation, the soil cover is often dominated by Podzols and Histosols, respectively. Acidic pH values and low Ca and Mg concentrations (soft water) in these soils along with high precipitation and low temperatures favor leaching of DOM into the rivers (Lobbes *et al.,* 2000; van Hees, 1998). The aquatic NOM in these oligothrophic rivers seems to be of terrestrial origin rather than aquatic phyto-

plankton (Hedges & Oades, 1997). Thus, riverine NOM may reflect the properties of the surrounding soils as well as the vegetation and climate of the region (Lydersen, 1995). On seasonal variation of riverine DOM in boreal catchments, only few studies can be found in the literature. Gjessing et al. (1999) speculated that increased precipitation during summer season may accelerate the elution of DOM, compared to the winter season. Moran & Zepp (1997) showed that exposure to solar radiation plays an important role in the degradation of DOM in lakes, increasing its bioavailability significantly. Consequently, decreased retention times in lake waters cause decreased photochemical reactions and will therefore lead to enhanced color and DOM concentrations (Tranvik, 2003). Skjelvåle et al. (2001) and Hongve et al. (2004) reported that fluctuations in the amount and intensity of precipitation are the main reason for the observed changes in surface water chemistry as well as DOM concentrations in Scandinavia. Heikkinen (1994) reported seasonal differences of DOM extracted from a boreal river drainage basin in the ability to bind iron, which result from changes in temperature-dependent microbiological processes. The author further stated the importance of these processes during the summer season due to active microbial breakdown of plant litter and intensive growth of Sphagnum as a primary source of DOM. Kaiser et al. (2001) studied changes in the chemical composition of DOM in forest floor layer leachates and found ^{13}C-NMR results to exhibit seasonal variations for alkyl, O-alkyl and aromatic carbon. They examined DOM samples from seepage waters from beech and pine forests over a 27-month period. According to liquid-state ^{13}C-NMR spectroscopy, the summer samples had larger abundances of aromatic and aliphatic structures as well as higher proportions of carboxyl groups, whereas the winter and spring samples were dominated by resonances indicating carbohydrates. The trends in temporal variations were found to be remarkably similar for both sites. These results were explained by the fact that the winter samples were mainly controlled by leaching of fresh biomass debris with large contributions of bacterial and fungal-derived carbohydrates, whereas the summer samples were controlled by decomposition processes in the forest floor. These studies are in contrast to findings of Solinger et al. (2001), who investigated the dynamics of DOM in forest soils in central Europe. They showed that concentrations of DOM in the forest floor and mineral soil exhibited no seasonal variability. Moreover, Yano et al. (2004) speculated that the influence of seasonal variability of DOM decreased with soil depth, resulting in the generation of soil water DOM of uniform composition, which is not affected by seasonal changes.

These findings are consistent with results published by Porcal et al. (2004), who found that the chemical composition of NOM did not differ significantly between acidified surface and subsurface tributaries in Eastern Europe, although DOC concentrations varied considerably between summer and winter. Despite the somewhat contradictory findings in the studies regarding seasonal variability of DOM composition, it is fair to state that possible annual fluctuations in the carbon chemistry of DOM is likely to have an important influence on a range of issues as, e.g., trace metal speciation, the removal of DOM during water treatment (Gjessing *et al.,* 1999), and the biological activity in boreal aquatic environments, as reported by Heikkinen et al. (1994). It is therefore equally warranted that these fluctuations need to be investigated more intensively and at larger scales. In this study, we have characterized a set of ten aquatic DOM samples (Vogt *et al.,* 2004; Vogt *et al.,* 2001) isolated by reverse osmosis during spring and fall seasons in five forested catchments in Scandinavia. The DOM samples were analyzed by elemental analysis, FT-IR spectroscopy, CP-MAS ^{13}C-NMR spectroscopy, synchrotron-based C-1s NEXAFS spectroscopy, and radiocarbon (^{14}C) analysis. Our objectives were (i) to study the composition of the DOM in five catchments, which differ in climate and exhibit some variations in soil types and vegetation, and (ii) to explore whether seasonal variations are reflected in the composition of aquatic DOM of spring and fall samples collected at each site.

4.2 Materials and methods

4.2.1 Sampling sites

Five catchments in Norway, Sweden and Finland were selected within the framework of a larger project on NOM in the Nordic countries (Vogt *et al.,* 2001). The locations of the five sampling sites are depicted in Figure 4.1. Table 4.1 summarizes some key properties of the sites, which differ in climate, dominating soil type, and vegetation (Bergström, 1995; Gjessing *et al.,* 1999; Vogt *et al.,* 2001). The annual average temperature ranges from 0 to 7 °C and the average annual precipitation from 590 to 2500 mm. All sampling sites are forested by Scots pine (*Pinus sylvatica* L.) and Norway spruce (*Picea abies* (L.) Karst.) on soils developed on glacial till. The dominant soil types are dystric Cambisols at Valkea-Kotinen, humic Gleysols at Birkenes, and Podzols at Svartberget, Skjervatjern and Hietajärvi. In addition to these soil types, large areas of peatland are present in

all catchments, with Histosols contributing between 13 % and 45 % of the total area (Table 4.1).

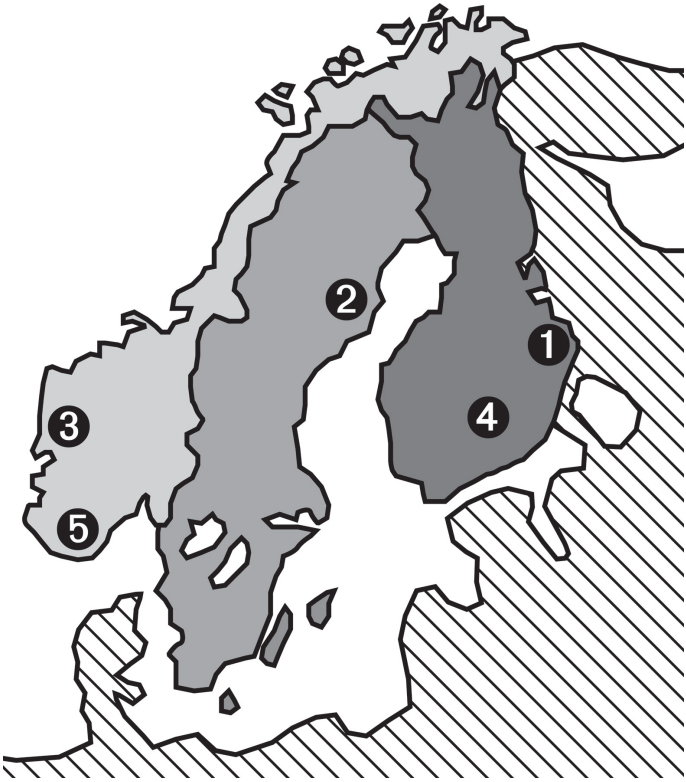

Figure 4.1:
Location of sampling sites: (1) Valkea-Kotinen, Finland, (2) Svartberget, Sweden, (3) Skjervatjern, Norway, (4) Hietajärvi, Finland, (5) Birkenes, Norway.

Table 4.1:
Main climatic data and site descriptions of the five selected sample sites after Bergström et al. (1995). Climate data, mean temperature and precipitation have been recorded by weather stations from 1990-1992. Air temperature, precipitation volume, discharge and evapotranspiration have been recorded during the period from 1991-1993.

Sampling site	Valkea-Kotinen #1	Svart-berget #2	Skjer-vatjern #3	Hietajärvi #4	Birkenes #5
Country	Finland	Sweden	Norway	Finland	Norway
Phytogeographic zone	Boreal	Boreal	Boreal-coastal	Middle Boreal	Boreal-nemoral
Forest type	Spruce	Spruce	Pine	Pine/ Spruce	Spruce
Elevation [m a.s.l.]	150	235	136	165	190
Precipitation [mm yr^{-1}]	618	720	2560	592	1500
Mean Temperature [°C]	3.1	0.0	5.5	2.0	6.6
Evapotrans-piration [mm]	432	395	NA	176	300
Discharge [mm]	186	325	NA	416	1200
Bedrock	Grano-diorite	Gneiss/ Schist	Gneiss	Grano-diorite	Granite
Dominant soil type	Dystric Cambisol	Ferric Podzol	Gleyic Podzol	Haplic Podzol	Humic Gleysol
Histosol coverage [%] *	25	16	42	45	13

NA denotes not available

** Values are given as percentages of the total soil coverage in the catchment*

4.2.2 Isolation of DOM

DOM was isolated from surface water collected at all five sites during base flow conditions in fall (September 26 to October 12, 1999) and spring (April 22 to Mai 26, 2000), respectively. At each site, 500 to 1100 L of surface water was processed through a mobile reverse osmosis (RO) unit (PROS/2S, RealSoft, Kansas City, MO, USA) as described by Serkiz and Perdue (1990). Briefly, the surface water was passed through a pre-filter into a reservoir, from where it was pumped through a sodium-saturated cation exchange resin (Dowex 50, Dow Chemical Comp., Michigan, MI, USA) to prevent precipitation of insoluble salts. The water was then passed through the RO membranes with pores of about 150 Å. In the RO membranes, the water was separated into a permeate solution,

containing virtually no solutes and a retentate solution that contained nearly all of the dissolved inorganic and organic material. The permeate solution was discharged and the retentate solution was recycled back into the reservoir. At the end of the RO treatment, 25 L of concentrated solution were filtered through a 0.45 µm filter (Nucleopore) and further concentrated by a rotary evaporator at 30 °C to a volume of about 5 L and then freeze-dried (Vogt *et al.,* 2001).

4.2.3 Elemental analysis

The freeze-dried, solid-state RO isolates were analyzed for total C, H, N, and S contents using a micro-CHNS analyzer (CHNS-932, Leco, St. Joseph, MI, USA). Five replicates were analyzed for each sample, using 2 mg subsamples. Inorganic cations and anions were analyzed after dissolving 1 mg of the freeze-dried RO isolates in 10 mL deionized water. The concentrations of SO_4^{2-}, NO_3^-, and Cl^- were measured by ion chromatography (761 Compact IC, Metrohm, Appenzell, Switzerland). The concentrations of Na, Ca, Mg, K, Al, Fe, Mn, and Si were analyzed by ICP-OES (Vista-MPX, Varian, Darmstadt, Germany) after acidifying the solutions with ultra-pure nitric acid. All concentrations were corrected for the moisture content of the samples, which was determined gravimetrically after drying the samples at 105 °C during 24 h.

4.2.4 FT-IR spectroscopy

Transmission mode Fourier-transform infrared (FT-IR) spectra were collected in ambient air at room temperature using 300 mg KBr pellets containing 0.5 mg of freeze-dried RO isolate (Spectrum One, Perkin Elmer, Fremont, CA, USA). For each sample, 20 scans were collected from 500 to 4000 cm^{-1} with a resolution of 4 cm^{-1}, background corrected and averaged.

4.2.5 Solid-state CP-MAS ^{13}C-NMR spectroscopy

The RO isolates were analyzed by solid-state cross polarization magic-angle spinning ^{13}C-nuclear magnetic resonance (CP-MAS ^{13}C-NMR) spectroscopy (DSX 200, Bruker, Rheinstetten, Germany). The NMR spectra were collected at a resonance frequency of 50.3 MHz, using a magic-angle spinning speed of 6.8 kHz and a contact time of 1 ms. A pulse delay of 400 ms was used. A ramped ^{1}H pulse decreasing was used in order to avoid spin modulations of Hartmann-Hahn conditions (Peersen *et al.,* 1993). The number of scans for each sample varied from 18'000 to 20'000.

For quantitative analysis, each spectrum was divided into six chemical shift regions which were assigned to alkyl carbon (0-45 ppm), O-alkyl carbon (45-110 ppm), aromatic carbon (110-160 ppm), phenolic carbon (140-160 ppm), carboxyl carbon (160-185 ppm) and carbonyl carbon (185-220 ppm), respectively The relative intensity of these peaks was determined by numerical integration of the spectral regions. Further details on the quantitative interpretation of NMR-spectra are given in Knicker and Kögel-Knabner (1998).

4.2.6 C-1s NEXAFS spectroscopy

Near edge X-ray absorption fine structure (NEXAFS) spectra at the C-1s edge were measured using the Stony Brook Scanning Transmission X-ray Microscope (STXM) at the NSLS beamline X-1A (National Synchrotron Light Source, Upton, N.Y.). The STXM was operated inside a helium-purged enclosure at room temperature and atmospheric pressure. A detailed description of the instrument can be found in Jacobsen et al. (1996). For specimen preparation, 2 mg of freeze-dried RO isolate were dissolved in 500 µL deionized water. A droplet of this solution was deposited onto a X-ray transparent Si_3N_4 window (Silson Ltd., Northampton, UK) and air-dried, resulting in a 50-200 nm thick film of organic carbon. On each specimen, absorbance spectra were collected from 280 to 310 eV at 25 different spots on the dry film and averaged. At least four spectra of the clean Si_3N_4 window were collected, averaged, and used for background correction of the C-1s NEXAFS spectra. For comparison of the spectra of different films, which can vary in thickness, the averaged spectra were normalized relative to their absorbance at 310 eV. The normalized NEXAFS spectra were deconvoluted by fitting the spectral region between 280 and 310 eV with seven Gaussian peaks representing the main 1s-π^* and 1s-σ^* transitions and one arctangent function for the ionization step at around 290eV (Schumacher *et al.,* 2005). For quantification, the fitted areas of the peaks at 285 eV, 286.5 eV, 288.5 eV, 289.5 eV, and 290.5 eV were converted into percentages of carbon bound as aromatic, phenolic, carboxyl, O-alkyl, and carbonyl carbon, respectively, using the empirical correlation functions given by Schumacher et al. (2005).

4.2.7 Radiocarbon dating

All samples were analyzed for the carbon isotopes ^{12}C, ^{13}C and ^{14}C. For the graphitization of the samples, the method described by Vogel et al. (1984) was applied. Briefly, cobalt powder was used as a catalyst for the reduction of CO_2 to C by H_2. The weight ratio of C to CO_2 was about 0.29. After measuring the CO_2 volume

of a sample, a subsample of the CO_2, which was equivalent to 0.5 – 2 mg of C, was transferred to the reactor. The amount of hydrogen gas added into the reactor equaled 2.05 times the partial pressure of CO_2. For the reduction, the gas was heated to 625 °C. Carbon isotope measurements of the so-obtained graphite materials were performed at the PSI/ETH compact accelerator mass spectrometry (AMS) facility in Zurich, Switzerland, which contains a 500 kV pelletron accelerator (Synal *et al.,* 2000). Details on sample preparation and the instruments specifications are reported elsewhere (Hajdas *et al.,* 2004; Szidat *et al.,* 2004). From the AMS results, the conventional ^{14}C-age relative to the NBS oxalic acid standard from 1950 was calculated for each sample (Stuiver & Polach, 1977). All ^{14}C-age values were corrected for isotope fractionation using the $\delta\ ^{13}C$ values measured for the samples and the reference material PDB (Stuiver & Polach, 1977).

4.3 Results and Discussion

4.3.1 Elemental composition

The RO isolates contained between 29 to 66 % inorganic material (ash) (Vogt *et al.,* 2001), which is typical for RO isolates (Gjessing *et al.,* 1999; Serkiz & Perdue, 1990). The ash consisted mainly of sodium sulfates and chlorides. In addition, small amounts of calcium, magnesium and silicate were identified. The high portion of sodium in the samples resulted from the use of a sodium-saturated cation exchange resin for the sample isolation. The amounts of sulfate in the samples from Skjervatjern and in the spring sample from Svartberget, having the lowest sulfur deposition among the sites, were low in comparison to their carbon content. Instead, these three samples exhibited the highest contents of silicates compared to the other samples. The elemental composition of the organic fraction of the RO isolates, the DOM, is reported in Table 4.2. The carbon content of the DOM was rather constant (535 ± 21 g kg^{-1} C) and the median value (525 g kg^{-1} C) was in good agreement with the median carbon content (496 g kg^{-1} C) of freshwater DOM samples compiled by Perdue and Ritchie (2003).

Table 4.2:
Total organic carbon (TOC) contents of original water samples and elemental composition of isolated DOM. The values for the elemental composition are corrected for ash contents.

Sample		TOC * [mg L^{-1}]	C [g kg^{-1}]	H [g kg^{-1}]	N [g kg^{-1}]	S [g kg^{-1}]	C/N
Birkenes	**Fall**	5	511	38	16	9	33
	Spring	4	524	71	18	12	30
Hietajärvi	**Fall**	6	520	37	9	9	59
	Spring	5	546	46	12	10	44
Skjervatjern	**Fall**	10	516	39	8	6	61
	Spring	6	526	42	7	5	76
Svartberget	**Fall**	11	569	32	7	7	82
	Spring	19	520	41	4	2	119
Valkea-Kotinen	**Fall**	9	551	40	13	7	41
	Spring	11	565	40	10	6	57
Average ± SD	**Fall**	8 ± 3	533 ± 25	37 ± 3	11 ± 4	7 ± 1	55 ± 19
Average ± SD	**Spring**	9 ± 6	536 ± 11	48 ± 13	10 ± 5	7 ± 4	65 ± 35
Average ± SD	**Total**	9 ± 5	535 ± 21	43 ± 11	11 ± 4	7 ± 3	58 ± 27

** from Vogt et al. (2001)*

The differences between the carbon contents of the DOM samples isolated in spring and fall were remarkably small and statistically not significant (P = 0.09). Furthermore, the contents of hydrogen and nitrogen were in good agreement with values published by Alberts and Takács (1999), who carried out elemental analysis of eight RO samples of DOM from Norwegian sites (i.e., NOM-typing project, Gjessing *et al.*, 1999).

4.3.2 FT-IR spectroscopy

The normalized FT-IR spectra of the RO isolates and the three reference materials peat fulvic acid (IHSS 1R103F), peat humic acid (IHSS 1R103H), and aquatic Suwannee River (SR) NOM (IHSS 1R101N) are presented in Figure 4.2. All spectra exhibit the typical absorption bands of natural organic matter and humic substances reported by Clapp et al. (1994) and Stevenson et al. (1982). In the following, we briefly resume the interpretation of the main absorption bands observed for our samples. The broad absorption band around 3400 to 3300 cm^{-1} corresponds to stretching vibrations of H-bonded hydroxyl groups.

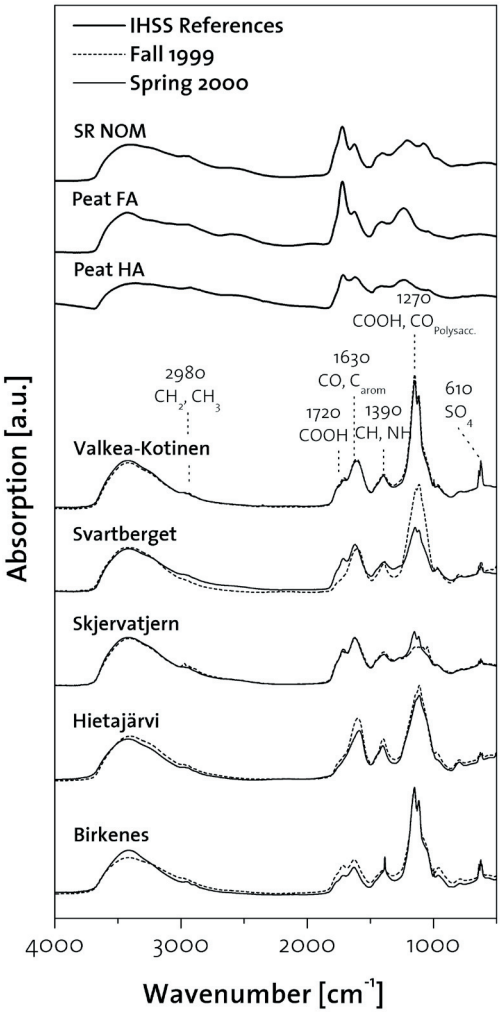

Figure 4.2:
FT-IR spectra of the DOM samples. Spectra from samples taken in fall 1999 and spring 2000 are plotted with dotted and solid lines, respectively. Spectra of IHSS peat fulvic (FA), IHSS humic acid (HA), and IHSS NOM are plotted for comparison.

The very weak bands at 2980 to 2900 cm^{-1} represent aliphatic C-H stretching vibrations. The band at 1720 cm^{-1} is attributed mainly to C=O stretching of carboxylic groups and ketones. The band at 1630 cm^{-1} is due to C=O stretching of H-bonded carboxylic groups, quinones, or conjugated ketones and to aromatic C=C vibrations (Stevenson, 1982). The bands at 1390 cm^{-1} may arise from O-H deformation and C-O stretching of phenolic OH, C-H deformation of CH_2 and CH_3 groups, and COO- asymmetric stretching, respectively. The bands around 1270 cm^{-1} can be assigned to C-O stretching of aryl ethers and phenols, and to C-O stretching as well as O-H deformation of carboxyl groups and polysaccharides. The bands at 610 cm^{-1} may be due to out-of-plane bending of aromatic C-H (Senesi, 1990). In addition, also inorganic constituents of the RO isolates contribute to the FT-IR spectra. For example, Si-O bonds in silicates may contribute to a small extent to the absorption bands at 1270 cm^{-1} and 610 cm^{-1}, respectively (Haberhauer & Gerzabek, 1998; Orlov, 1992).

More importantly, sulfate may contribute to the absorption band at 1270 cm^{-1}, as sulfate has several absorption bands between 1110 cm^{-1} and 1280 cm^{-1} (Nakamoto, 1997; Smidt *et al.,* 2002). The influence of sulfate may be responsible for the observation that the absorption bands between 1110 cm^{-1} and 1280 cm^{-1} are smaller for both samples from Skjervatjern and for the spring sample from the Svartberget site than for all other samples. As mentioned in the previous section, these three samples have low sulfate contents compared to their amounts of carbon. In comparison of the FT-IR spectra for our DOM samples, the peat fulvic acid, the peat humic acid and the Suwannee River NOM sample reveal that all DOM samples investigated possess evidently higher contents of inorganic contents such as silicates and sulfate, which contribute to the respective absorption bands but lower contents of carboxyl carbon. The most striking feature of the FT-IR spectra is the similarity between the spring and fall samples, all of which were collected during base flow conditions. For the Valkea-Kotinen site, the FT-IR spectra of spring and fall samples were virtually identical. For the Skjervatjern, Hietajärvi, and Birkenes sites, only minor spectral differences were observed and the relative intensities of most peaks remained constant. Larger differences between spring and fall samples were only observed for the Svartberget catchment, which may mainly be caused by their differences in the inorganic constituents.

4.3.3 Solid-state CP-MAS ^{13}C-NMR spectroscopy

The CP-MAS ^{13}C-NMR spectra of the sample set and the three reference samples are presented in Figure 4.3. The spectral differences between the spring and fall samples from each site were again minor. Note, that this was also true for the Svartberget site, which exhibited the largest differences in FT-IR spectra. This result support our interpretation that differences in FT-IR spectra between the Svartberget fall and spring samples were mainly due to inorganic compounds. The quantitative evaluation of the ^{13}C-NMR spectra is summarized in Table 4.3, together with average values and standard deviations for the fall samples, the spring samples and the total sample set.

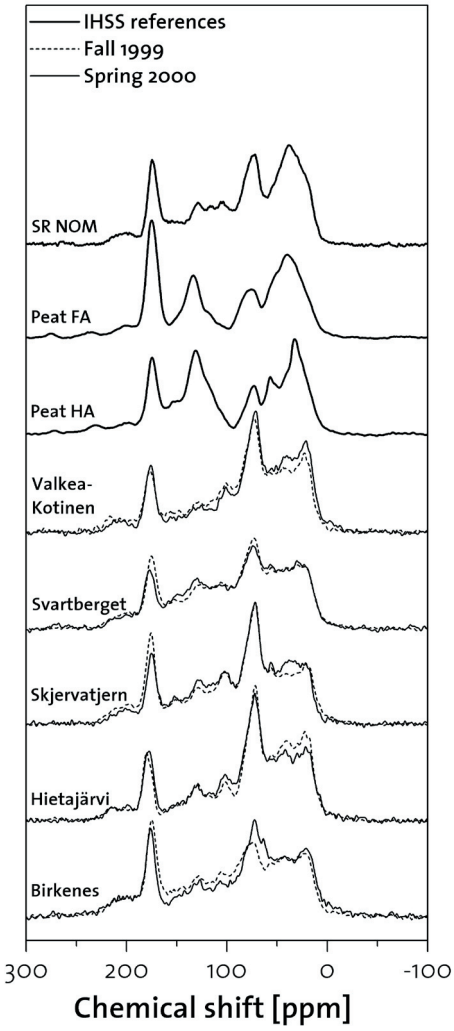

Figure 4.3:
Solid-state CP-MAS ^{13}C-NMR spectra of the DOM samples. Spectra from samples taken in fall 1999 and spring 2000 are plotted with dotted and solid lines, respectively. Spectra of IHSS peat fulvic (FA), IHSS humic acid (HA), and IHSS NOM are plotted for comparison.

All ten ^{13}C-NMR spectra exhibited strong peaks in the chemical shift region assigned to O-alkyl carbon including alcohols, ethers and hemiacetals (45-110 ppm) and the region assigned to carboxyl carbon (160-185 ppm). On average, the DOM samples contained 42 % O-alkyl carbon, which is slightly higher than the median O-alkyl carbon content of freshwater DOM reported in the literature (Perdue & Ritchie, 2003). The DOM samples had an average carboxyl carbon content of 11 %, which is comparably low. Perdue and Ritchie (2003) reported that the median carboxyl carbon content of freshwater DOM was 19 % of the total carbon as estimated from ^{13}C-NMR data. The average content of total aromatic carbon in our DOM samples was 15 %, which is lower than the median contents of freshwater NOM reported in the literature (Abbt-Braun & Frimmel, 1999). The average contents of carbonyl carbon (6 %) and alkyl carbon (26 %) were very similar to literature median values (Abbt-Braun & Frimmel, 1999; Perdue & Ritchie, 2003). When comparing the composition of DOM from the five sampling sites, some small differences between sites can be observed. The Birkenes and Svartberget DOM, which are both sampled in stream water, contained slightly less O-alkyl carbon.

Table 4.3:
Carbon distribution as derived from integrated solid-state CP-MAS ^{13}C-NMR spectra.

Functional group		Alkyl	O-Alkyl	Aromatic*	Phenolic	Carboxyl	Carbonyl
Spectral region [ppm]		*0-45*	*45-110*	*110-140*	*140-160*	*160-185*	*185-220*
Birkenes	**Fall**	23	37	11	6	15	8
	Spring	27	39	7	4	13	8
Hietajärvi	**Fall**	27	45	10	3	10	5
	Spring	30	43	9	3	9	6
Skjervatjern	**Fall**	22	42	11	5	13	7
	Spring	22	44	12	5	11	6
Svartberget	**Fall**	24	40	14	7	10	5
	Spring	23	40	13	6	12	6
Valkea-Kotinen	**Fall**	26	45	9	4	10	6
	Spring	31	44	8	3	10	4
Average ± SD	**Fall**	24 ± 2	42 ± 3	11 ± 2	5 ± 2	12 ± 2	6 ± 1
Average ± SD	**Spring**	27 ± 4	42 ± 2	10 ± 3	4 ± 1	11 ± 2	6 ± 1
Average ± SD	**Total**	26 ± 3	42 ± 3	10 ± 2	5 ± 1	11 ± 2	6 ± 1

** without phenolic carbon*

In addition, the samples from Birkenes, the catchment with the highest S deposition, exhibited slightly higher contents of carbonyl carbon than the DOM from the other sites. The DOM from Svartberget had the highest content of total aromatic carbon, while the Hietajärvi and Valkea-Kotinen samples had the lowest contents of total aromatic carbon. However, the differences in aromaticity are relatively small, particularly when comparing the values with the average composition of DOM reported in the literature (Perdue & Ritchie, 2003). Concerning seasonal variation between the samples from spring and fall, no significant differences were observed (Table 4.3). Comparison of the ^{13}C-NMR spectra obtained for our DOM samples with the IHSS reference samples reveals that all DOM samples investigated possess evidently higher contents of O-alkyl carbon, but much lower contents of aromatic carbon as well as alkyl carbon and compared to peat fulvic acid, also lower contents of carboxyl carbon (Figure 4.3). This finding indicates that the DOM samples are more hydrophilic than the reference fulvic and humic acid samples. The clear differences between DOM samples and

IHSS references materials suggest that leaching of fulvic and humic acids from peatlands into the discharge system contributes only to a minor extent to the riverine DOM contents at base flow conditions. For the catchment at Svartberget, Laudon et al. (2004) showed that freshwater TOC concentrations are mainly controlled by water inputs such as precipitation and snow melting. Similar observations were reported for DOC concentrations in Norwegian lakes by Hongve et al. (2004). Laudon et al. (2004) further found, that TOC concentrations in the discharge system also correlated the percentage of wetland coverage in the respective area. We conclude that at base flow conditions, the composition of riverine DOM in boreal catchments is fairly constant and not strongly affected by seasonal variations. Significant variations in DOM composition may however be caused by changes in hydrologic conditions.

4.3.4 C-1s NEXAFS spectroscopy

In addition to ^{13}C-NMR spectroscopy, C-1s NEXAFS spectroscopy was carried out to probe the chemical bonding environment of carbon in the DOM samples. Figure 4.4 shows the averaged and normalized C-1s NEXAFS spectrum of the Birkenes fall DOM as an example to explain how the C-1s NEXAFS spectra were interpreted. The spectrum exhibits four well-developed peaks, which arise from the excitation of core 1s-electrons up to low-energy unoccupied molecular orbitals, e.g., antibonding (π^*) orbitals. At higher X-ray energies near and above the ionization energy (290 eV), 1s-σ^* transitions give rise to broad absorption peaks. The first peak at 285.5 eV corresponds to C=C 1s-π^* transitions of aromatic carbon (protonated and alkylated to carbonyl-substituted) and may also include quinone carbon and possibly olefinic carbon (Boyce *et al.,* 2002; Cody *et al.,* 1996; Kong *et al.,* 1998). The second peak at 286.5 eV is typical for the C-O 1s-π^* transition of phenolic carbon, including O-substituted aryl carbon as well as aromatic carbon substituted with other electron-withdrawing groups (Hitchcock *et al.,* 1997; Urquhart *et al.,* 1999). The sharp peak at 288.0 eV is assigned to the C=O 1s-π^* transition of carboxyl carbon (Ishii & Hitchcock, 1988; Urquhart *et al.,* 1999), whereas the signal around 289.5 eV can be assigned to C-O transitions present in O-alkyl carbon (Scheinost *et al.,* 2001). The peak at 290.5 eV corresponds to C=O 1s-π^* transitions in carbonyl carbon (Boyce *et al.,* 2002; Urquhart & Ade, 2002).

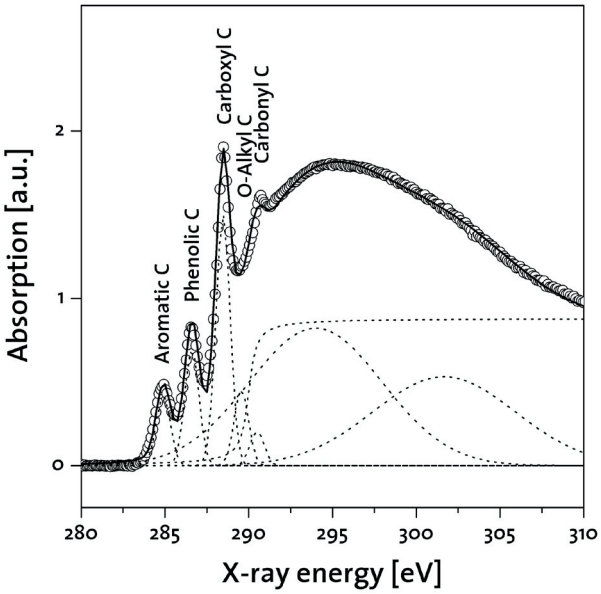

Figure 4.4:
Spectral deconvolution of a C-1s NEXAFS spectrum of the fall sample from Birkenes. Circles represent the experimental data, whereas the solid line corresponds to the fitted spectrum calculated as sum of single components shown in dotted lines.

In this study, the C-1s NEXAFS spectra were deconvoluted by fitting five Gaussian peaks representing the main transitions discussed above, two broad Gaussian peaks representing 1s-σ* transitions above the ionization threshold, and one arctangent function for the ionization step around 290 eV (Schumacher *et al.,* 2005). The example in Figure 4.4 demonstrates that the fitting scheme resulted in a good representation of the overall spectrum. The C-1s NEXAFS spectra of all DOM samples are depicted in Figure 4.5. In order to obtain quantitative information from C-1s NEXAFS spectra, relative peaks areas for aromatic carbon (285.0 eV), phenolic carbon (286.5 eV), carboxyl carbon (288.5 eV), O-alkyl carbon (289.4 eV), and carbonyl carbon (290.5 eV) were converted to values representing the carbon distribution (Table 4.4). For the conversion, we applied the correlation functions for the respective carbon bond type, which were reported by Schumacher et al. (2005). The spectral differences between the fall and spring samples were again extremely small and statistically not significant ($P = 0.11$). Only for the Svartberget fall and spring sample, the C-1s NEXAFS

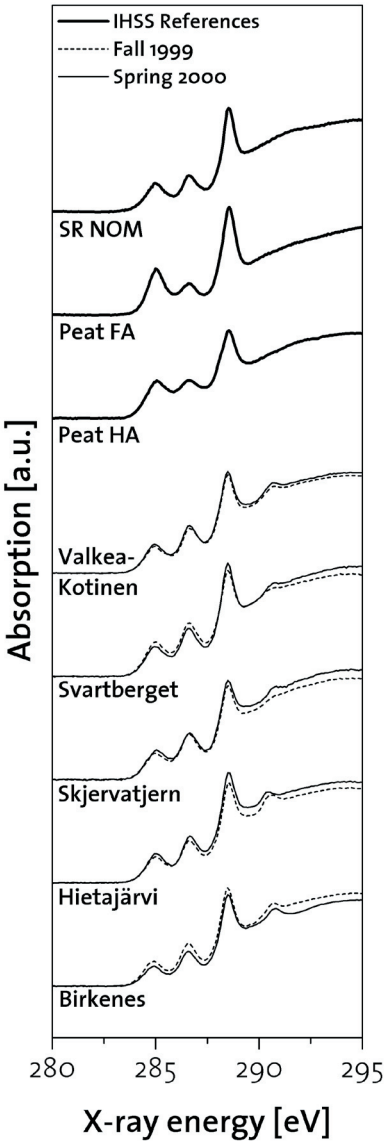

Figure 4.5:
C-1s NEXAFS spectra of the DOM samples. Spectra of samples taken in fall 1999 and spring 2000 are plotted with dotted and solid lines, respectively. Spectra of IHSS peat fulvic (FA), IHSS humic acid (HA), and IHSS NOM are plotted for comparison.

spectroscopy revealed differences in all functional groups, showing slightly higher contents of aromatic, phenolic, and O-alkyl carbon and slightly lower carboxyl and carbonyl carbon contents for the fall sample (Table 4.4). The C-1s NEXFAS spectra of DOM samples from the five catchments were also similar to one another, although some minor differences were observed. The amounts of aromatic and phenolic carbon were slightly elevated for the Svartberget and Skjervatjern sites, which is consistent with our NMR results. In addition, DOM from the Svartberget and Skjervatjern sites tended to have lower carbonyl carbon contents. However, no clear differences or trends between the DOM from the five catchments were found by C1-s NEXAFS spectroscopy. This finding is in good agreement with the FT-IR and ^{13}C-NMR results and the elemental composition of the samples. A comparison of the C-1s NEXAFS spectra obtained for our DOM samples and for the three reference materials shows that even the spectrum of the aquatic NOM sample isolated from the Suwannee River, USA, is very similar to the spectra of the Scandinavian samples (Figure 4.5). The humic acid spectrum exhibited a slightly higher absorbance in the aromatic region and a slightly lower absorbance in the carboxyl region compared to the IHSS NOM sample and the DOM samples.

Table 4.4:
Carbon functional group distribution calculated from C-1s NEXAFS spectra. For the quantification of C-1s NEXAFS spectra, peak areas of the respective spectral regions were converted into percentages of carbon bound as aromatic, phenolic, carboxyl, O-alkyl, or carbonyl carbon applying the correlation of C-1s NEXAFS and ^{13}C-NMR data given by Schumacher et al. (2005).

Functional group		**Aromatic***	**Phenolic**	**Carboxyl**	**O-Alkyl**	**Carbonyl**
Spectral region [eV]		*285.0 ± 0.1*	*286.5 ± 0.1*	*288.5 ± 0.1*	*289.5 ± 0.2*	*290.5 ± 0.1*
Birkenes	**Fall**	9	8	16	31	9
	Spring	6	6	17	39	11
Hietajärvi	**Fall**	9	7	15	33	11
	Spring	10	7	15	33	9
Skjervatjern	**Fall**	11	9	14	37	5
	Spring	12	9	13	36	7
Svartberget	**Fall**	13	10	13	31	6
	Spring	11	8	16	30	8
Valkea-Kotinen	**Fall**	10	8	15	34	8
	Spring	10	8	14	33	10
Average ± SD	**Fall**	10 ± 2	8 ± 1	15 ± 1	33 ± 2	8 ± 2
Average ± SD	**Spring**	10 ± 2	8 ± 1	15 ± 2	34 ± 3	9 ± 2
Average ± SD	**Total**	10 ± 2	8 ± 1	15 ± 1	34 ± 3	8 ± 2

** without phenolic carbon*

The fulvic acid spectrum, however, showed clear differences at 285 eV and 288.5 eV indicating a higher aromatic and carboxyl carbon content compared to IHSS NOM and the DOM samples. Comparison of quantitative results obtained by ^{13}C-NMR and C-1s NEXAFS spectroscopy shows that the values agree well for aromatic and carbonyl carbon (Tables 4.3 and 4.4). For phenolic, and carboxyl carbon, quantitative values derived from C-1s NEXAFS spectra tend to slightly exceed values derived from ^{13}C-NMR spectra. The largest deviations were found for O-alkyl carbon, where the estimated values derived from C-1s NEXAFS spectra were slightly lower than the values determined by ^{13}C-NMR spectroscopy. This may be due to the relative low response of the 1s-σ* transition of O-alkyl carbon in C-1s NEXAFS spectra. Since the quantitative results of ^{13}C-NMR and C-1s NEXAFS spectroscopy are in good agreement for aromatic, phenolic, carboxyl, and carbonyl carbon, we conclude that for NOM samples, reasonable estimates

for these carbon types can be derived from C-1s NEXAFS spectra using the fitting scheme and the empirical correlation functions reported by Schumacher et al. (2005).

4.3.5 Radiocarbon dating

The results of the radiocarbon analysis are reported in Table 4.5. Calculated conventional ^{14}C-age data are given in years before present time (yr BP), i.e, relative to the oxalic acid standard from 1950 provided by the US National Bureau of Standards. All ^{14}C-age data were corrected for carbon isotope fractionation by normalizing the values to the δ ^{13}C values with respect to PDB (Stuiver & Polach, 1977). For all samples, the percent modern relative to the year 1950 was calculated. For all DOM samples investigated the calculated conventional ^{14}C-age values are negative indicating that all samples were highly enriched in ^{14}C compared to the oxalic acid standard. Due to nuclear weapon tests in the 1950's and 1960's, the atmospheric ^{14}C concentration was strongly increased.

Table 4.5:
Results of carbon isotope analysis and conventional ^{14}C-age.

Sample		AMS ^{14}C-age [yr BP]	δ ^{13}C [‰]	Percent modern [%]
Birkenes	**Fall**	-740 ± 50	-26.9 ± 1.2	109.33 ± 0.68
	Spring	-625 ± 45	-25.1 ± 1.2	107.37 ± 0.60
Hietajärvi	**Fall**	-1270 ± 45	-28.6 ± 1.2	116.35 ± 0.55
	Spring	-1155 ± 45	-31.5 ± 1.2	114.75 ± 0.64
Skjervatjern	**Fall**	-1095 ± 45	-31.3 ± 1.2	113.84 ± 0.69
	Spring	-1110 ± 45	-30.2 ± 1.2	114.06 ± 0.64
Svartberget	**Fall**	-410 ± 45	-30.9 ± 1.2	104.54 ± 0.58
	Spring	-1275 ± 40	-31.2 ± 1.2	116.42 ± 0.58
Valkea-Kotinen	**Fall**	-1640 ± 45	-28.3 ± 1.2	121.84 ± 0.68
	Spring	-1335 ± 40	-30.0 ± 1.2	117.30 ± 0.58
Average ± SD	**Fall**	-1031 ± 46	-29.2 ± 1.2	113.18 ± 6.61
Average ± SD	**Spring**	-1100 ± 43	-29.6 ± 1.2	113.98 ± 3.91
Average ± SD	**Total**	-1065 ± 45	-29.4 ± 1.2	113.58 ± 5.14

In all organic matter generated after this period, the concentrations of ^{14}C are typically increased to a large extent. Based on the radiocarbon age data, we conclude that the mean residence time of carbon bound in the DOM is less than 50 years for all samples. This fact is also reflected in the percent modern values given in Table 4.5. For all DOM samples, the percent Modern values are over 100 % suggesting that all DOM samples contain a large portion of nuclear bomb ^{14}C and were therefore formed mainly after 1950. This finding indicates that our DOM samples consist mainly of recent organic material rather than of fulvic and humic acids, which typically exhibit radiocarbon ages of several hundred to a few thousand years. The calculated $\delta\,^{13}C$ values, given relative to the PDB standard, range from -25 ‰ to -32 ‰ for our DOM samples (Table 4.5). This range is typical for fresh litter such as tree leaves, as well as for humus or peat (Stuiver & Polach, 1977; Szidat *et al.,* 2004). Aquatic organisms and fresh water plant materials usually show $\delta\,^{13}C$ values between -10 ‰ to -20 ‰ (Stuiver & Polach, 1977). The $\delta\,^{13}C$ values of our DOM samples indicate that most organic material in our DOM samples is of terrestrial origin rather than from aquatic environments.

4.4 Conclusions

Our analysis of DOM samples isolated during the fall and spring seasons in five boreal forested catchments suggests that seasonal variations in DOM composition during base flow conditions are negligibly small. In addition, the striking similarity of the DOM samples from the five river catchments suggests that the differences in climate, dominating soil type, and vegetation had little influence on DOM composition in the rivers. The chemical characterization revealed the all DOM samples were rich in hydrophobic moieties indicated by high contents of O-alkyl carbon. Compared to the peat fulvic acid and peat humic acid samples, the DOM samples showed far smaller signals of hydrophobic moieties, such as aromatic and alkyl carbon in both the C-1s NEXAFS spectra and ^{13}C-NMR spectra. Carbon isotope analysis revealed that all DOM samples can clearly be dated after the period of thermonuclear bomb test in the 1950's and 1960's. In addition, $\delta\,^{13}C$ values suggest that the DOM samples are of terrestrial origin, mainly. We conclude that during base flow conditions, DOM isolated from rivers in boreal catchments mainly consists of fresh terrestrial, hydrophilic organic matter. As long as the discharge in the catchments is close

to base flow conditions, the DOM composition in the rivers is likely to be rather stable and unaffected by seasonal variations in temperature. However, the DOM composition may change considerably when the discharge is strongly increased, leading to an enhanced input of humic materials leached from surrounding peatlands and forest floors.

Acknowledgements

The NEXAFS spectra were recorded on the STXM beamline X-1A, NSLS, Brookhaven National Laboratory, Upton, N.Y.. The STXM was developed by the group of J. Kirz and C. Jacobsen at SUNY Stony Brook with support from the Office of Biological and Environmental Research, U.S. DoE under contract DE-FG02-89ER60858 and the NSF under grant DBI-9605045. We are also grateful to Heike Knicker (TU Munich, Germany) for recording NMR spectra, Andreas C. Scheinost (Research Center Rossendorf, Germany) for valuable discussions and critical comments, and Sue Wirick (X1A, NSLS) for her help at the beamline.

Literature cited

Abbt-Braun, G. & Frimmel, F.H. 1999. Basic characterization of Norwegian NOM samples - Similarities and differences. *Environ. Int.* **25**: 161-180.

Alberts, J.J. & Takacs, M. 1999. Characterization of Natural Organic Matter from eight Norwegian surface waters: The effect of ash on molecular size distributions and CHN content. *Environ. Int.* **25**: 237-244.

Bergström, I. 1995. *Integrated Monitoring Programme in Finland*, National Report. Finnish Ministry of the Environment, Helsinki.

Boyce, C.K., Cody, G.D., Feser, M., Jacobsen, C., Knoll, A.H. & Wirick, S. 2002. Organic chemical differentiation within fossil plant cell walls detected with X-ray spectromicroscopy. *Geology*. **30**: 1039-1042.

Buffle, J., Mota, A.M. & Goncalves, M. 1987. Adsorption of Fulvic-Like Organic-Ligands and Their Cd and Pb Complexes at a Mercury-Electrode. *Journal of Electroanalytical Chemistry*. **223**: 235-262.

Clapp, C.E., Hayes, M.B.H., Senesi, N. & Griffith, S.M. 1994. *Humic Substances and Organic Matter in Soil and Water Environments: Characterization, Transformations, and Interactions*. In: Proceedings of the 7th International Conference of the International Humic Substances Society, IHSS, University of the West Indies, St- Augustine, Trinidad and Tobago.

Cody, G.D., Botto, R.E., Ade, H. & Wirick, S. 1996. The application of soft X-ray microscopy to the in-situ analysis of sporinite in coal. *Int. J. Coal Geol.* **32**: 69-86.

Gjessing, E., Egeberg, P.K. & Hakedal, J. 1999. Natural organic matter in drinking water - The "NOM-typing project", Background and basic characteristics of original water samples and NOM isolates. *Environ. Int.* **25**: 145-159.

Haberhauer, G. & Gerzabek, M.H. 1998. Drift and transmission FT-IR spectroscopy of forest soils: an approach to determine decomposition processes of forest litter. *Vib. Spectrosc.* **19**: 413-417.

Hajdas, I., Bonani, G., Thut, J., Leone, G., Pfenninger, R. & Maden, C. 2004. A report on sample preparation at the ETH/PSI AMS facility in Zurich. *Nucl. Instrum. Meth. B*. **223-224**: 267-271.

Hedges, J.I. & Oades, J.M. 1997. Comparative organic geochemistries of soils and marine sediments. *Org. Geochem.* **27**: 319-361.

Heikkinen, K. 1994. Organic matter, iron and nutrient transport and nature of dissolved organic matter in the drainage basin of a boreal humic river in northern Finland. *Sci. Total Environ.* **152**: 81-89.

Hitchcock, A.P., Urquhart, S.G., Wen, A.T., Kilcoyne, A.L.D., Tyliszczak, T., Ruhl, E., Kosugi, N., Bozek, J.D., Spencer, J.T., McIlroy, D.N. & Dowben, P.A. 1997. Inner-shell excitation spectroscopy of closo-carboranes. *J. Phys. Chem. B*. **101**: 3483-3493.

Hongve, D., Riise, G. & Kristiansen, J.F. 2004. Increased colour and organic acid concentrations in Norwegian forest lakes and drinking water – a result of increased precipitation? *Aquatic Sciences*. **66**: 231-238.

Ishii, I. & Hitchcock, A.P. 1988. The oscillator strengths for C1s and O1s excitation of some saturated and unsaturated organic alcohols, acids and esters. *J. Electron Spectrosc.* **46**: 55-84.

Jacobsen, C., Chapman, H.N., Fu, J., Kalinovsky, A., Kirz, J., Maser, J., Osanna, A., Spector, S.J., Tennant, D.M., Wang, S., Wirick, S. & Zhang, X. 1996. Biological microscopy and soft x-ray optics at Stony Brook. *J. Electron Spectrosc.* **80**: 337-341.

Knicker, H. & Kogel-Knabner, I. 1998. In: *Nitrogen-Containing Macromolecules in the Bio- and Geosphere* Vol. 707, p. 339-356.

Kong, M.J., Teplyakov, A.V., Lyubovitsky, J.G. & Bent, S.F. 1998. NEXAFS studies of adsorption of benzene on Si(100)-2 x 1. *Surf. Sci.* **411**: 286-293.

Laudon, H., Kohler, S. & Buffam, I. 2004. Seasonal TOC export from seven boreal catchments in northern Sweden. *Aquatic Sciences*. **66**: 223-230.

Leenheer, J.A. & Croue, J.P. 2003. Characterizing aquatic dissolved organic matter. *Environ. Sci. Technol.* **37**: 18A-26A.

Lobbes, J.M., Fitznar, H.P. & Kattner, G. 2000. Biogeochemical characteristics of dissolved and particulate organic matter in Russian rivers entering the Arctic Ocean. *Geochim. Cosmochim. Acta*. **64**: 2973-2983.

Lydersen, E. 1995. Effect of cold and warm years on the water chemistry at the Birkenes catchment. *Water Air Soil Poll.* **84**: 217-232.

Moran, M.A. & Zepp, R.G. 1997. Role of photoreactions in the formation of biologically labile compounds from dissolved organic matter. *Limnol. Oceanogr.* **42**:

Nakamoto, K. 1997. *Infrared and Raman Spectra of inorganic and coordination compounds. Part A: Theory and Applications in Inorganic Chemistry*. John Wiley & Sons, New York.

Orlov, D.S. 1992. *Soil Chemistry*. Balkema, Rotterdam.

Peersen, O.B., Wu, X., Kustanovich, I. & Smith, S.O. 1993. Variable-amplitude cross-polarization MAS-NMR. *J. Magn. Reson. Ser. A*. **104**: 334-339.

Perdue, E.M. & Ritchie, J.D. 2003. In: *Treatise on Geochemistry* (H.D. Holland & K.K. Turekian eds.) Vol. 5, Elsevier, p. 273-318.

Porcal, P., Hejzlar, J. & Kopacek, J. 2004. Seasonal and photochemical changes of DOM in an acidified forest lake and its tributaries. *Aquatic Sciences*. **66**: 211-222.

Scheinost, A.C., Kretzschmar, R., Christl, I. & Jacobsen, C. 2001. In: *Humic Substances: Structures, Models and Functions* (E.A. Ghabbour & G. Davies eds.) Royal Society of Chemistry, Cambridge. p. 37 -40.

Schnitzer, M. 1991. Soil organic matter: The next 75 years. *Soil Sci.* **151**: 41-58.

Schumacher, M., Scheinost, A.C., Christl, I., Jacobsen, C. & Kretzschmar, R. 2005. Can C-1s NEXAFS spectroscopy be used to quantify functional C groups in humic substances? *Eur. J. Soil Sci.* submitted.

Senesi, N. 1990. Fluorescence Spectroscopy Applied to the Study of Humic Substances from Soil and Soil Related Materials - a Review. *Abstr. Pap. Am. Chem. S.* **199**: 8-ENVR.

Serkiz, S.M. & Perdue, E.M. 1990. Isolation of dissolved organic matter from the Suwannee river using reverse osmosis. *Water Res.* **24**: 911-916.

Skjelvale, B.L., Mannio, Y., Wiklander, A. & Andersen, T. 2001. Recovery from acidification of lakes in Finland, Norway and Sweden 1990-1999. *Hydrol. Earth Syst. Sc.* **5**: 327-337.

Smidt, E., Lechner, P., Schwanninger, M., Haberhauer, G. & Gerzabek, M.H. 2002. Characterization of waste organic matter by FT-IR spectroscopy: Application of waste science. *Appl. Spectrosc.* **56**: 1170-1175.

Solinger, S., Kalbitz, K. & Matzner, E. 2001. Controls on the dynamics of dissolved organic carbon and nitrogen in a Central European deciduous forest. *Biogeochemistry*. **55**: 327-349.

Stevenson, F.J. 1982. *Humus chemistry: Genesis, Composition, Reactions*. John Wiley & Sons, New York.

Stuiver, M. & Polach, H.A. 1977. Discussion reporting of ^{14}C data. *Radiocarbon*. **19**: 355-363.

Synal, H.A., Jacob, S. & Suter, M. 2000. The PSI/ETH small radiocarbon dating system. *Nucl. Instrum. Meth. B*. **172**: 1-7.

Szidat, S., Jenk, T.M., Gäggeler, H.W., Synal, H.A., Fisseha, R., Baltensperger, U., Kalberer, M., Samburova, V., Reimann, S., Kasper-Giebl, A. & Hajdas, I. 2004. Radiocarbon (^{14}C)-deduced biogenic and anthropogenic contributions to organic carbon (OC) of urban aerosols from Zürich, Switzerland. *Atmos. Environ.* **38**: 4035-4044.

Tipping, E., Rey-Castro, C., Bryan, S.E. & Hamilton-Taylor, J. 2002. Al(III) and Fe(III) binding by humic substances in freshwaters, and implications for trace metal speciation. *Geochim. Cosmochim. Acta*. **66**: 3211-3224.

Tranvik, L. 2003. *Microbial and photochemical degradation of dissolved organic matter*. In: Workshop on changes in quality and quantity of dissolved NOM: Causes and consequences, NORDTEST, Atna.

Urquhart, S.G. & Ade, H. 2002. Trends in the carbonyl core (C 1s, O 1s) - π^* C=O transition in the near-edge X-ray absorption fine structure spectra of organic molecules. *J. Phys. Chem. B*. **106**: 8531-8538.

Urquhart, S.G., Smith, A.P., Ade, H., Hitchcock, A.P., Rightor, E.G. & Lidy, W. 1999. Near-edge x-ray absorption fine structure spectroscopy of MDI and TDI polyurethane polymers. *J. Phys. Chem. B*. **103**: 4603-4610.

van Hees, P. 1998. *Low molecular weight organic acids and their aluminum complexes in forest soils*. Linköping Studies in Science and Technology.

Vogel, J.S., Southon, J.R., Nelson, D.E. & Brown, T.A. 1984. Performance of catalytically condensed carbon for use in accelerator mass spectrometry. *Nucl. Instrum. Meth. B*. **5**: 289-293.

Vogt, R.D., Akkanen, J., Andersen, D.O., Bruggemann, R., Chatterjee, B., Gjessing, E., Kukkonen, J.V.K., Larsen, H.E., Luster, J., Paul, A., Pflugmacher, S., Starr, M., Steinberg, C.E.W., Schmitt-Kopplin, P. & Zsolnay, A. 2004. Key site variables governing the functional characteristics of Dissolved Natural Organic Matter (DNOM) in Nordic forested catchments. *Aquatic Sciences*. **66**: 195-210.

Vogt, R.D., Gjessing, E., Andersen, D.O., Clarke, N., Gadmar, T., Bishop, K., Lundström, U. & Starr, M. 2001. *Natural Organic Matter in the Nordic countries*, NT Technical report. NORDTEST, Espoo.

Yano, Y., Lajtha, K., Sollins, P. & Caldwell, B.A. 2004. Chemical and seasonal controls on the dynamics of dissolved organic matter in a confiferous old-growth stand in the Pacific Northwest, USA. *Biogeochemistry*. **71**: 197-223.

5 Heterogeneity of water-dispersible soil colloids investigated by Scanning Transmission X-ray Microscopy and C-1s NEXAFS microspectroscopy

M. Schumacher, I. Christl, A.C. Scheinost, C. Jacobsen and R. Kretzschmar
Submitted for publication in Environmental Science & Technology

Summary

Colloid release and deposition in natural porous media and the sorption of inorganic and organic pollutants to mobile colloids are strongly influenced by the composition and chemical heterogeneity of the colloidal particles. To investigate the chemical heterogeneity of organic soil colloids at the particle scale, we used synchrotron scanning transmission X-ray microscopy (STXM) and C-1s near edge X-ray absorption fine structure (NEXAFS) spectroscopy on 49 individual particles isolated from the surface horizons of three forest soils. Stacks of 130 images of each particle were collected at different X-ray energies between 280 to 310 eV. From these image arrays, C-1s NEXAFS spectra were obtained and analyzed by principle component analysis and cluster analysis to characterize the intra-particle heterogeneity of the organic components. The chemical heterogeneity of the organic colloid components is discussed at different scales: (i) *intra-particle heterogeneity*, i.e., the chemical variations within individual particles, (ii) *inter-particle heterogeneity*, i.e., the chemical variations between particles isolated from the same soil horizon, and (iii) differences between colloidal particles isolated from different soils or soil horizons. The results demonstrate that the organic matter associated with water-dispersible soil colloids is heterogeneous at the single particle scale. However, differences in NEXAFS spectra obtained for different regions within single particles were in most cases smaller than the differences observed between the spectra of different particles isolated from the same soil horizon (*inter-particle heterogeneity*). At the soil profile scale, no significant differences in the average composition of water-dispersible colloids from H and Ah horizons could be detected due to the high inter-particle heterogeneity.

5.1 Introduction

Mobile colloidal particles can serve as carriers for strongly sorbing contaminants and thereby facilitate contaminant transport in soils, groundwater aquifers, and fractured rocks (Grolimund *et al.*, 1996; Kretzschmar *et al.*, 1999; McCarthy & Zachara, 1989; Saiers & Hornberger, 1996). In soils and surface-near aquifers, mobile colloids usually consist of mixtures or complexes of phyllosilicates, hydrous oxides of Si, Fe and Al and natural organic matter. The mobility of colloids, and therefore the importance of colloid-facilitated transport of contaminants, strongly depends on colloid chemistry and colloidal stability in the geochemical environment (Kretzschmar *et al.*, 1999; Ryan & Elimelech, 1996). The colloidal stability of clay mineral and oxide particles is often greatly enhanced by the presence of adsorbed natural organic matter (Gibbs, 1983; Kretzschmar *et al.*, 1998; Tiller & O'Melia, 1993). It has also been shown that the stability, transport, and deposition of colloids in porous media are strongly affected by the chemical heterogeneity of the colloidal particle and matrix surfaces (Johnson *et al.*, 1996; Song & Elimelech, 1994). However, little is known about the nature of natural organic matter associated with mobile soil colloids and the heterogeneity of the colloids at the particle scale.

At the soil profile scale, the chemical composition of soil organic matter (SOM) is often quite variable. For example, Spielvogel et al. (2004) demonstrated that the functional group distribution of SOM, determined by ^{13}C-NMR spectroscopy, exhibited large variations for 42 top soil horizons from different soil types located in Germany. This heterogeneity of SOM was explained by the variable organic input materials as well as differences in moisture and temperature conditions favoring different decomposition processes (Kögel-Knabner *et al.*, 1988; Lydersen, 1995). On the other hand, ^{13}C-NMR studies on chemical composition of SOM investigated as a function of soil depth, showed that the degradation of organic materials with different initial composition led to the formation of soil organic matter with remarkably similar functional group distribution (Dignac *et al.*, 2002; Mahieu *et al.*, 1999). Although ^{13}C-NMR spectroscopy is a very powerful tool to investigate the chemical composition of soil organic matter at the profile scale, no information can be obtained about the heterogeneity of soil colloids at the particle scale. In recent years, synchrotron scanning transmission X-ray microscopy (STXM) combined with near-edge X-ray absorption fine structure (NEXAFS) spectroscopy has been developed for combined imaging and spectroscopic characterization of thin organic specimen.

For example, this technique has been applied to quantify carbon bound in major functional groups in a variety of environmental samples, ranging from petroleum (Hitchcock *et al.*, 1986; Waldo *et al.*, 1991) and coal (Cody *et al.*, 1995; Spiro *et al.*, 1984) to atmospheric and interplanetary dust particles (Flynn *et al.*, 2003; Russell *et al.*, 2002). Thieme et al. (2003) investigated the structures of microorganisms and carbonate precipitates in soils using STXM and C-1s NEXAFS spectroscopy. First studies on the chemistry of soil organic matter (Scheinost *et al.*, 2001) and the characterization of organic colloids using STXM and NEXAFS spectroscopy are also available (Schäfer *et al.*, 2003). Here, we present the first study on the chemical heterogeneity of organic matter in water-dispersible soil colloids using synchrotron scanning transmission X-ray microscopy (STXM) and C-1s NEXAFS micro-spectroscopy. By investigating a total of 49 individual soil particles isolated from three soils, we obtained new information about the chemical heterogeneity within single particles (*intra-particle heterogeneity*) and the chemical variations between different particles from each soil horizon (*inter-particle heterogeneity*).

5.2 Materials and Methods

5.2.1 Soil samples and isolation of water-dispersible colloids

Soil samples were taken along a toposequence located on a lateral moraine near Langenthal, northern Switzerland. The first site (Riedhof, RH, 525 m elevation) is situated on top of the lateral moraine and the soil is classified as a Dystric Luvisol (ISSS-ISRIC-FAO, 1998). The second site (Oberrickenzopfen, ORZ, 505 m elevation) is located on the mid-slope of the moraine and the soil is a humic Gleysol. The third site (Unterrickenzopfen, URZ, 490 m elevation) is located at the bottom of the moraine and the soil is also classified as a humic Gleysol. All three sites are forested, with beech trees (*Fagus sylvatica*) dominating at the Riedhof site and spruce trees (*Picea abies*) dominating at the other two sites, respectively. The region has a humid-temperate climate, with an annual mean temperature of 8.7 °C and 1154 mm mean annual precipitation. At all three sites, we sampled the well-humified organic surface horizons (H) and the top mineral horizons (Ah). After sampling, the field-moist soil material was passed through a 5-mm sieve and stored in the dark at -17 °C. Water-dispersible soil colloids were isolated from frozen soil samples using the following procedure. Two hundred grams of moist soil was suspended in 1 L of deionized water, shaken for 8 h at 25 ± 1 °C, and centrifuged for 6 min at 2500 g. Aliquots of the supernatant suspensions containing the water-dispersible soil colloids were transferred into 50-mL glass vials, stored in the dark at room temperature and analyzed within a few days.

In addition to water-dispersible colloids, we also isolated the humic acid and fulvic acid fractions of each soil horizon using standard IHSS procedures (Thurman & Malcolm, 1981) and a water-soluble dissolved organic carbon (DOC) fraction. The DOC was obtained by suspending two hundred grams of most soil in 1 L of deionized water, shaking it for 12 h at 25 ± 1 °C and centrifuging at for 20 min at 900 g. The supernatant suspension was passed through a 0.45 µm membrane filter (Schleicher & Schüll, Dassel, Germany), dialysed for one week against deionized water (SpectraPor 2, Spectrum, Breda, Netherlands) and freeze-dried.

5.2.2 X-ray microscopy and micro-spectroscopy

In total, 49 colloidal particles from the six different soil horizons were imaged using STXM and further characterized by C-1s NEXAFS micro-spectroscopy on beamline X-1A at the National Synchrotron Light Source, Brookhaven National

Laboratory, Upton, NY. For specimen preparation, one drop of soil colloid suspension was deposited onto a Si_3N_4 window (Silson Ltd., Northampton, UK) with 100 nm thickness, which was previously glued onto the wet-cell of the microscope. The wet-cell was then closed by covering it with another Si_3N_4 window and screwing both parts together (Neuhäusler *et al.*, 2000). A mean sample thickness of about 100 nm was obtained with three adjustable screws in the wet-cell. The sample thickness is important in order to obtain a good signal-to-noise ratio in NEXAFS spectroscopy (Urquhart *et al.*, 1999a). A sample thickness of 100 nm is ideal, whereas thinner samples suffer from poor signal-to-noise ratios and thicker samples show split absorption peaks due to absorption saturation. The STXM was operated inside a He purge enclosure at room temperature and atmospheric pressure. For calibration purposes, CO_2 gas was added to the He purge in the microscope and normalized to -8.01 eV relative to the C-1s→3s transition (292.8 eV). Details on the instruments specifications have been reported elsewhere (Jacobsen *et al.*, 1991; Kirz *et al.*, 1991). After mounting the wet-cell sample on the sample holder, spectra were recorded using an automated imaging routine, which collects sets of images at X-ray energies ranging from 280 eV to 310 eV in energy steps of 0.5 eV, except near the absorption edge (282 to 290 eV), where the step size was reduced to 0.1 eV. In total, 130 images were recorded from each particle and aligned afterwards using an autocorrelation routine in order to remove possible offsets in the image array. Particular care was taken of the background correction of the spectra. Image regions which did not contain detectable amounts of carbon were chosen and used as the background I_o. Absorbance (A) spectra were then derived from the transmitted X-ray intensity (I), assuming validity of Beer's law with $A = \mu\rho t = -\ln(I/I_o)$, where μ is the energy dependent mass absorption coefficient, ρ is the sample density and t is the sample thickness (Kirz *et al.*, 1991). In order to allow quantitative comparisons, all collected spectra were normalized to the absorbance at 310 eV (Stöhr, 1996). The spectral data was extracted from the image stacks by using the IDL routines "stack_analyze" and "spectra_gui", written by Jacobsen et al. (2000). Principal component analysis (PCA) and cluster analysis (CA) were carried out on the same image stacks, using an IDL program routine written by Lerotic et al. (2004). A semi-quantitative analysis of NEXAFS spectra was carried out by peak deconvolution using the program WinXAS 3.1 (Ressler, 2004).

Table 5.1:
C-1s NEXAFS peak energies, corresponding transitions and assignments.

Energy	Transition	Functional group
285.0 eV	C (1s)→π*	C_{arom}–H, C_{arom}–C Aromatic C
286.5 eV	C (1s)→π*	C_{arom}–O Phenolic C
288.5 eV	C (1s)→π*	COOH Carboxyl C
289.5 eV	C (1s)→π*	C–O O-Alkyl C
290.5 eV	C (1s)→π*	C=O Carbonyl C

The following peak assignments were considered as given in Table 5.1. The peak at energies around 285 eV was assigned to the photoinduced transition of an electron from the 1s orbital to an aromatic π* orbital (Urquhart *et al.*, 2000) and will herein be referred to as aromatic C. The second peak at around 286.5 eV was assigned to transitions taking place for O-substituted aromatic carbon, as in the case of phenol or aryl ether (Cody *et al.*, 1995) and will be referred to as phenolic C. The most intense peak at 288.5 eV was assigned to carboxyl carbon (Urquhart *et al.*, 1999b). The spectral feature at 289.5 eV was assigned to transitions of O-alkyl carbon (Scheinost *et al.*, 2001), whereas the last peak could be assigned to carbonyl carbon (Urquhart & Ade, 2002). For all spectral assignments listed above, Gaussian peaks with a fixed full width at half maximum (FWHM) of 1 eV were fitted to the data from 280 eV to 310 eV. The ionization threshold was described with an arctangent function at 290 eV with a FWHM of 1. In addition, σ*-transitions were simulated by two Gaussian functions with maxima around 294 eV and 303 eV and FWHMs of ≤ 10 eV and ≤ 8 eV, respectively. In order avoid deformation of these two Gaussian functions, the region of K L_{II}- and L_{III}-edges between 295 eV and 302 eV was omitted in the spectral deconvolution of all particles. Although only K-bearing particles were affected by spectral distortions within this specific region during the fitting procedure, it was applied to all particle spectra in order to assure spectral comparability of all particles. For all 49 particle spectra included in the analysis, the sum of the residuals of the fit was less than 8. For the quantitative analysis, the sum of all five π*-transitions (aromatic, phenolic, carboxyl, O-alkyl and carbonyl C) was set to 100 %. The peak areas of the π*-transitions were transformed into values representing

the percentage of carbon bound in the respective functional carbon group. The correlation functions used for data transformation were taken from Schumacher et al. (2005). Since for most colloids, C-1s NEXAFS peak areas of O-alkyl carbon exceeded the calibration range reported by Schumacher et al. (2005), transformed values are not reliable for O-alkyl carbon and will not be reported.

5.3 Results and Discussion

5.3.1 Heterogeneity of colloids at the particle scale

The heterogeneity of organic matter associated with water-dispersible soil colloids was first investigated at the particle scale. Figure 5.1 shows an example of a particle isolated from the H horizon of the Unterrickenzopfen (URZ) soil. The first image (Fig. 5.1a) was recorded at an X-ray energy of 280 eV, that is, below the C-1s edge energy of carbon (283 eV). The image contrast is produced mainly by absorption of X-ray energy by inorganic components within the particle. The second image (Fig. 5.1b) was recorded at an X-ray energy of 290 eV, i.e., above the C-1s absorption edge of carbon. In this case, carbon also produces a strong image contrast and organic-rich regions within the colloidal particle also become visible. Further characterization of the heterogeneity of natural organic matter associated with the colloidal particles was achieved by principle component and cluster analysis (PCA-CA) of C-1s NEXAFS spectra. Figures 5.1c and 5.1d show the results, in this case yielding three distinct regions. The blue color represents the background without detectable amounts of carbon. The inner region (red) appeared denser and was slightly richer in aromatic carbon, while the outer region (green) appeared to be less dense and richer in carboxyl, O-alkyl and carbonyl carbon. Possibly, the components rich in carboxyl carbon were more negatively charged and more hydrophilic, while the dense inner region was more aromatic and therefore more hydrophobic. Figure 5.2 shows the corresponding results for a water-dispersible colloidal particle isolated from the organic Ah horizon of the Unterrickenzopfen soil. The two images (Fig. 5.2a, 5.2b) recorded below and above the C-1s absorption edge demonstrate that the particle (or aggregate), which is about 2 µm in diameter, is composed of both mineral and organic components. Again, PCA-CA analysis yielded two distinct regions within the colloidal particle (Fig. 5.2c).

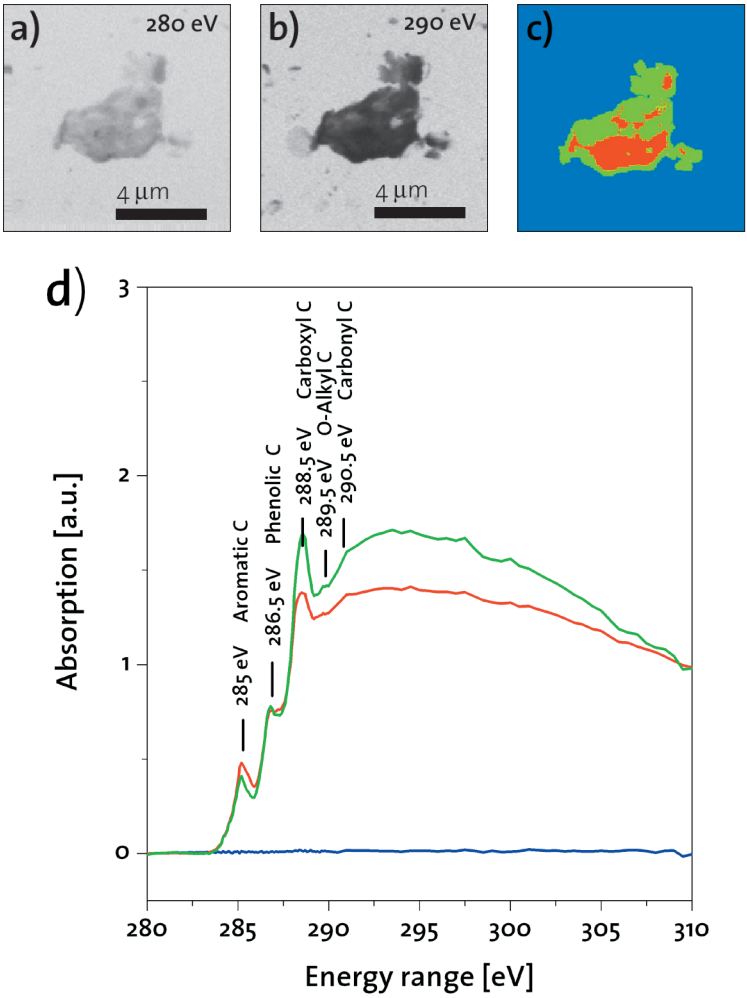

Figure 5.1:
Intra-particular heterogeneities of a colloidal particle from the H-horizon at Unterrickenzopfen. Images a) and b) were taken at 280 eV and 290 eV, i.e., below and above the C-1s absorption threshold. Figures c) and d) show the areas of the three chemically different regions as evaluated by cluster analysis and the respective average C-1s spectra in corresponding colors.

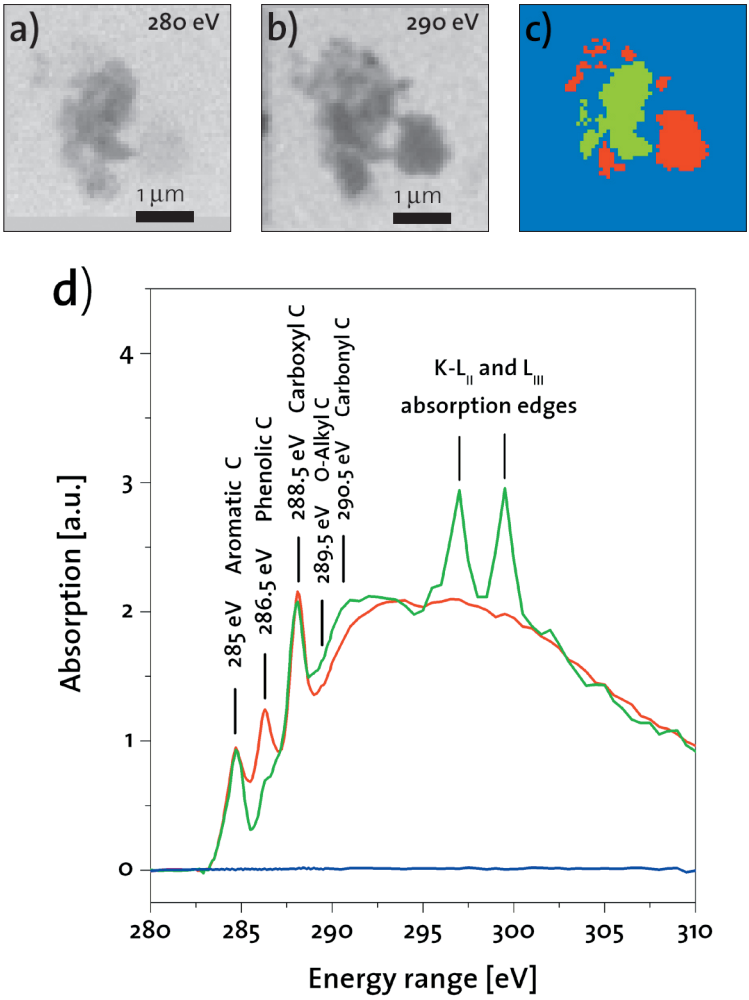

Figure 5.2:
Intra-particular heterogeneity of a colloidal particle from the Ah-horizon at Unterrickenzopfen. Images a) and b) were taken at 280 eV and 290 eV, i.e., below and above the C-1s absorption threshold. Figures c) and d) show the areas of the three chemically different regions as evaluated by cluster analysis and the respective average C-1s spectra in corresponding colors.

The C-1s spectra of the two distinct regions within the particle show remarkable differences (Fig. 5.2d). This time, the green color represents regions within the particle that contain mineral components in addition to organic carbon, while the red color represents regions that contain mainly organic substances. The peak intensities for aromatic (285.0 eV) and carboxyl (288.5 eV) carbon in both spectra are very similar. However, the highly organic regions (red) appear richer in phenolic carbon, as indicated by a stronger peak at 286.6 eV. The strong peaks at 297 and 300 eV in the spectrum for the mineral-rich regions (green) are due to the potassium L_{II}- and L_{III}-absorption edges, respectively. This suggests that the mineral components may consist of K-bearing phyllosilicates, such as illite.
The two examples, which served to illustrate characteristic features observed for 49 particles, demonstrate for the first time that the organic matter associated with water-dispersible soil colloids is chemically heterogeneous at the particle scale. In the H horizons, the greatest differences tended to be observed in the contents of aromatic, carboxyl and O-alkyl carbon, while the peaks for phenolic and carbonyl carbon were rather invariable. In Ah horizons, we observed the greatest differences in the contents of phenolic and O-alkyl carbon, while the peak intensities assigned to aromatic, carboxyl, and carbonyl carbon tended to be rather constant. Although clearly detectable, the differences in NEXAFS spectra between regions of single particles (intra-particle heterogeneity) were much smaller than differences between averaged spectra of different particles isolated from the same horizon (inter-particle heterogeneity). This inter-particle heterogeneity is discussed in the next section.

5.3.2 Inter-particle heterogeneity

The inter-particle chemical heterogeneity of the water-dispersible soil colloids was analyzed on the basis of the C-1s NEXAFS spectra of all particles analyzed from each horizon (n = 3 to 14). The single particle spectra were obtained by averaging normalized NEXAFS spectra for all pixels within the entire particle region, e.g., the red and green regions in Figure 5.1 and 5.2. The average of all single particle spectra for each horizon then gave a mean spectrum for the water-dispersible colloids of that respective soil horizon. Selected spectra for the Unterrickenzopfen H horizon are presented in Figure 5.3. The first spectrum shows the averaged spectrum representing the entire population of water-dispersible colloids. The following four spectra are examples of single particle spectra within that population of particles, illustrating the variability of particles within this soil horizon. The bottom three spectra are from the humic acid (HA), fulvic acid (FA), and

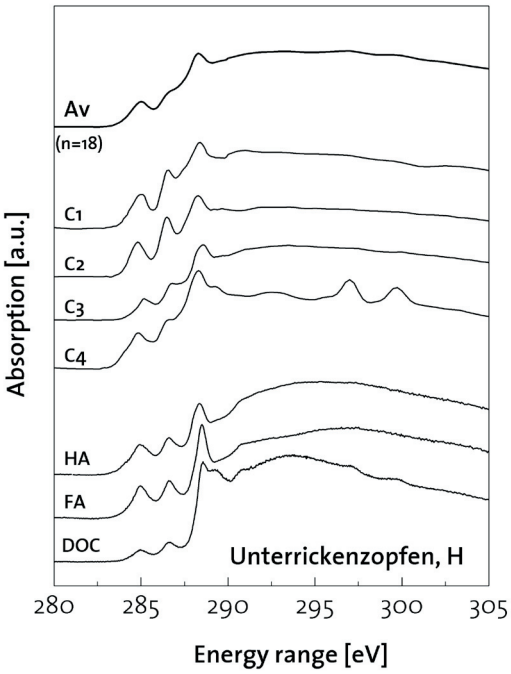

Figure 5.3:
C-1s NEXAFS spectra of four colloidal particles (C1 – C4) extracted from the H-horizon at Unterrickenzopfen. The average spectrum (Av) represents the averaged spectra for all investigated particles of the respective soil horizon. The number of n corresponds to the total number of particles evaluated. At the bottom, spectra for extracted humic acid (HA), fulvic acid (FA) and DOC are shown.

dissolved organic carbon (DOC) isolated from the same soil for comparison. The single particle spectra of the H horizon exhibited a rather large variability in peak intensities for aromatic and phenolic carbon, while the peak intensities for carboxyl, O-alkyl and carbonyl carbon were less variable. One of total fourteen particles showed clear potassium absorption peaks at 297 eV and 300 eV, suggesting that this particle was an association of clay minerals and organic matter. In order to compare the composition of organic components associated with water-dispersible soil colloids with more traditional fractions of soil organic matter, we also analyzed the humic acid (HA), fulvic acid (FA) and water-soluble organic carbon (DOC) fractions of the H horizon (Fig. 5.3). The spectrum for HA and FA had similar peak intensities for aromatic, phenolic, O-alkyl and carbonyl carbon, but the FA exhibited a much stronger peak for carboxyl carbon. The DOC spectrum showed a somewhat different pattern: Peak intensities arising from aromatic and phenolic carbon were lower for DOC than for humic and fulvic acid. In addition, very pronounced peaks appeared in the DOC spectrum for carboxyl, O-alkyl and carbonyl carbon. Comparison of the spectra suggests that the organic matter associated with water-dispersible soil colloids was most similar to the humic acid fraction.

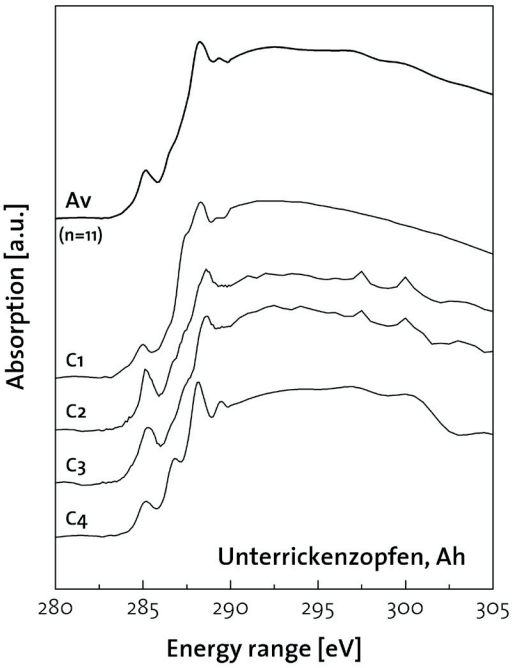

Figure 5.4:
C-1s NEXAFS spectra of four colloidal particles (C1 – C4) extracted from the Ah-horizon at Unterrickenzopfen. The average spectrum (Av) represents the averaged spectra for all investigated particles of the respective soil horizon. The number of n corresponds to the total number of particles evaluated.

The average spectrum of water-dispersible colloids from the Unterrickenzopfen Ah horizon and selected single particle spectra of that population are depicted in Figure 5.4. The particle spectra showed distinct differences in peak intensities for aromatic and carboxyl carbon, while peak intensities for phenolic, O-alkyl and carbonyl carbon remained fairly stable. Four of total eleven particles showed potassium absorption features in their spectra, again suggesting the presence of K-bearing clay minerals. This is expected, since the Ah horizon is a mineral soil horizon containing large quantities of clay minerals. The relative amounts of aromatic, phenolic, carboxyl, and carbonyl carbon of all 49 single particles from six soil horizons are summarized in Figure 5.5. The box plots show the minimum and maximum (stars), 25 and 75 percentiles (upper and lower corners of open polygons), median (dashed line) and mean value (square symbol). The plot depicts the relative amounts of carbon groups as determined by C-1s NEXAFS spectroscopy, calibrated against ^{13}C-NMR spectroscopy (Schumacher *et al.*, 2005). Overall, the inter-particle heterogeneity of organic functional group composition was somewhat larger in the H horizons than in the Ah horizons, especially in abundances of aromatic carbon groups. The contrary could be observed for abundances of carboxyl carbon groups, where particles extracted from Ah horizons exhibited larger variations than particles derived from the H horizons, as explained in the next section.

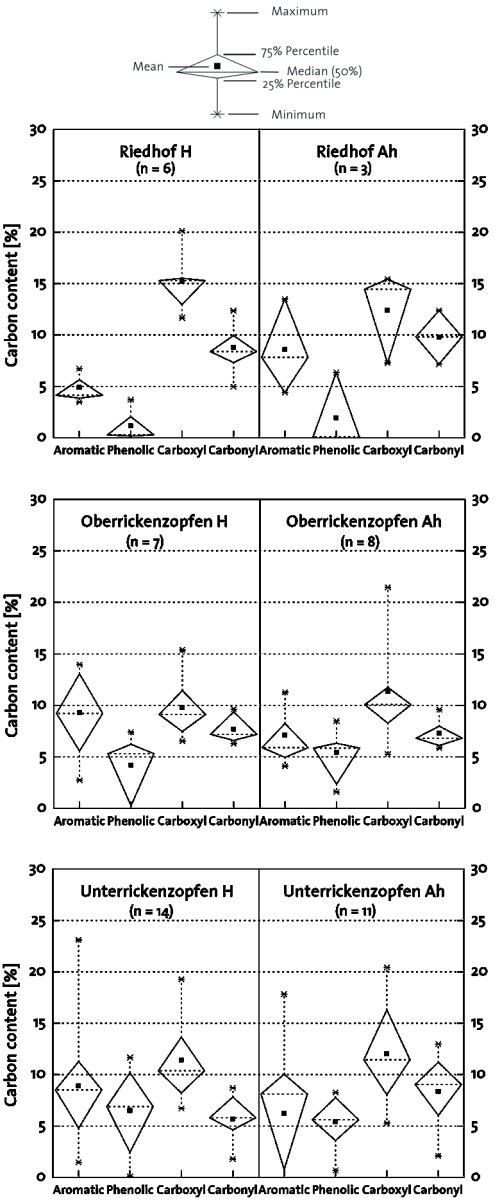

Figure 5.5:
Distribution of carbon functional groups as determined by C-1s NEXAFS spectroscopy for water-dispersible colloids extracted from organic soil horizons (H) and top mineral soil horizons (Ah) of the locations Riedhof, Oberrickenzopfen and Unterrickenzopfen. The value of n corresponds to the total number of particles evaluated for the respective horizon. Note the legend on top for description.

5.3.3 Water-dispersible colloids from different soil horizons

The average functional group composition of organic matter associated with water-dispersible soil colloids isolated from the H and Ah horizons of the three forest soils can also be compared in Figure 5.5. Due to the large inter-particle variability discussed in the previous section, significant differences between the H and Ah horizons were not be detected. However, several trends can be observed. The median values for amounts of aromatic carbon in all soil horizons ranged between 5 % and 9 %. No significant differences between H and Ah horizons were observed. The amounts for phenolic carbon were slightly more variable and the median values ranged from 0 % in the Riedhof H to 7 % in the Unterrickenzopfen H horizon. Amounts for carboxyl carbon exhibited the same variability with median values ranging from 9 % for the Oberrickenzopfen H to 15 % in the Riedhof H. Finally, carbonyl carbon gave median amounts between 6 % in the Unterrickenzopfen H and 10 % in the Riedhof Ah horizons whereas the variability for all horizons was smallest for this carbon group. In summary, evaluation of C-1s NEXAFS spectra of 49 water-dispersible soil colloids extracted from six different soil horizons revealed a high inter-particle variability in organic functional group composition, especially in abundances of aromatic and carboxyl carbon. Particles extracted from H horizons exhibited slightly larger variations in contents of aromatic carbon groups, whereas particles extracted from Ah showed higher differences in amounts of carboxyl bound carbon. This may be explained by increasing humification of organic matter components with increasing soil depth, where aromatic structures are broken down and oxidized with further formation of carboxyl functional groups with increasing depth. Mahieu et al. (1999) reported that ^{13}C-NMR spectra of soil organic matter from various soils were increasingly similar to each other with increasing soil depth, which was also explained by the degree of humification. Chemical heterogeneities within single colloidal particles (intra-particle heterogeneity) were clearly detectable, but the differences were relatively small compared to the very large inter-particle heterogeneity that was observed for all 49 particles investigated.

Acknowledgements

This project was financially supported by the ETH Zurich (TH project Nr. 01753). All NEXAFS analyses were performed at beamline X-1A at the National Synchrotron Light Source at the Brookhaven National Laboratory in Upton, N.Y., which is supported by the U.S. Department of Energy. Operation of the Stony Brook STXM is supported by National Science Foundation grants CHE-0221934 and OCE-0221029. Furthermore, the authors would like to gratefully acknowledge S. Wirick, Dr. T. Beetz and Dr. M. Feser of the Department of Physics, SUNY Stony Brook, and K. Barmettler from ETH Zurich for their contribution and support to this work.

Literature cited

Cody, G.D., Botto, R.E., Ade, H., Behal, S., Disko, M. & Wirick, S. 1995. Inner-shell spectroscopy and imaging of a subbituminous coal: In-situ analysis of organic and inorganic microstructure using C(1s)-, Ca(2p)-, and Cl(2s)-NEXAFS. *Energ. Fuel.* **9**: 525-533.

Dignac, M.-F., Kögel-Knabner, I., Michel, K., Matzner, E. & Knicker, H. 2002. Chemistry of soil organic matter as related to C:N in Norway spruce forest (Picea abies (L.) Karst.) floors and mineral soils. *J. Plant Nutr. Soil Sci.* **165**: 281-289.

Flynn, G., Keller, L.P., Wirick, S., Jacobsen, C. & Sutton, S.R. 2003. Analysis of interplanetary dust particles by soft and hard X-ray microscopy. *J. Phys. IV*. **104**: 367-372.

Gibbs, R.J. 1983. Effect of natural organic matter coatings on the coagulation of particles. *Environ. Sci. Technol.* **17**: 237-240.

Grolimund, D., Borkovec, M., Barmettler, K. & Sticher, H. 1996. Colloid-facilitated transport of strongly sorbing contaminants in natural porous media: A laboratory column study. *Environ. Sci. Technol.* **30**: 3118-3123.

Hitchcock, A.P., Newbury, D.C., Ishii, I., Stöhr, J., Horsley, J.A., Redwing, R.D., Johnson, A.L. & Sette, F. 1986. Carbon K-shell excitation of gaseous and condensed cyclic hydrocarbons: C_3H_6, C_4H_8, CH_8, C_5H_{10}, C_6H_{10}, C_6H_{12} and C_8H_8. *J. Chem. Phys.* **85**: 4849-4862.

ISSS-ISRIC-FAO. 1998. *World Reference Base for Soil Resources*. International Society of Soil Science, Rome.

Jacobsen, C., Williams, S., Anderson, E., Browne, M.T., Buckley, C., Kern, D., Kirz, J., M., R. & Zhang, X. 1991. Diffraction-limited imaging in a scanning transmission x-ray microscope. *Opt. Commun.* **86**: 351-364.

Jacobsen, C., Wirick, S., Flynn, G. & Zimba, C. 2000. Soft x-ray spectroscopy from image sequences with sub-100nm spatial resolution. *J. Microsc.* **197**: 173-184.

Johnson, P.R., Sun, N. & Elimelech, M. 1996. Colloid transport in geochemically heterogeneous porous media: Modeling and measurements. *Environ. Sci. Technol.* **30**: 3284-3293.

Kirz, J., Ade, H., Jacobsen, C., Ko, C.H., Lindaas, S., McNulty, I., Sayre, D., Williams, S., Zhang, X. & Howells, M. 1991. Soft x-ray microscopy with coherent x-rays. *Rev. Sci. Instrum.* **63**: 557-563.

Kögel-Knabner, I., Zech, W. & Hatcher, P. 1988. Chemical composition of the organic matter in forest soils: The humus layer. *Z. Pflanzenern. Bodenkunde*. **151**: 331-340.

Kretzschmar, R., Borkovec, M., Grolimund, D. & Elimelech, M. 1999. Mobile subsurface colloids and their role in contaminant transport. *Adv. Agron.* **66**: 121-194.

Kretzschmar, R., Holthoff, H. & Sticher, H. 1998. Influence of pH and humic acid on coagulation kinetics of kaolinite: A dynamic light scattering study. *J. Colloid Interf. Sci.* **202**: 95-103.

Lerotic, M., Jacobsen, C., Schäfer, T. & Vogt, S. 2004. Cluster analysis of soft X-ray spectromicroscopy data. *Ultramicroscopy*. **100**: 35-57.

Lydersen, E. 1995. Effect of cold and warm years on the water chemistry at the Birkenes catchment. *Water Air Soil Poll.* **84**: 217-232.

Mahieu, N., Powlson, D.S. & Randall, E.W. 1999. Statistical analysis of published carbon-13 CP-MAS NMR spectra of soil organic matter. *Soil Sci. Soc. Am. J.* **63**: 307-319.

McCarthy, J.F. & Zachara, J.M. 1989. Subsurface transport of contaminants. *Environ. Sci. Technol.* **23**: 496-502.

Neuhäusler, U., Jacobsen, C., Schulze, D.G., Scott, D. & Abend, S. 2000. A specimen chamber for soft X-Ray spectromicroscopy on aqueous and liquid samples. *J. Synchrotron Radiat*. **7**: 110 -112.

Ressler, T. 2004. www.winxas.de.

Russell, L.M., Maria, S.F. & Myneni, S.C.B. 2002. Mapping organic coatings on atmospheric particles. *Geophys. Res. Lett*. **29**: 26/21-26/24.

Ryan, J.N. & Elimelech, M. 1996. Colloid mobilization and transport in groundwater. *Colloid Surface A*. **107**: 1-56.

Saiers, J.E. & Hornberger, G.M. 1996. The role of colloidal kaolinite in the transport of cesium through laboratory sand columns. *Water Resour. Res.* **32**: 33-41.

Schäfer, T., Claret, F., Bauer, A., Griffault, L., Ferrage, E. & Lanson, B. 2003. Natural organic matter (NOM)-clay association and impact on Callovo-Oxfordian clay stability in high alkaline solution: Spectromicroscopic evidence. *J. Phys. IV*. **104**: 413-416.

Scheinost, A.C., Kretzschmar, R., Christl, I. & Jacobsen, C. 2001. In: *Humic Substances: Structures, Models and Functions* (E.A. Ghabbour & G. Davies eds.) Royal Society of Chemistry, Cambridge. p. 37 -40.

Schumacher, M., Scheinost, A.C., Christl, I., Jacobsen, C. & Kretzschmar, R. 2005. Can C-1s NEXAFS spectroscopy be used to quantify functional C groups in humic substances? *Eur. J. Soil Sci.* submitted.

Song, L. & Elimelech, M. 1994. Transient deposition of colloidal particles in heterogeneous porous media. *J. Colloid Interf. Sci.* **167**: 301-313.

Spielvogel, S., Knicker, H. & Kögel-Knabner, I. 2004. Soil organic matter composition and soil lightness. *J. Plant Nutr. Soil Sci.* **167**: 545-555.

Spiro, C.L., Wong, J., Lytle, F.W., Geegor, R.B., Maylotte, D.H. & Lamson, S.H. 1984. X-ray absorption spectroscopic investigation of sulfur sites in coal: Organic sulfur identification. *Science*. **226**: 48-50.

Stöhr, J. 1996. *NEXAFS spectroscopy*. Springer, Berlin.

Thieme, J., Schneider, G. & Knöchel, C. 2003. X-ray tomography of a microhabitat of bacteria and other soil colloids with sub-100nm resolution. *Micron*. **34**: 339-344.

Thurman, E.M. & Malcolm, R.L. 1981. Preparative isolation of aquatic humic substances. *Environ. Sci. Technol.* **15**: 463-466.

Tiller, C.L. & O'Melia, C.R. 1993. Natural organic matter and colloidal stability: Models and measurements. *Colloid Surface A*. **73**: 89-102.

Urquhart, S.G. & Ade, H. 2002. Trends in the carbonyl core (C 1s, O 1s) - π^* C=O transition in the near-edge X-ray absorption fine structure spectra of organic molecules. *J. Phys. Chem. B*. **106**: 8531-8538.

Urquhart, S.G., Ade, H., Rafailovich, M., Sokolov, J.S. & Zhang, Y. 2000. Chemical and vibronic effects in the high-resolution near-edge X-ray absorption fine structure spectra of polystyrene isotopomers. *Chem. Phys. Lett*. **322**: 412 -418.

Urquhart, S.G., Hitchcock, A.P., Smith, A.P., Ade, H., Lidy, W., Rightor, E.G. & Mitchell, G.E. 1999a. NEXAFS spectromicroscopy of polymers: overview and quantitative analysis of polyurethane polymers. *J. Electron Spectrosc*. **100**: 119-135.

Urquhart, S.G., Smith, A.P., Ade, H., Hitchcock, A.P., Rightor, E.G. & Lidy, W. 1999b. Near-edge x-ray absorption fine structure spectroscopy of MDI and TDI polyurethane polymers. *J. Phys. Chem. B*. **103**: 4603-4610.

Waldo, G.S., Mullins, O.C., Penner-Hahn, J.E. & Cramer, S.P. 1991. Determination of the chemical environment of sulphur in petroleum asphaltenes by X-ray absorption spectroscopy. *Fuel*. **70**: 549-559.

6 Conclusions and outlook

This work focused on the investigation of the chemical heterogeneity occurring in natural organic matter and humic substances by the use of STXM and C-1s NEXAFS spectroscopy. The topic of the research conducted in this thesis was the improvement of the qualitative and quantitative interpretation of C-1s NEXAFS spectra in order to examine the chemical heterogeneity of humic substances and NOM as well as to provide an insight into NOM-mineral reactions at the particle scale.

In order to quantify the various features contributing to C-1s NEXAFS data, a spectral deconvolution scheme was applied on the C-1s NEXAFS spectra of well characterized reference humic substances. The results were compared with data derived from established quantification procedures, including statistical correlations. All deconvolution results were further compared with quantitative results obtained from solid-state CP-MAS ^{13}C-NMR spectroscopy. Calculated linear regression analysis demonstrated that a spectral deconvolution based on seven Gaussian lineshapes provided fair quantitative results for all major carbon groups present in humic substances. In order to resolve seasonal differences in carbon group chemistry of aquatic NOM, ten DOM samples taken in autumn and spring from five boreal freshwater catchments in Scandinavia were investigated by FT-IR, CP-MAS ^{13}C-NMR and C-1s NEXAFS spectroscopy. Spectral analysis revealed that particular seasonal variations within the carbon chemistry of the samples were not detectable by any of the three techniques and that all samples exhibited remarkable spectral uniformity. Determinations of radiocarbon ages showed that the average age of all samples was less than 50 years. These findings suggest the hypothesis that the DOM samples are derived from direct litter and biomass decomposition and are decomposed within very short timescales. However, since this carbon turnover seems to occur during several decades, seasonal variations between the samples are therefore not observable.

To investigate the chemical properties of the mobile fraction of natural organic matter in soils, the carbon functional group characteristics of 49 water-dispersible colloids, extracted from three different soils along a toposequence, were investigated by C-1s NEXAFS spectroscopy and STXM. Spectral analysis was carried out at the scale of particles, horizons and soils by using principal component and cluster analysis on all collected spectra. In order to quantify the changes in contents of reactive carbon functional groups, C-1s NEXAFS were deconvoluted according to the G-7 scheme presented in the previous chapter. The relative peak areas were further corrected and calibrated by applying calculated linear regressions obtained from ^{13}C-NMR spectroscopy. For the first time, the carbon group chemistry of hydrated colloidal particles could be investigated and quantified with high spatial resolution. Results showed that single particles, extracted from the same horizon and soil type, exhibited much higher differences in carbon functional group distribution than particles extracted from different soil types. Due to this high inter-particle heterogeneity, no significant variations between horizons or soil types could be observed.

The study of complex natural samples such as natural organic matter and humic substances is of great importance in environmental research. The use of STXM and C-1s NEXAFS spectroscopy techniques does not only permit the detection and quantification of specific carbon groups present in these environmental samples but also visualizes their spatial distribution at a micrometer scale. In situ investigation on hydrated environmental samples with high spatial resolution in combination with the capability of highlighting elements naturally by their absorbance is currently not possible by any other technique than STXM and is one of its intriguing advantages. Information about the chemical structure and the association of organic matter with clay minerals or iron-oxides in hydrated aggregates can be revealed and can help to develop further theoretical models about the interaction of these components in soil and aquatic environments. Spectral assignments of C-1s NEXAFS data and quantitative interpretation about the functional group chemistry of organic macromolecules are still in their early stages. The establishment of a NEXAFS spectroscopy database, similar to the spectroscopy database available for infrared spectroscopy, would greatly facilitate the identification and analysis of materials for which prior knowledge is very limited. In parallel to the development of such a database, theoretical modelling together with calculated electronic spectra, as performed by Kaznacheyev et al. (2002) for a wide range of amino acids, would help in the interpretation of NEXAFS spectra and the chemical structural information they

provide. The collection of NEXAFS spectra at the oxygen absorption edge may give additional information about the chemical bonding environment between carbon and oxygen. The correlation of C-1s with O-1s NEXAFS data can help in the development of a consistent quantification scheme that provides reliable data for at least all oxygen-containing carbon groups such as phenolic, carboxyl, O-alkyl or carbonyl C. Details on other complementary techniques such as small and wide angle X-ray scattering or X-ray emission could provide complementary information on the macromolecular structure of environmental samples and may help to establish C-1s NEXAFS spectroscopy and STXM as a substantial investigation tool in environmental research.

This work contributed to the development of a deeper knowledge of the physico-chemical properties of natural organic matter particles and their interaction with other chemical compounds in soil and aquatic ecosystems. The potential and limits of NEXAFS spectroscopy and STXM on the study of humic substances and natural organic matter as a novel tool for research in agriculture, forestry, soil and aquatic sciences have been described and offer the chance to make significant contributions to the understanding of the complex chemistry of NOM and its important role in environmental processes.

Appendix A

Location: Riedhof / BE

Soil type: Dystric Luvisol

Coordinates: 629.000 / 229.500

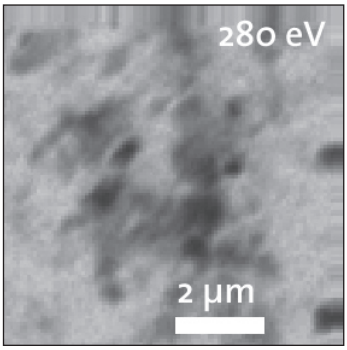

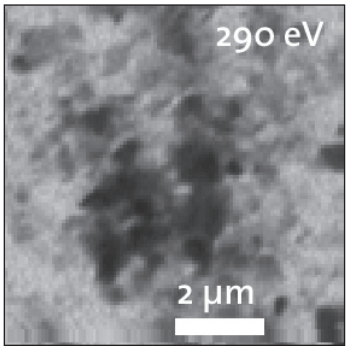

Riedhof

H-horizon

Stack 1

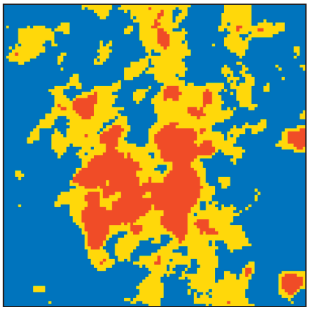

November
2003

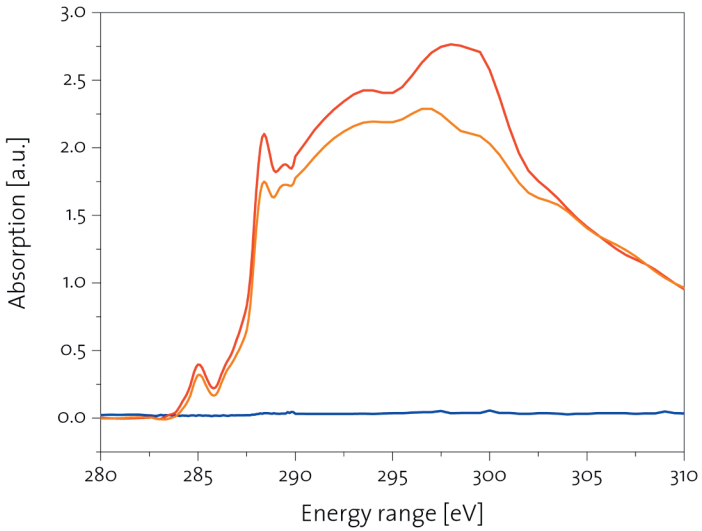

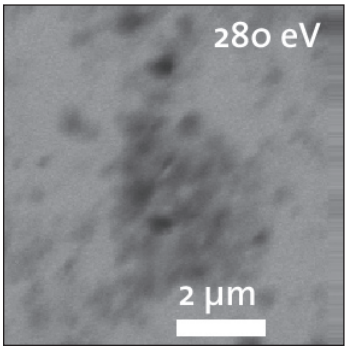

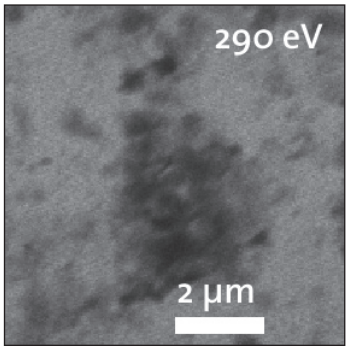

Riedhof

H-horizon

Stack 2

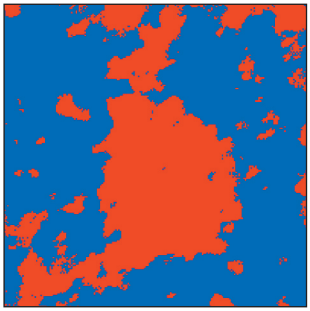

November
2003

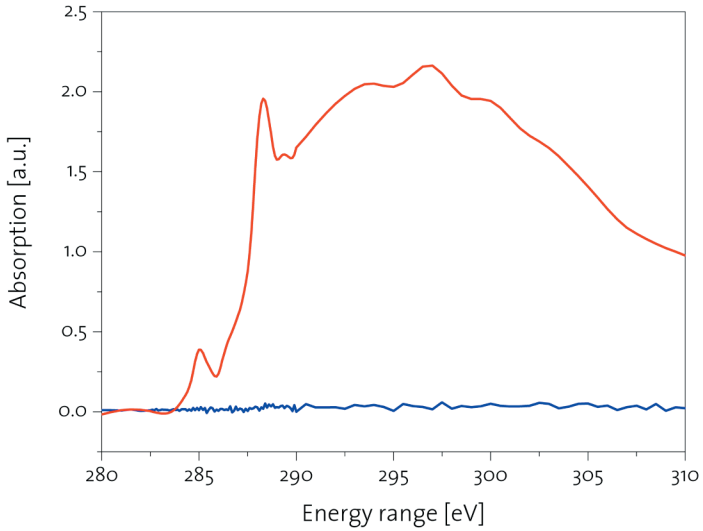

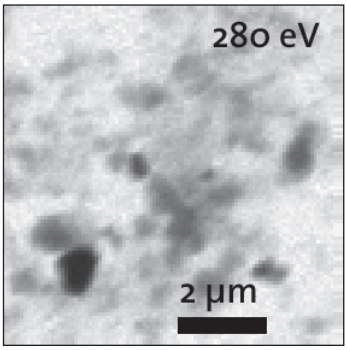

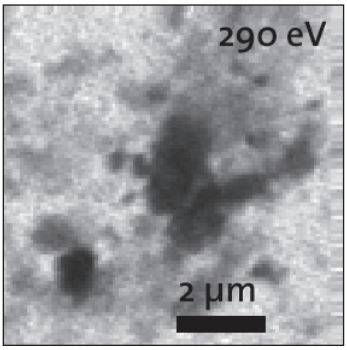

Riedhof

H-horizon

Stack 3

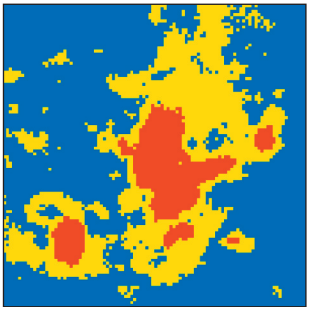

November
2003

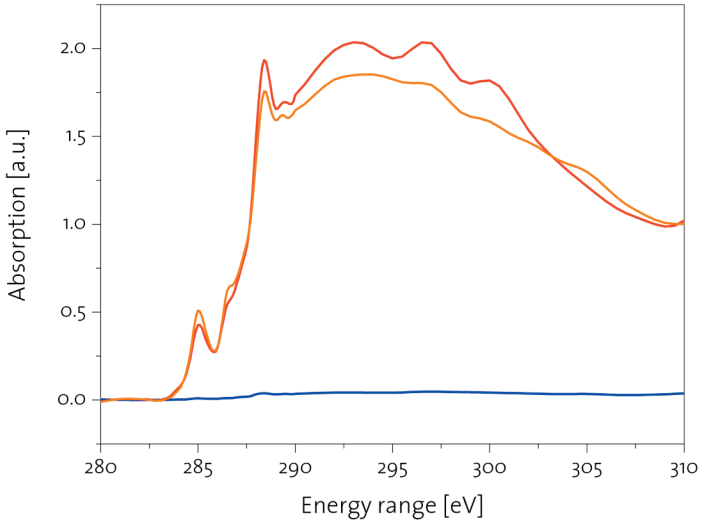

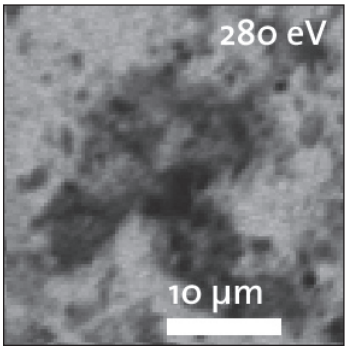

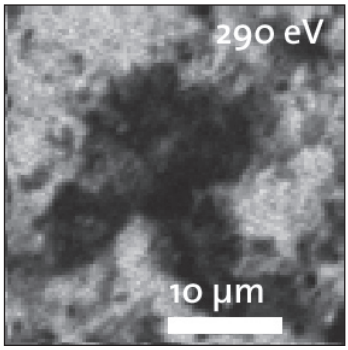

Riedhof

H-horizon

Stack 4

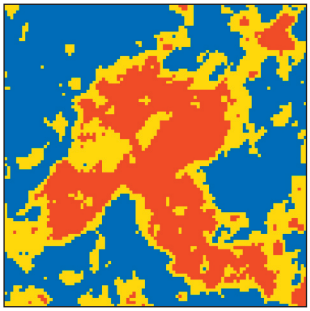

November
2003

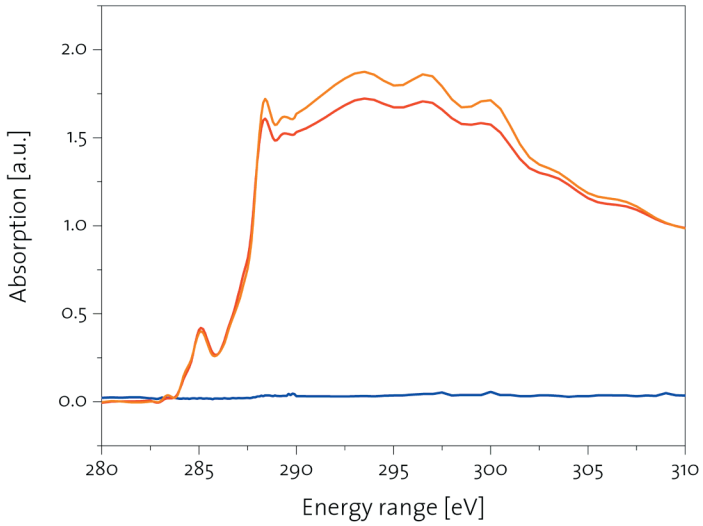

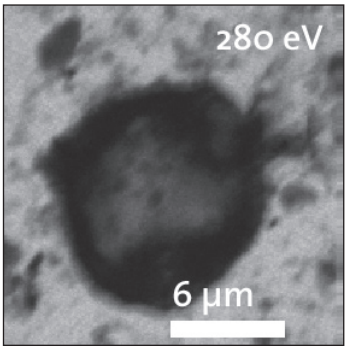

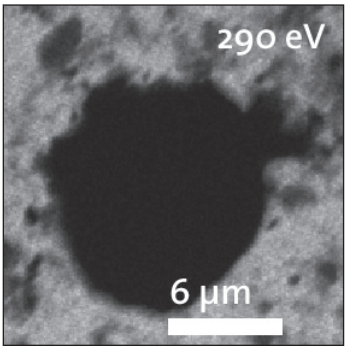

Riedhof

H-horizon

Stack 5

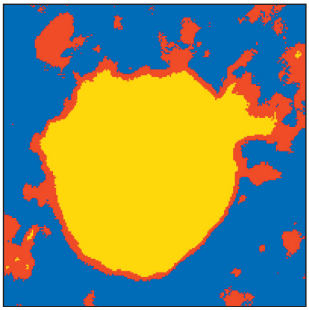

November
2003

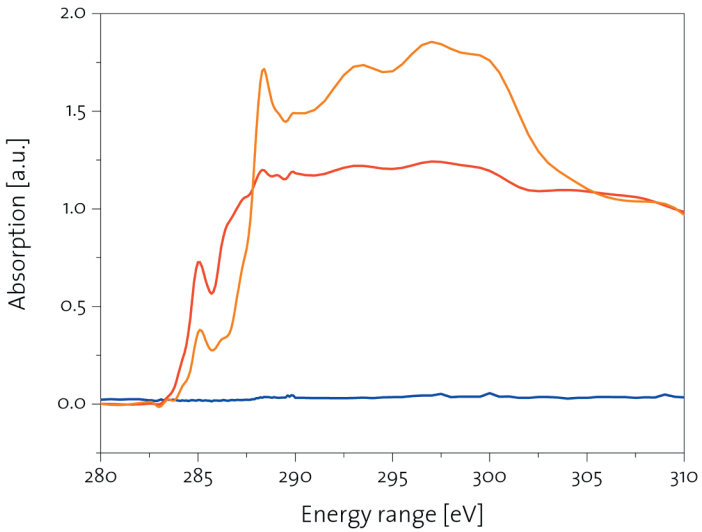

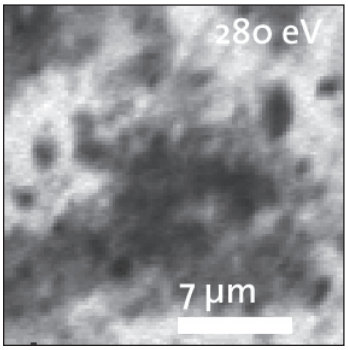

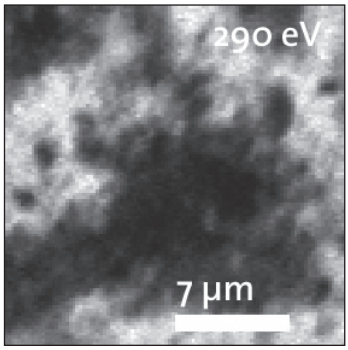

Riedhof

H-horizon

Stack 6

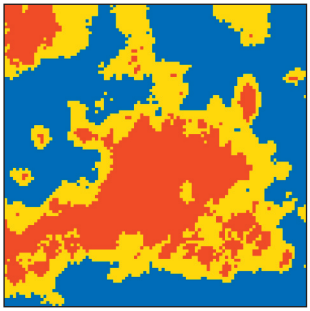

November
2003

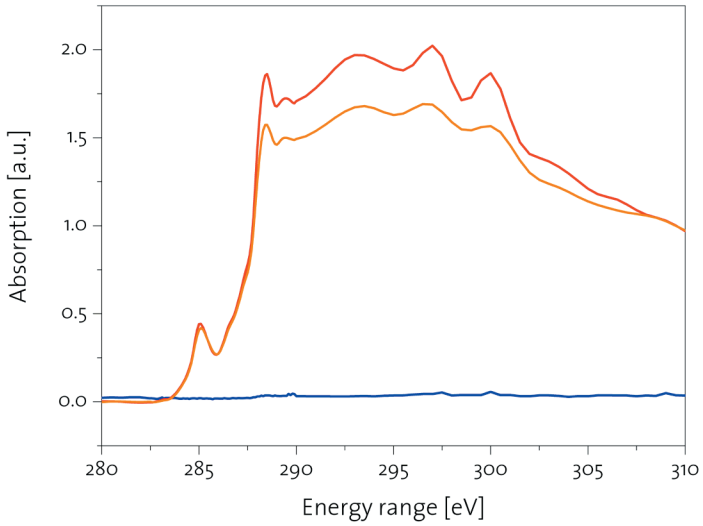

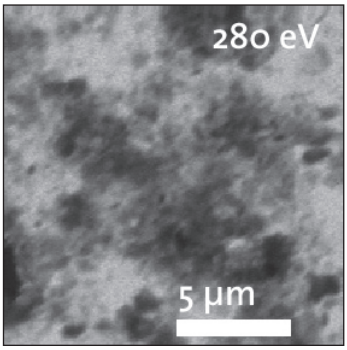

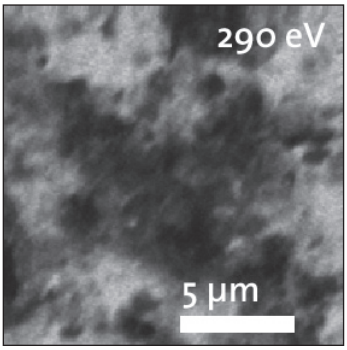

Riedhof

H-horizon

Stack 7

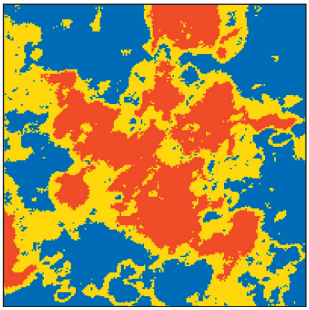

November
2003

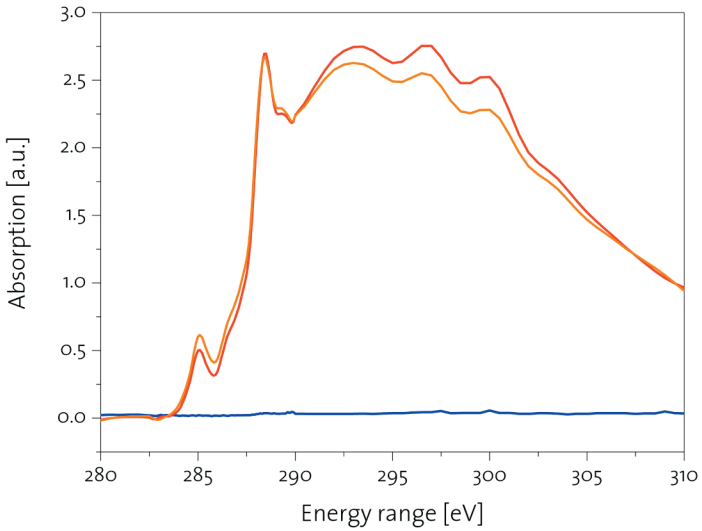

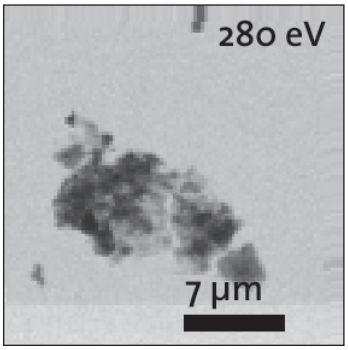

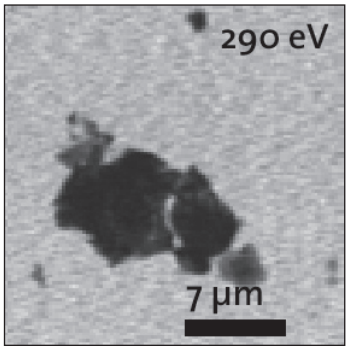

Riedhof

Ah-horizon

Stack 1

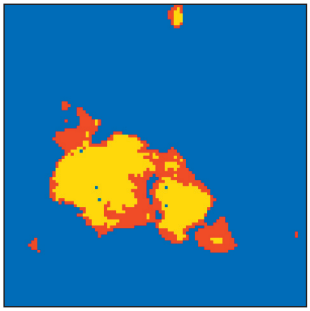

November
2002

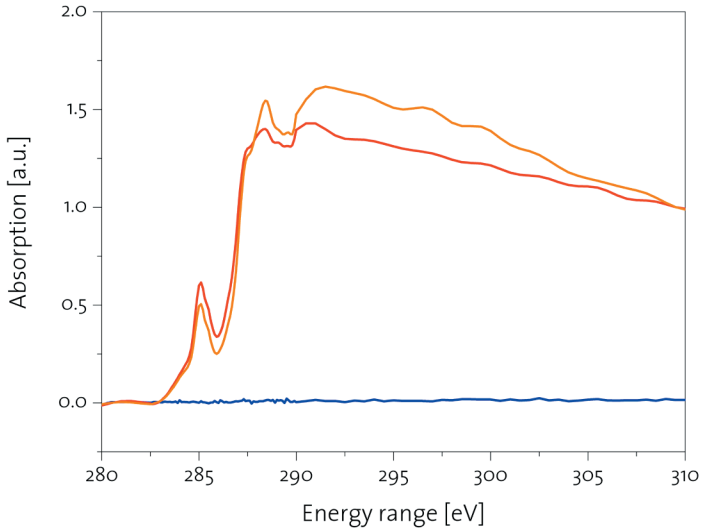

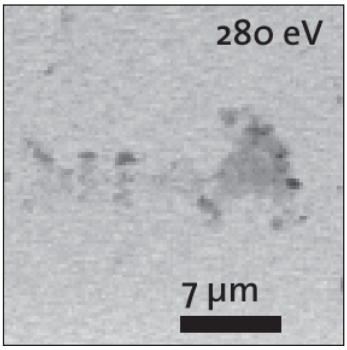

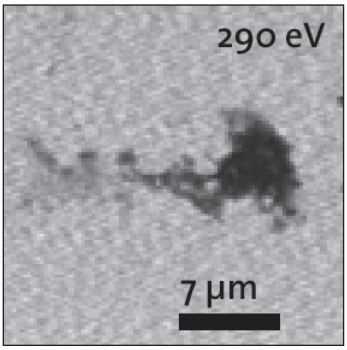

Riedhof

Ah-horizon

Stack 2

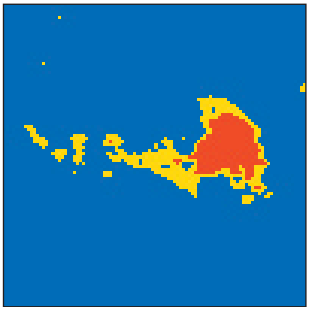

November
2002

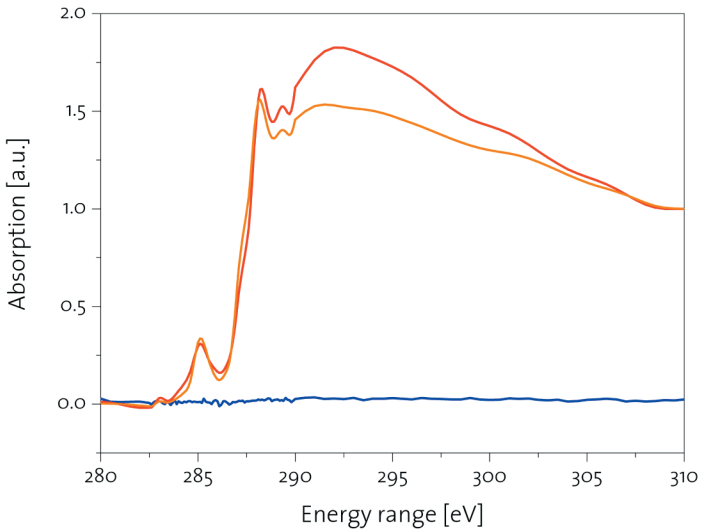

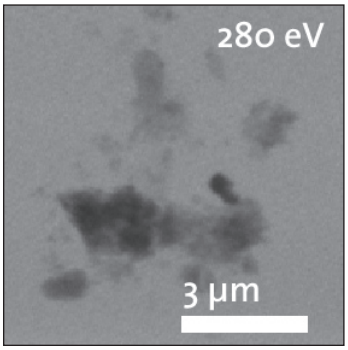

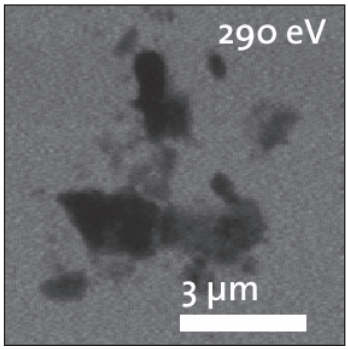

Riedhof

Ah-horizon

Stack 3

November
2002

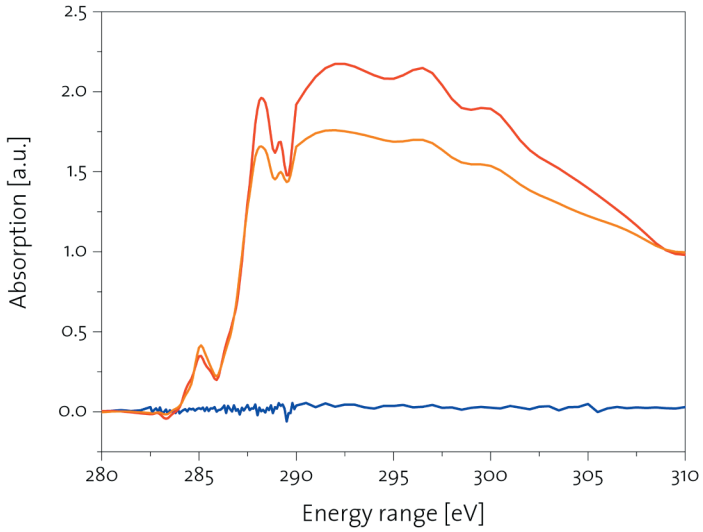

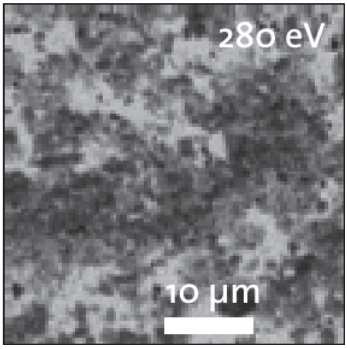

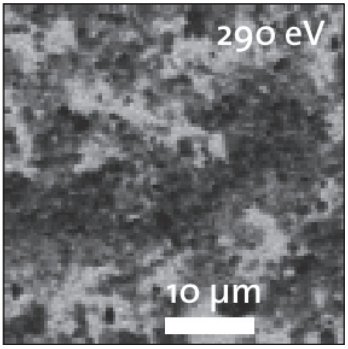

Riedhof

Ah-horizon

Stack 1

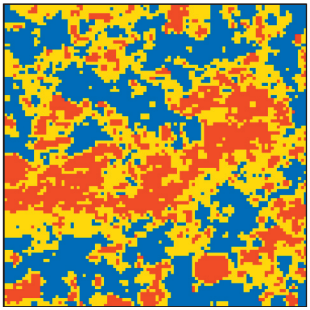

November
2003

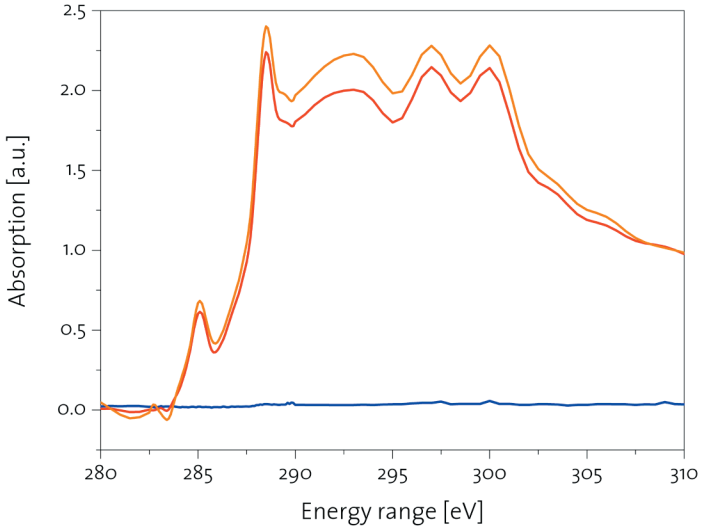

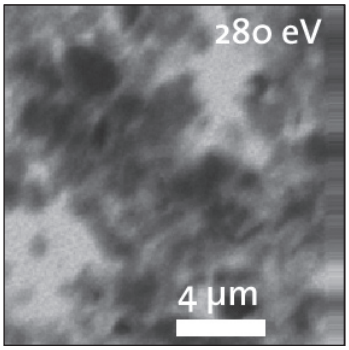

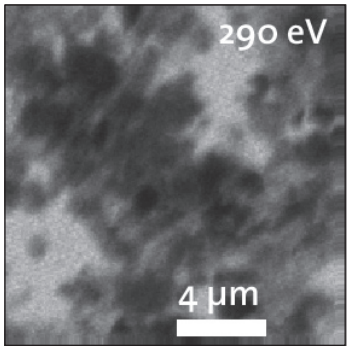

Riedhof

Ah-horizon

Stack 2

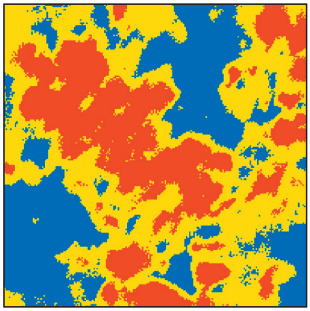

November
2003

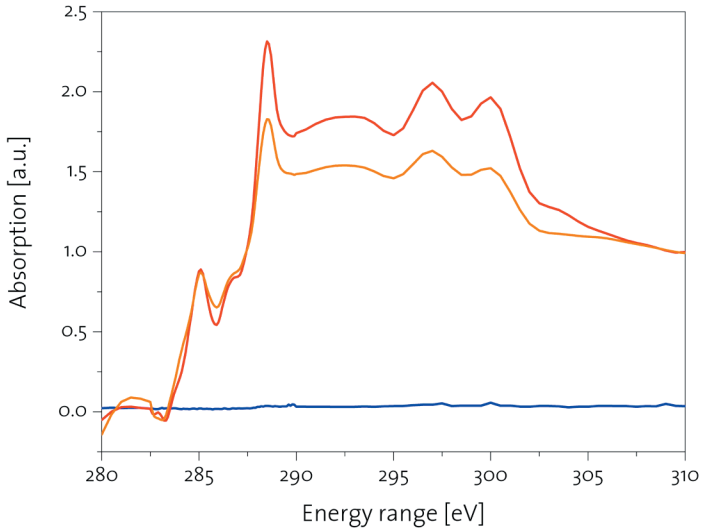

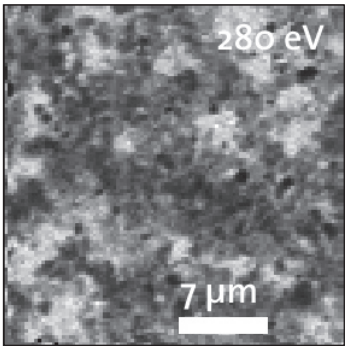

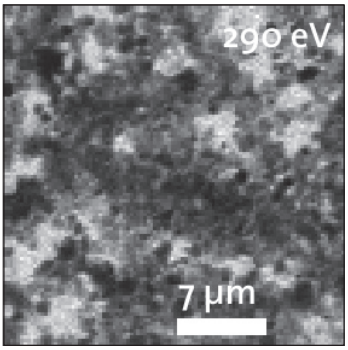

Riedhof

Ah-horizon

Stack 3

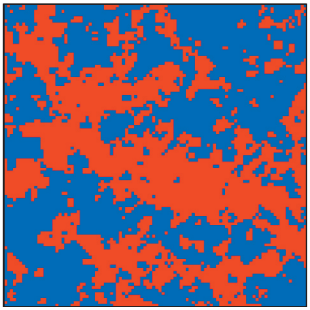

November
2003

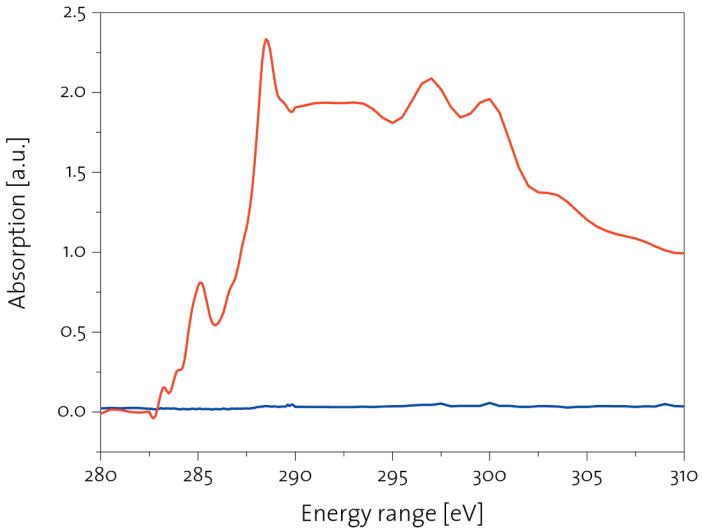

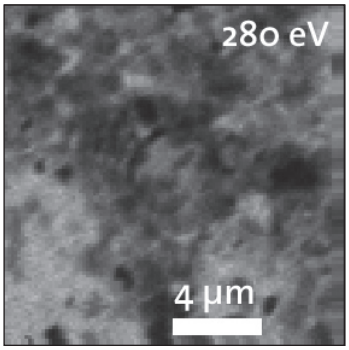

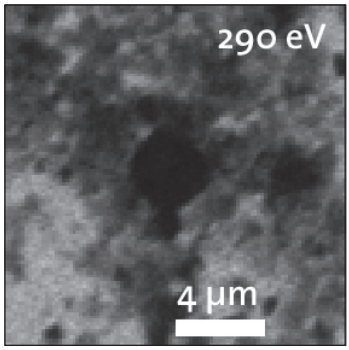

Riedhof

Ah-horizon

Stack 4

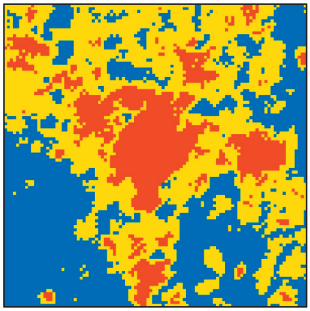

November
2003

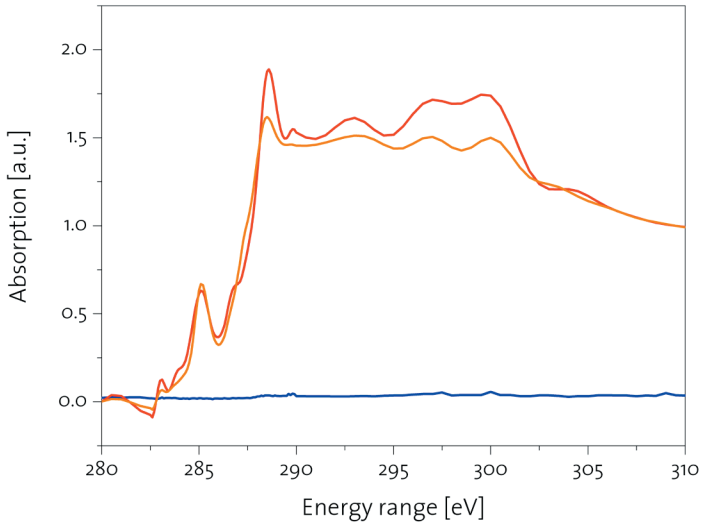

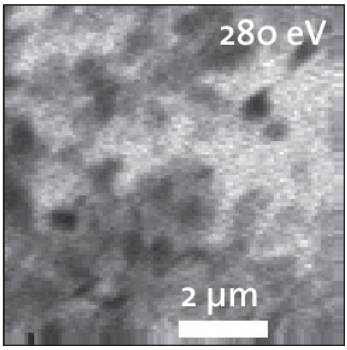

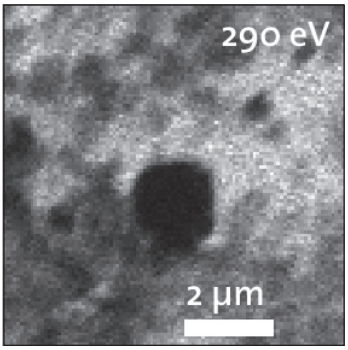

Riedhof

Ah-horizon

Stack 5

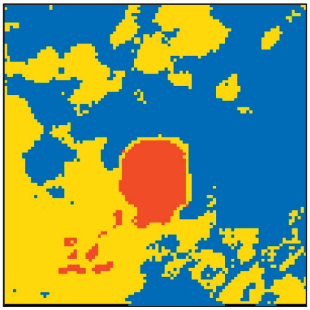

November
2003

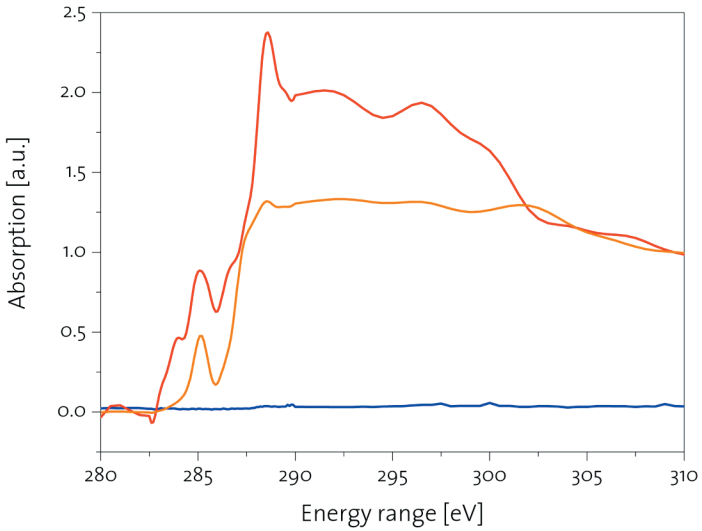

Appendix B

Location: Oberrickenzopfen / BE

Soil type: Humic Gleysol
Coordinates: 629.000 / 229.450

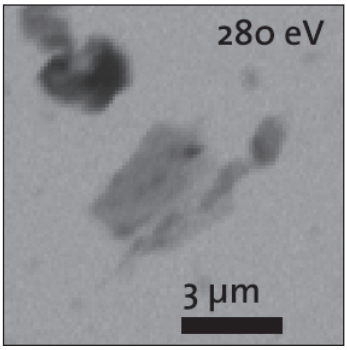

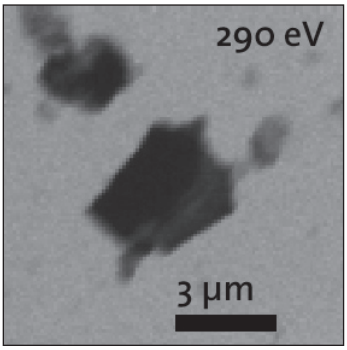

Ober-
Rickenzopfen

H-horizon

Stack 1

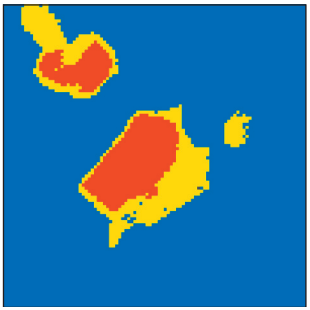

August
2003

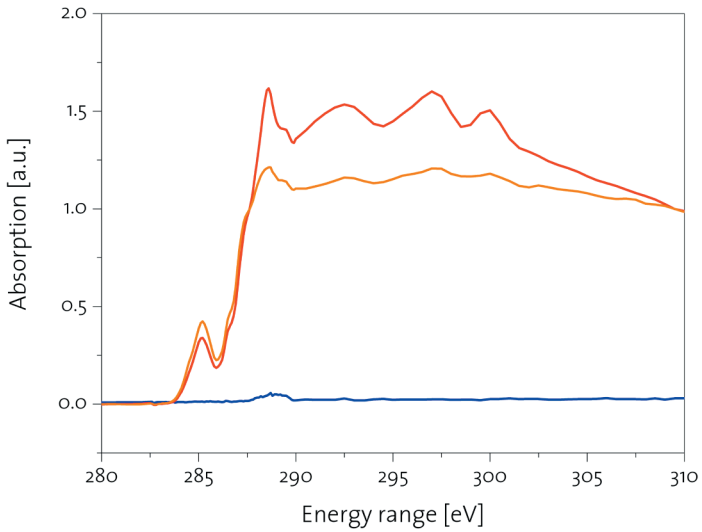

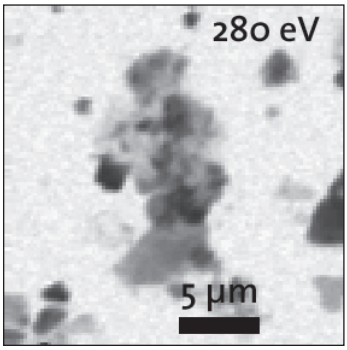

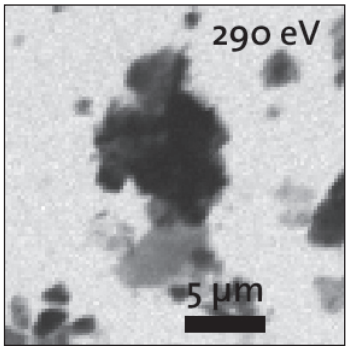

Ober-
Rickenzopfen

H-horizon

Stack 2

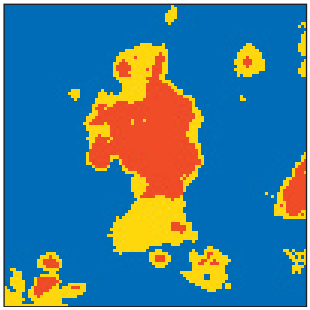

August
2003

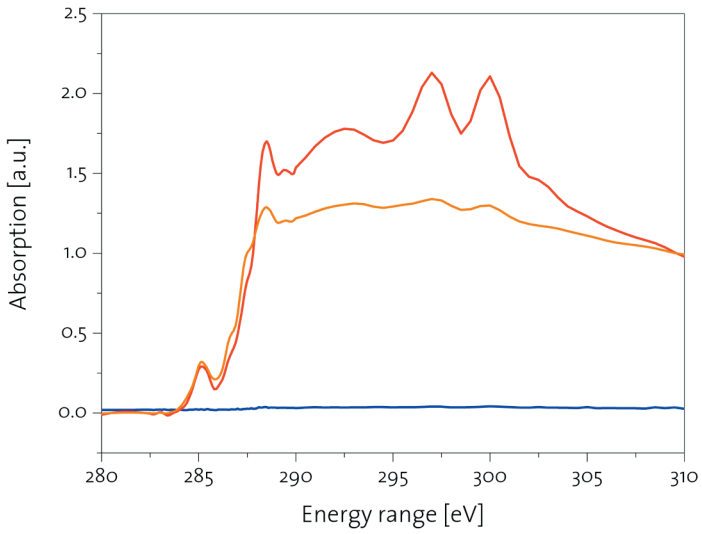

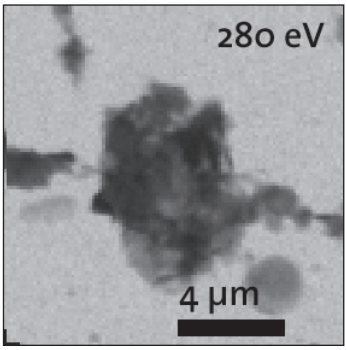

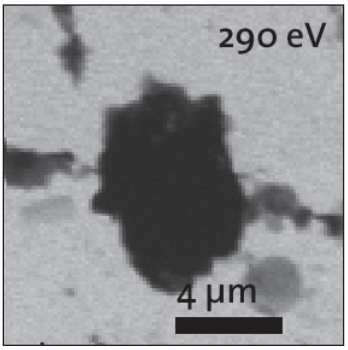

Ober-
Rickenzopfen

H-horizon

Stack 3

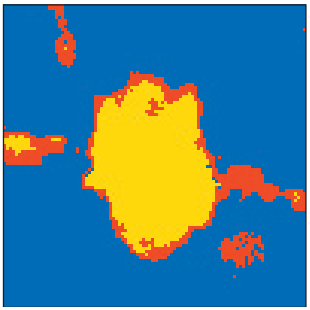

August
2003

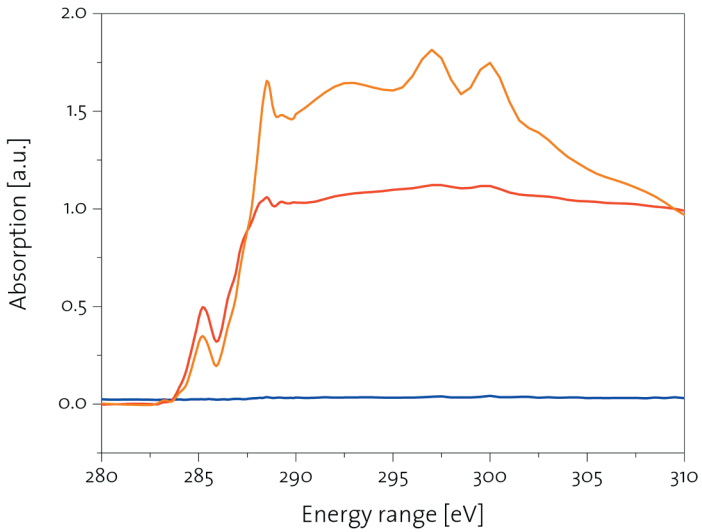

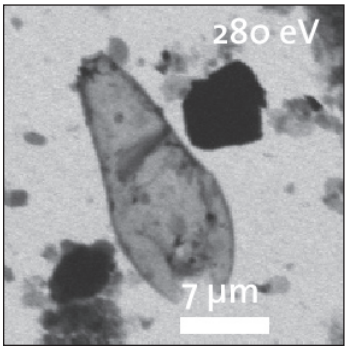

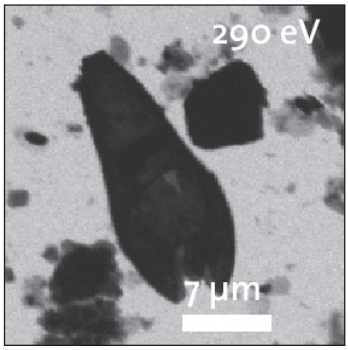

Ober-
Rickenzopfen

H-horizon

Stack 4

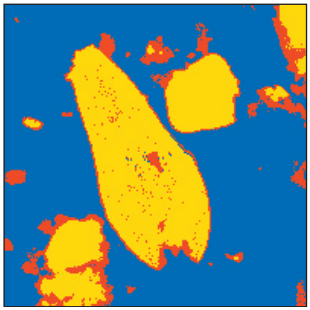

August
2003

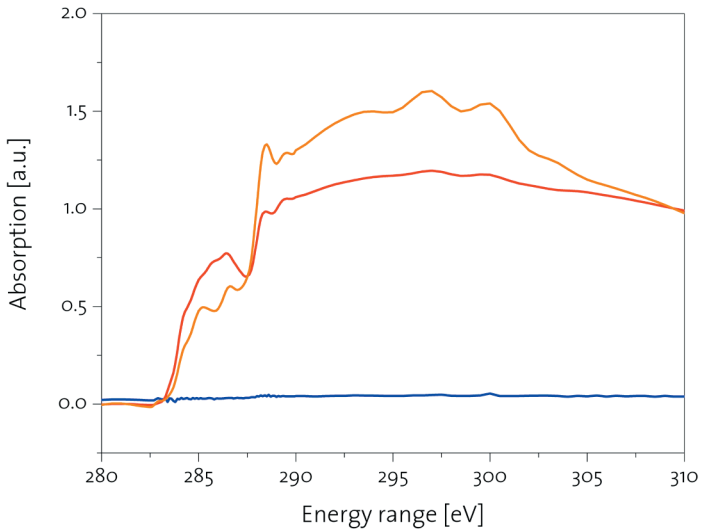

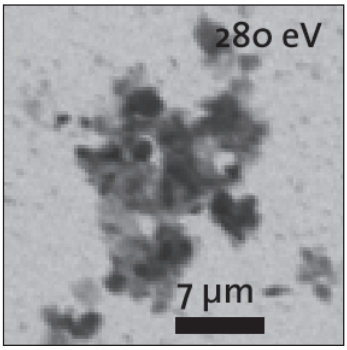

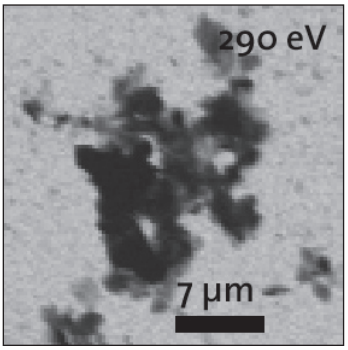

Ober-
Rickenzopfen

H-horizon

Stack 5

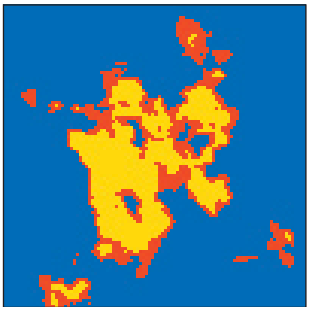

August
2003

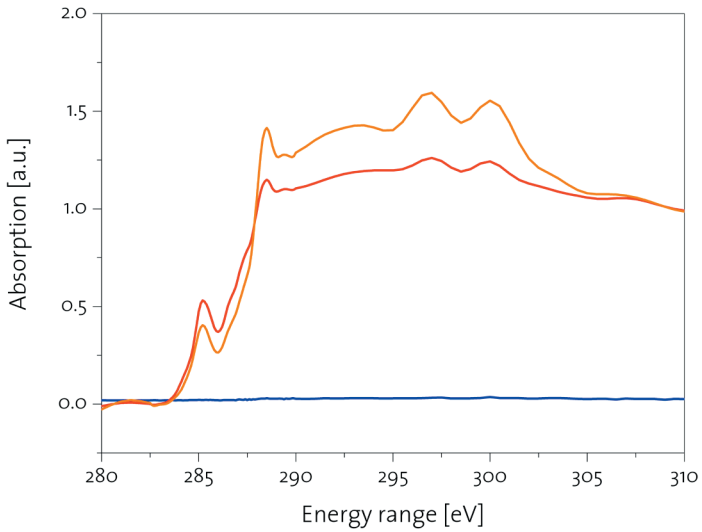

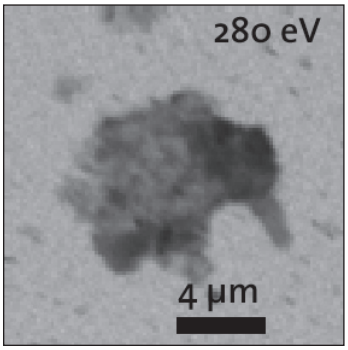

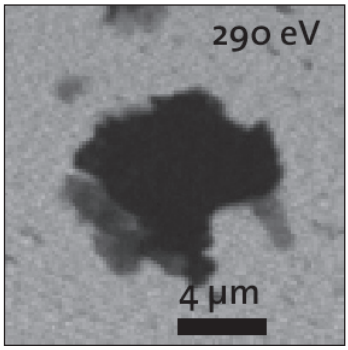

Ober-
Rickenzopfen

H-horizon

Stack 6

August
2003

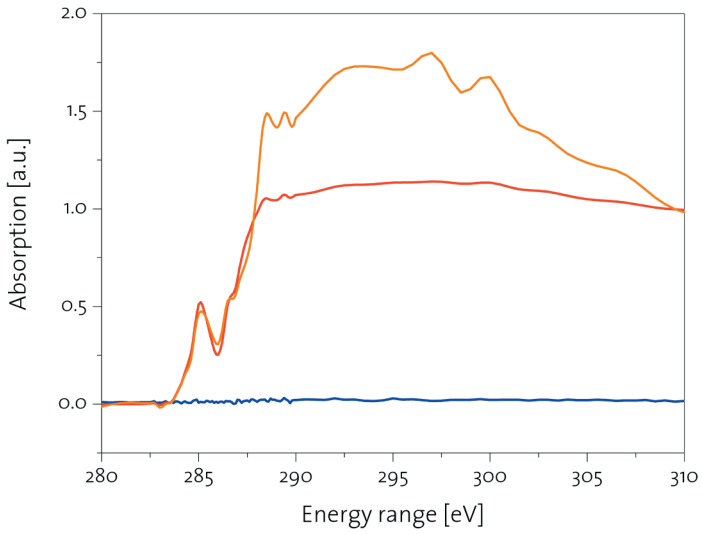

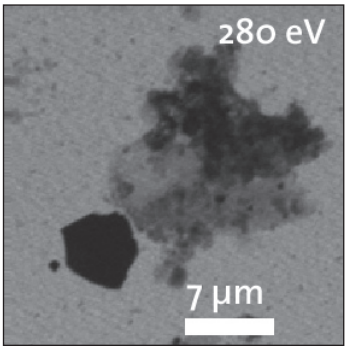

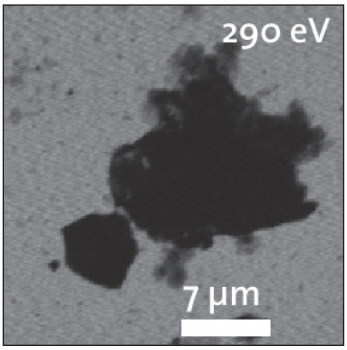

Ober-
Rickenzopfen

H-horizon

Stack 7

August
2003

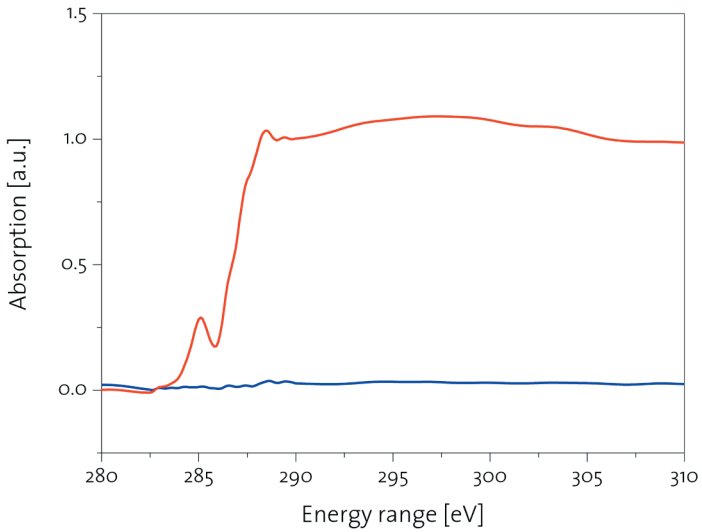

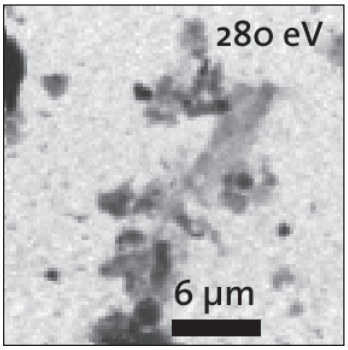

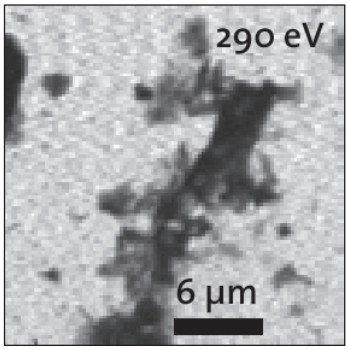

Ober-
Rickenzopfen

H-horizon

Stack 8

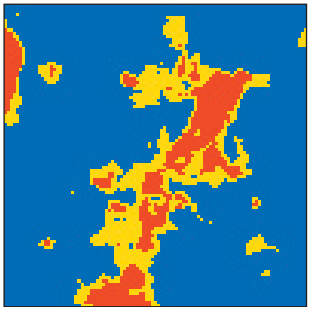

August
2003

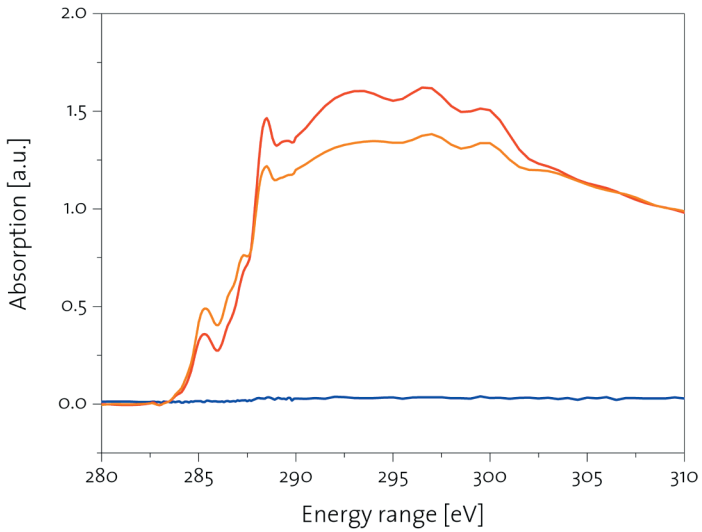

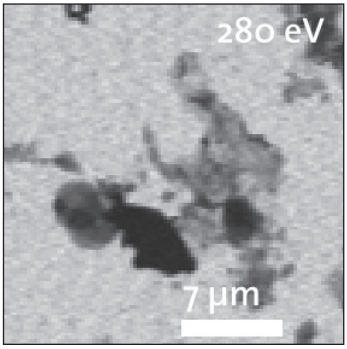

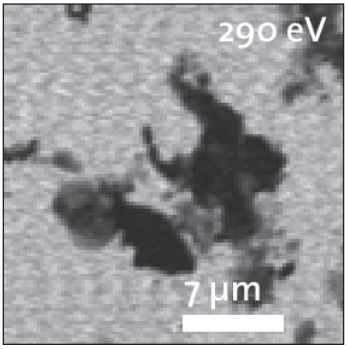

Ober-
Rickenzopfen

H-horizon

Stack 9

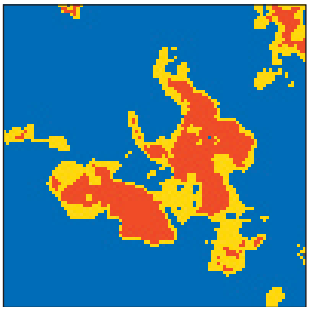

August
2003

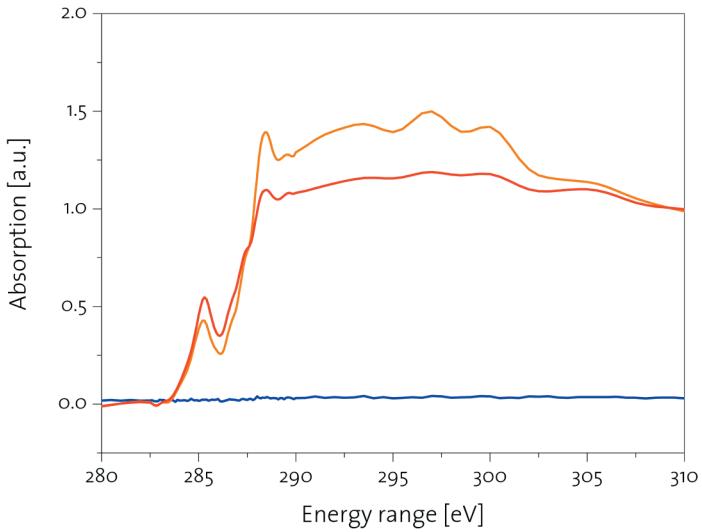

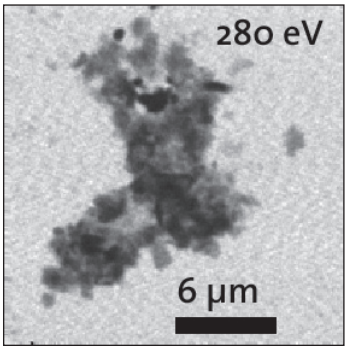

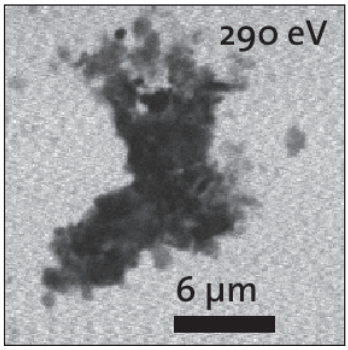

Ober-
Rickenzopfen

H-horizon

Stack 10

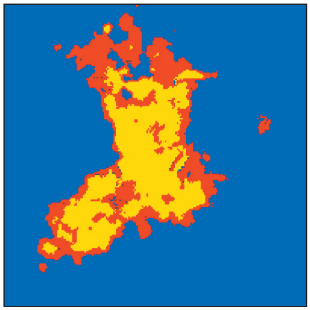

August
2003

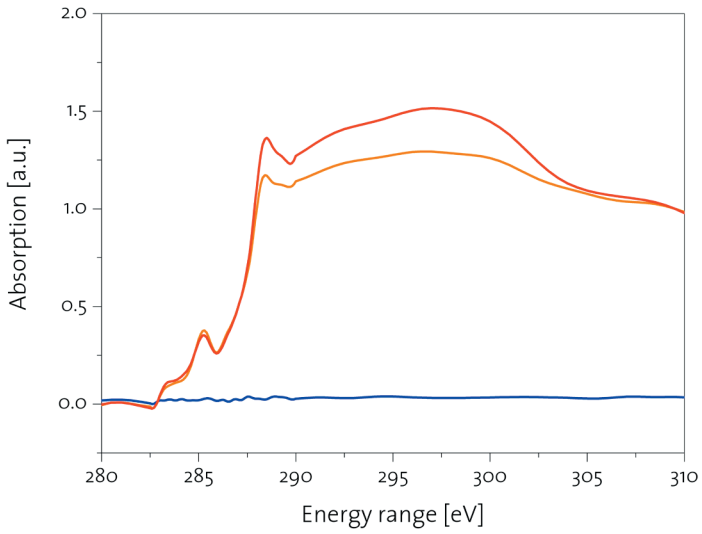

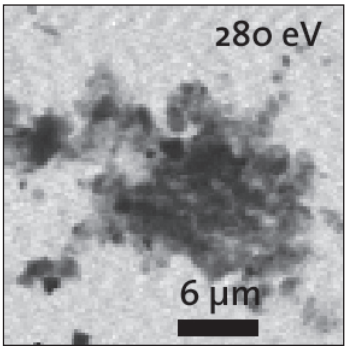

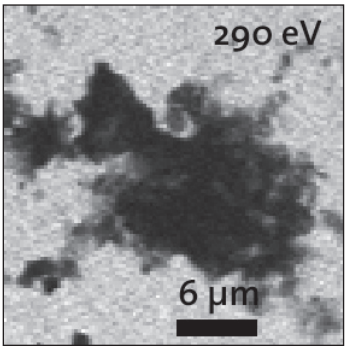

Ober-
Rickenzopfen

H-horizon

Stack 11

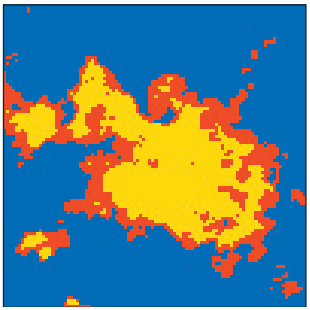

August
2003

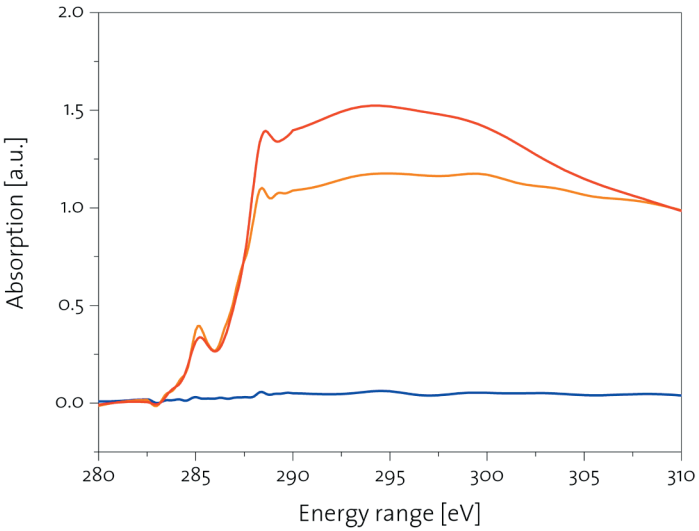

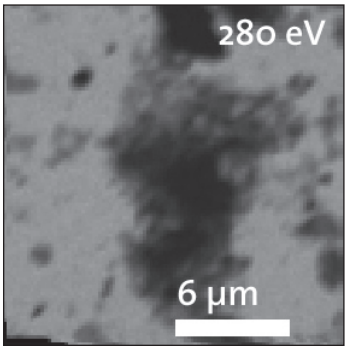

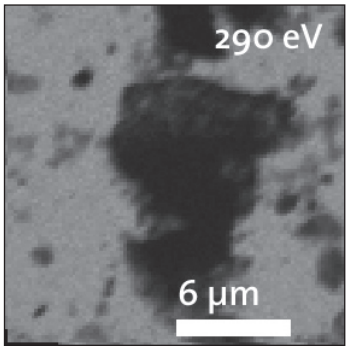

Ober-
Rickenzopfen

H-horizon

Stack 1

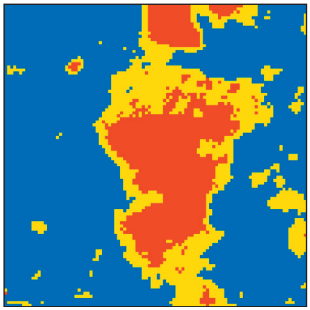

April
2004

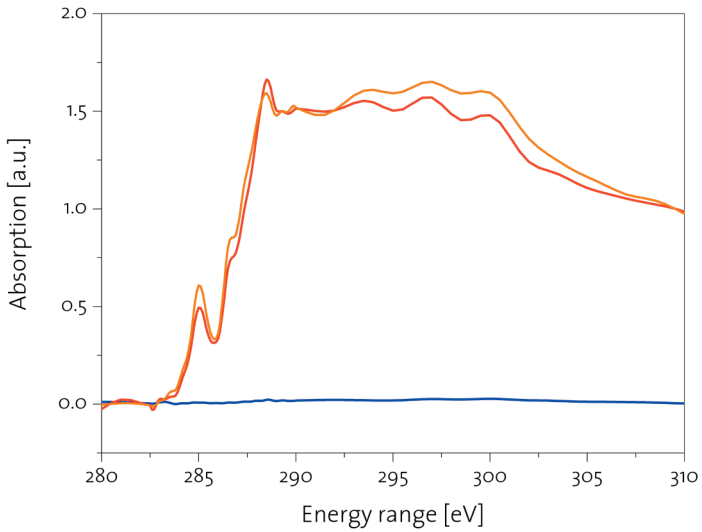

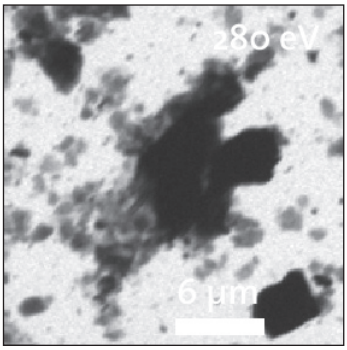

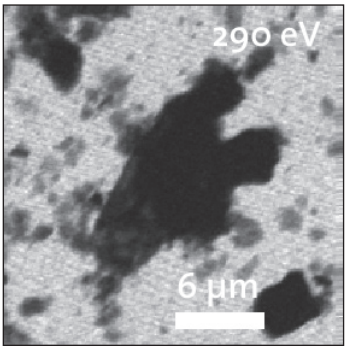

Ober-
Rickenzopfen

H-horizon

Stack 2

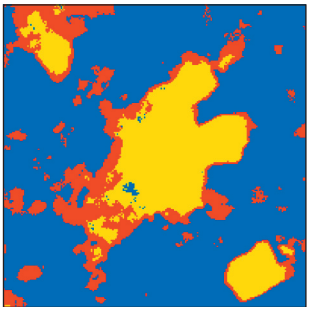

April
2004

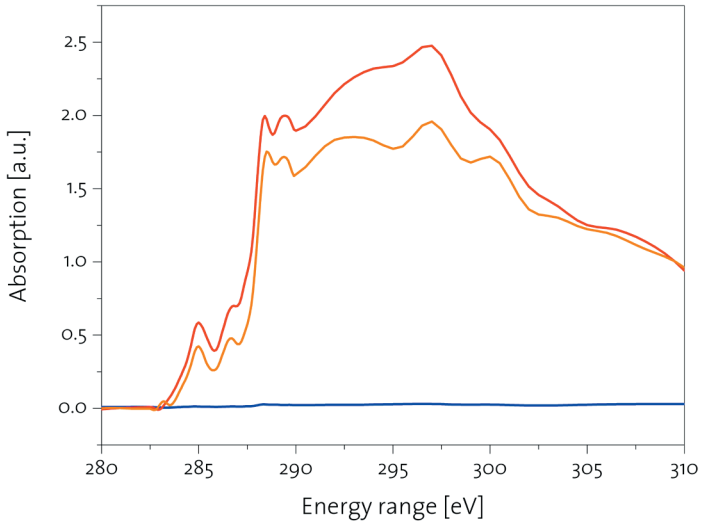

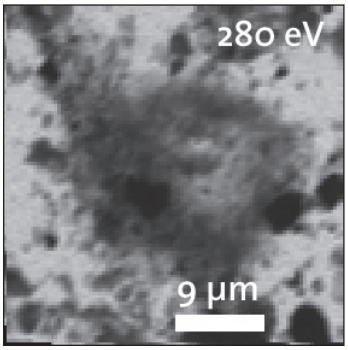

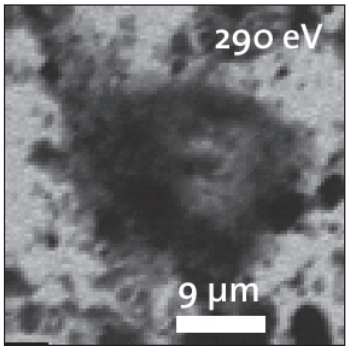

Ober-
Rickenzopfen

H-horizon

Stack 3

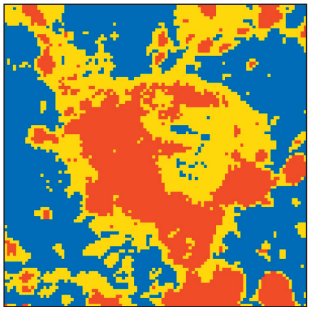

April
2004

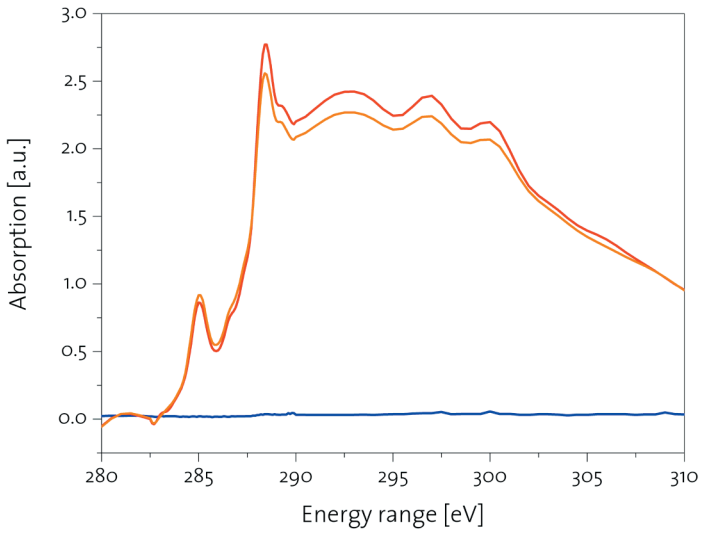

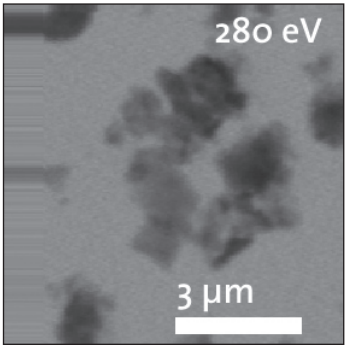

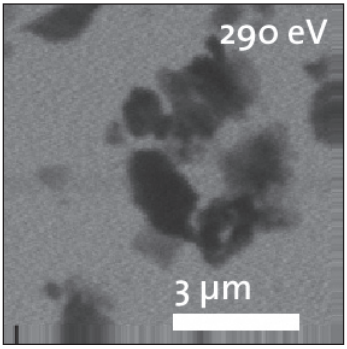

Ober-
Rickenzopfen

Ah-horizon

Stack 1

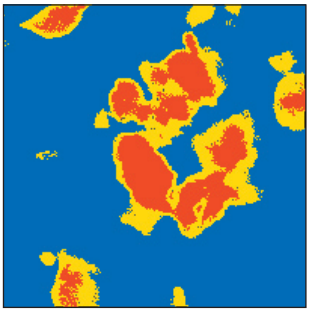

March
2003

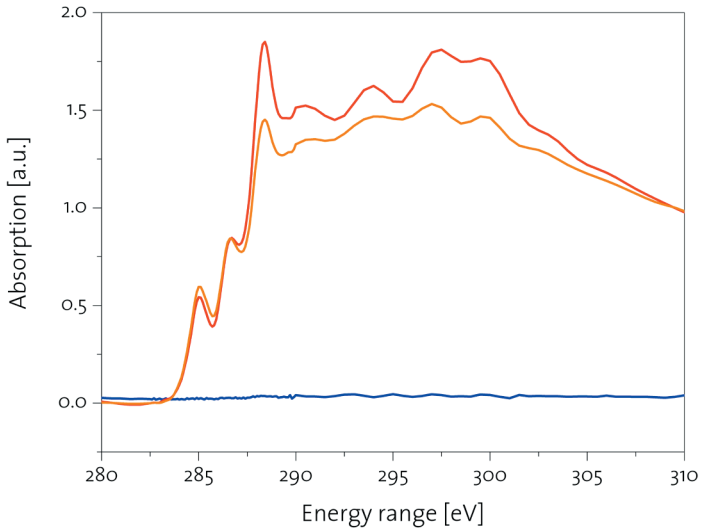

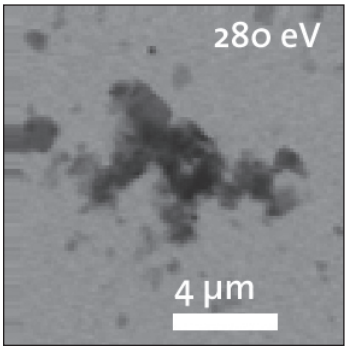

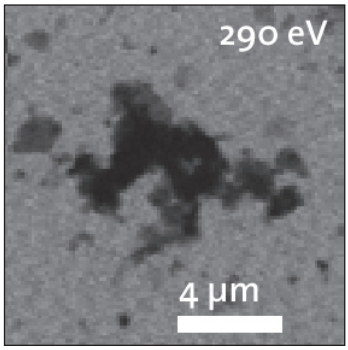

Ober-
Rickenzopfen

Ah-horizon

Stack 2

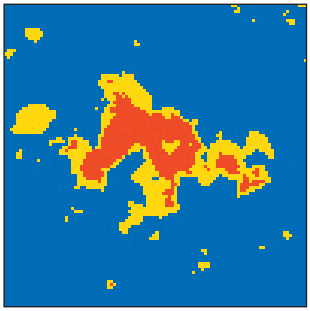

March
2003

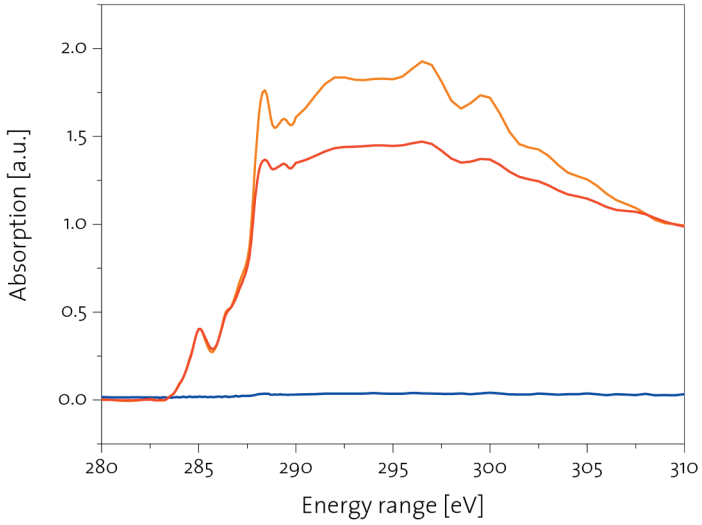

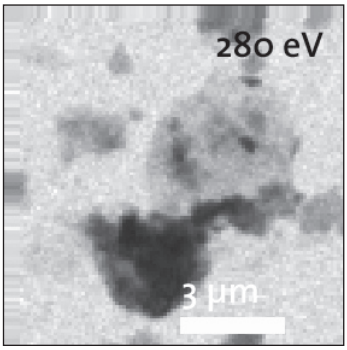

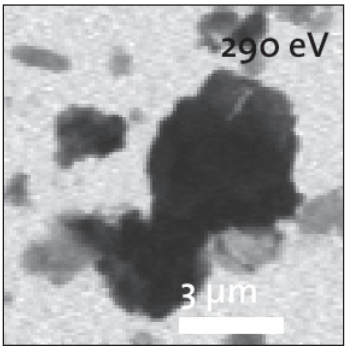

Ober-
Rickenzopfen

Ah-horizon

Stack 3

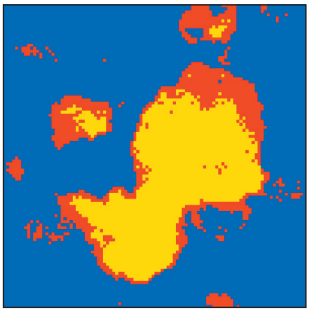

March
2003

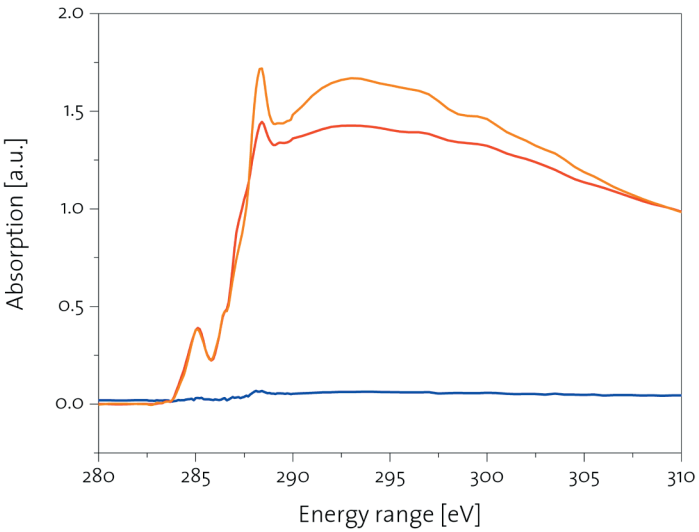

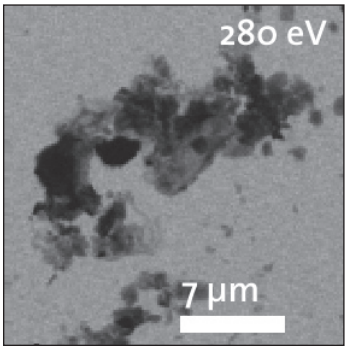

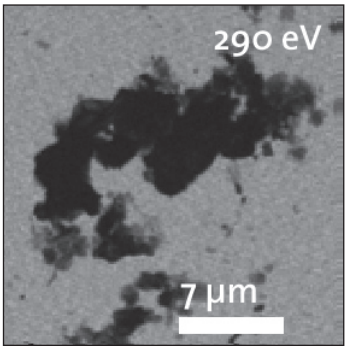

Ober-
Rickenzopfen

Ah-horizon

Stack 4

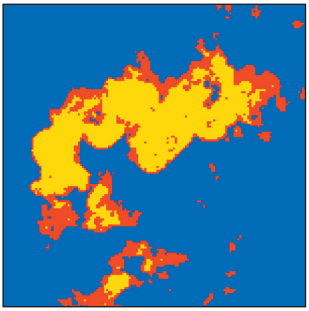

March
2003

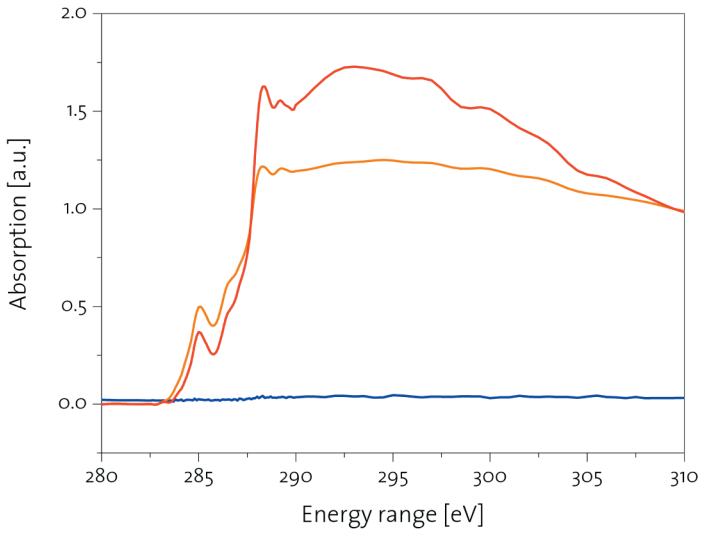

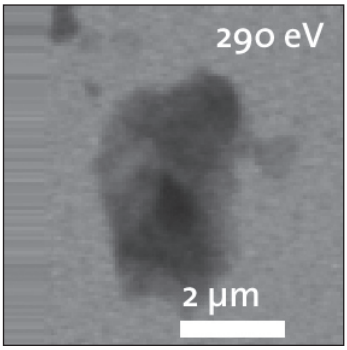

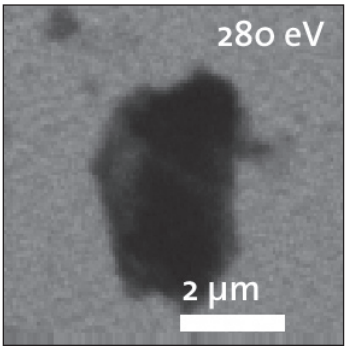

Ober-
Rickenzopfen

Ah-horizon

Stack 5

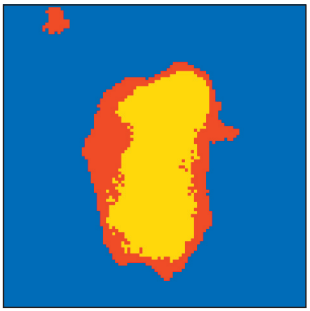

March
2003

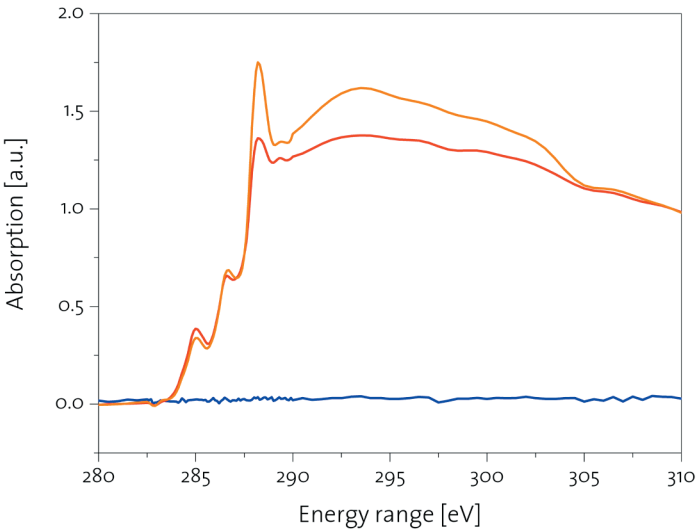

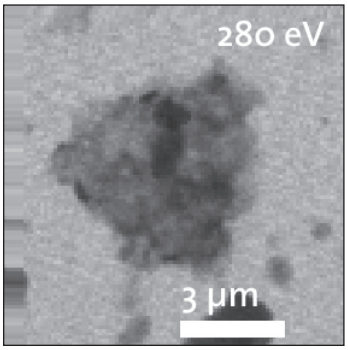

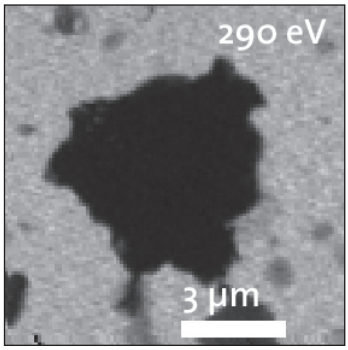

Ober-
Rickenzopfen

Ah-horizon

Stack 6

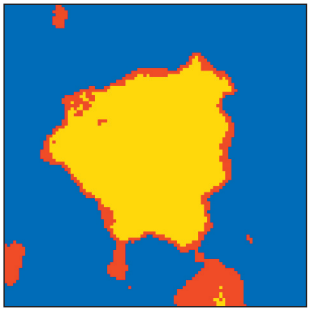

March
2003

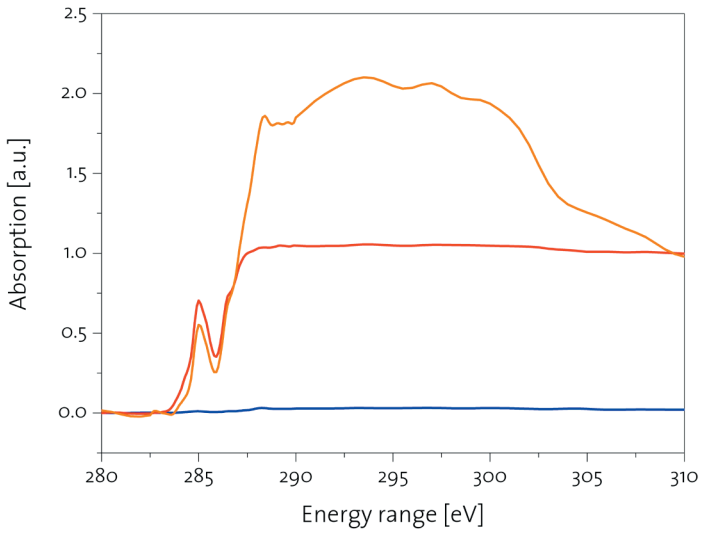

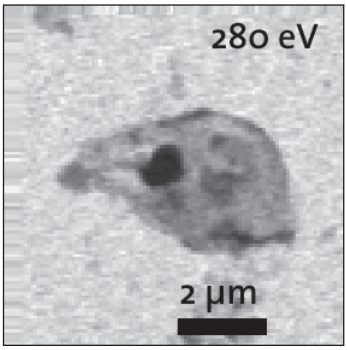

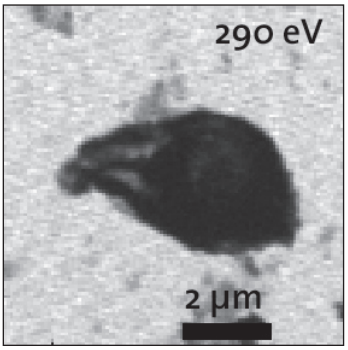

Ober-
Rickenzopfen

Ah-horizon

Stack 7

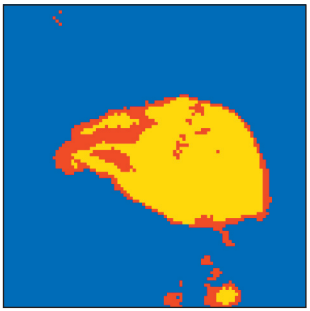

March
2003

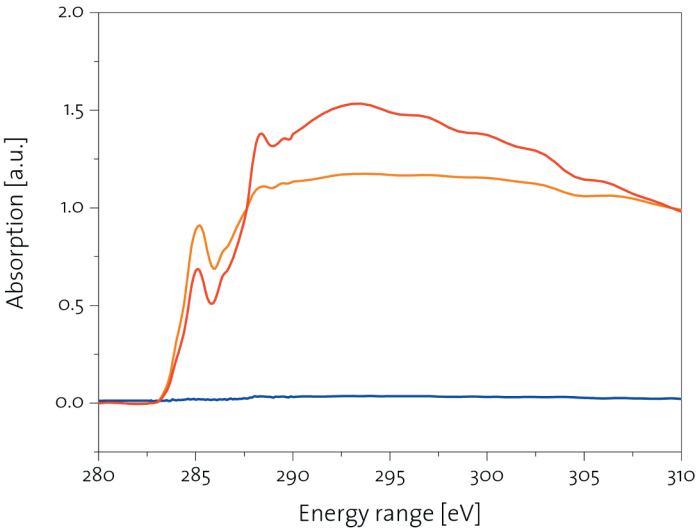

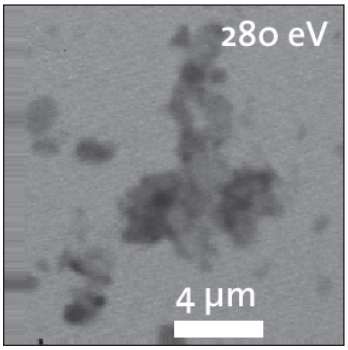

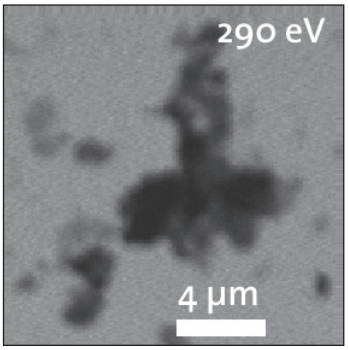

Ober-
Rickenzopfen

Ah-horizon

Stack 8

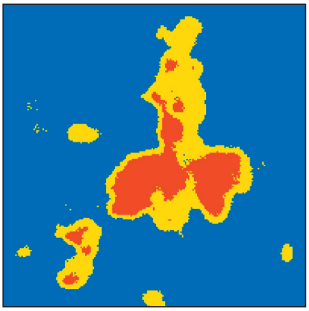

March
2003

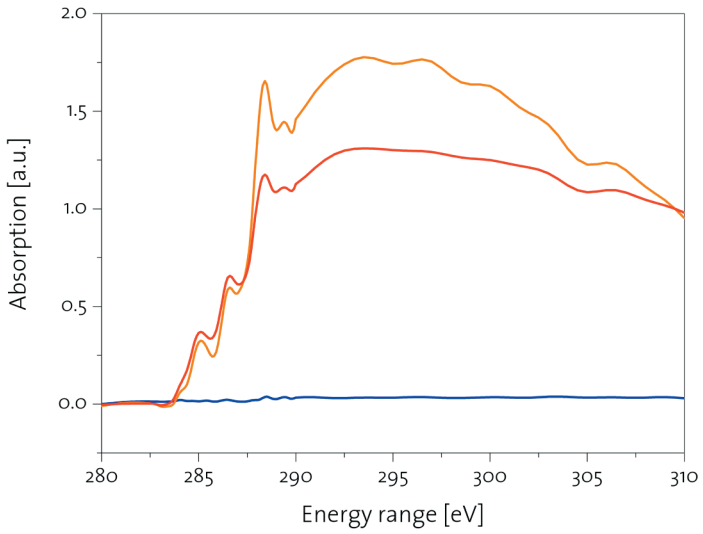

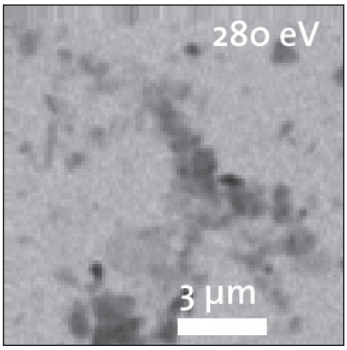

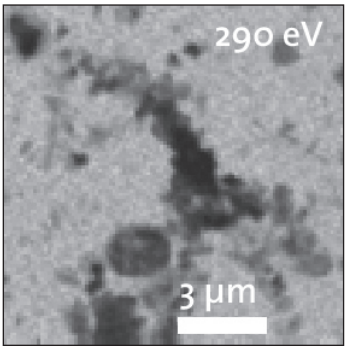

Ober-
Rickenzopfen

Ah-horizon

Stack 9

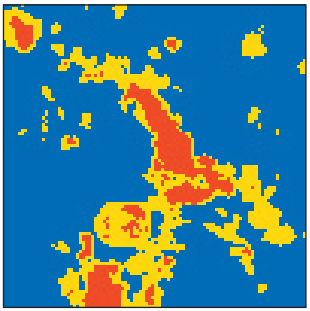

March
2003

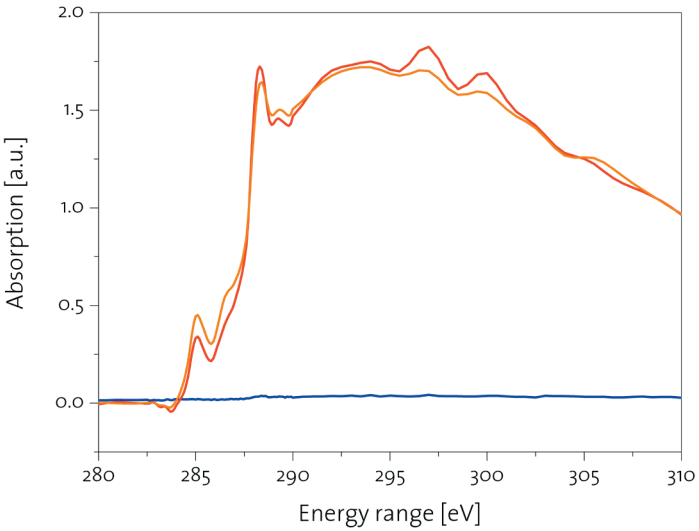

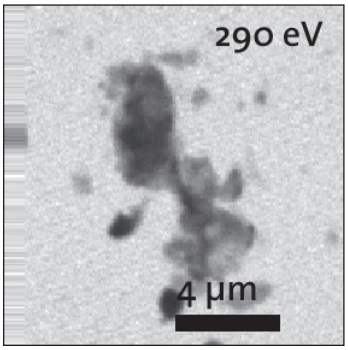

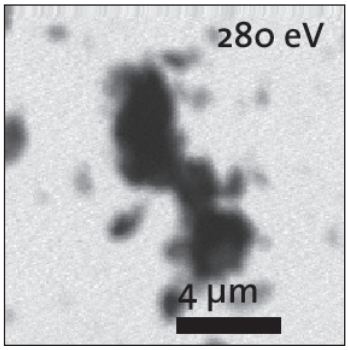

Ober-
Rickenzopfen

Ah-horizon

Stack 10

March
2003

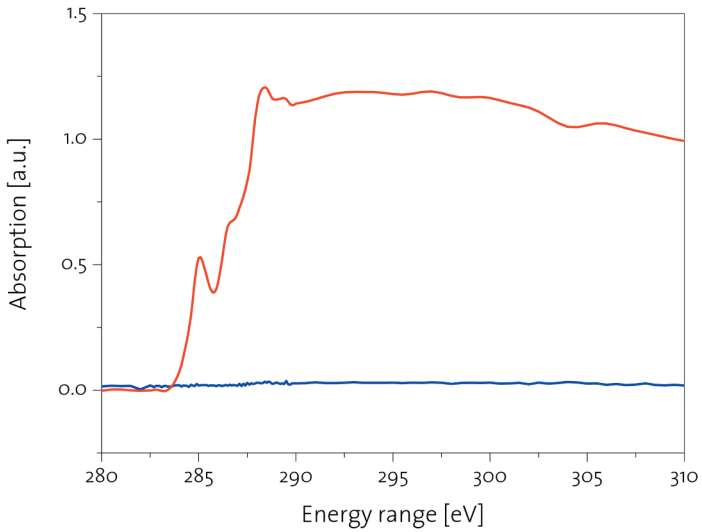

Appendix C

Location: Unterrickenzopfen / BE

Soil type: Humic Gleysol
Coordinates: 629.520 / 229.500

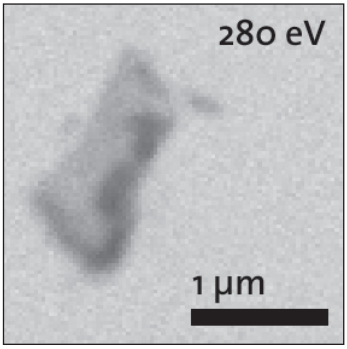

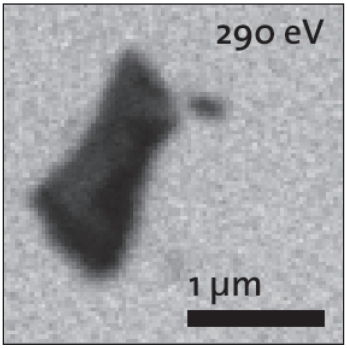

Unter-
Rickenzopfen

H-horizon

Stack 1

April
2001

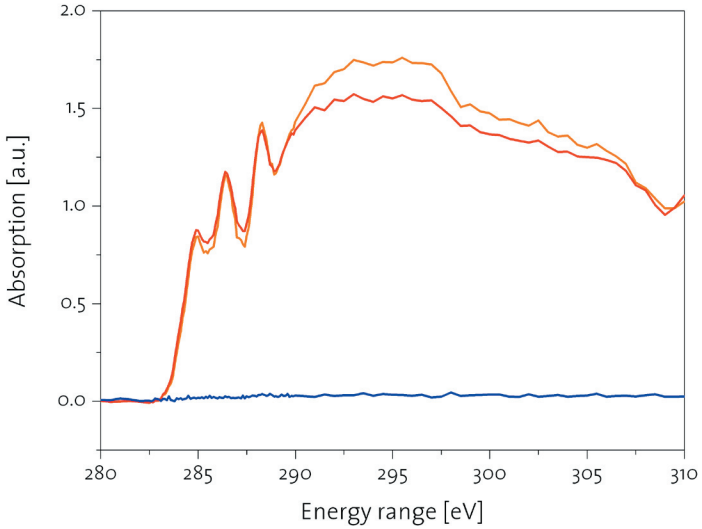

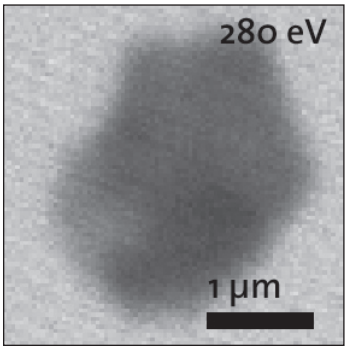

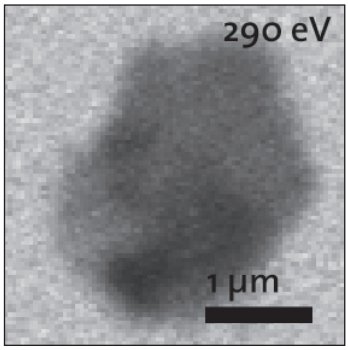

Unter-
Rickenzopfen

H-horizon

Stack 2

April
2001

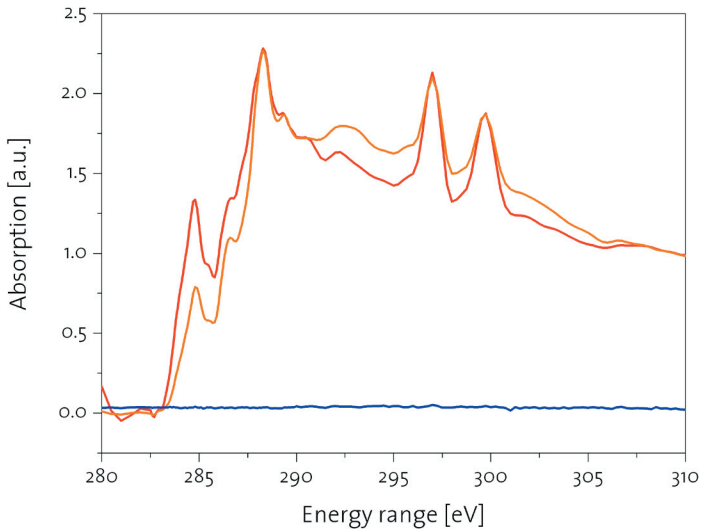

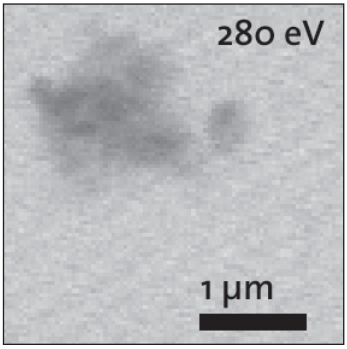

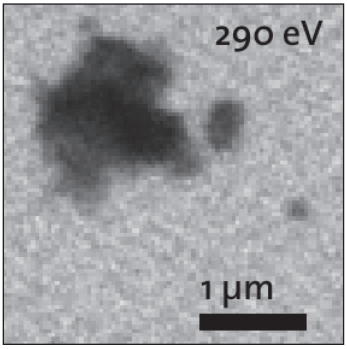

Unter-
Rickenzopfen

H-horizon

Stack 3

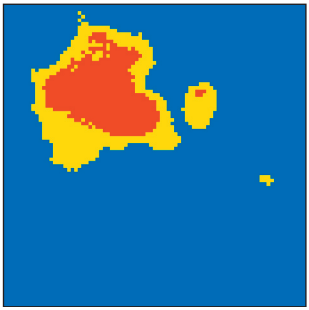

April
2001

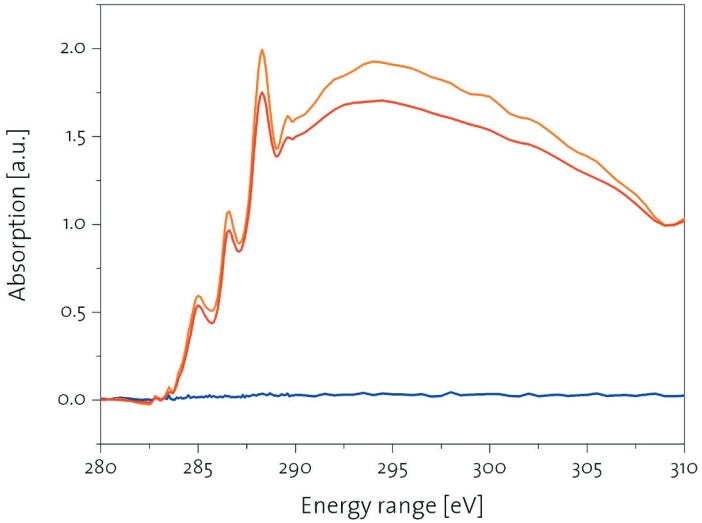

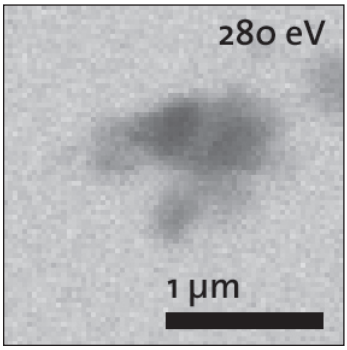

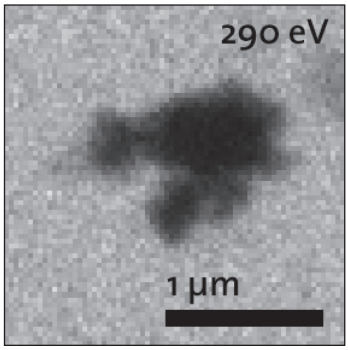

Unter-
Rickenzopfen

H-horizon

Stack 4

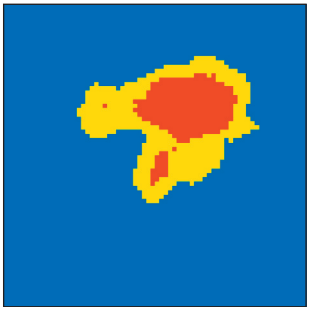

April
2001

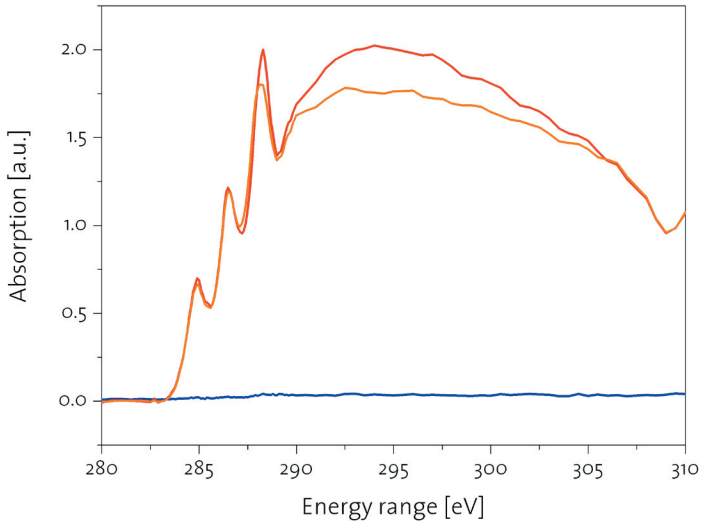

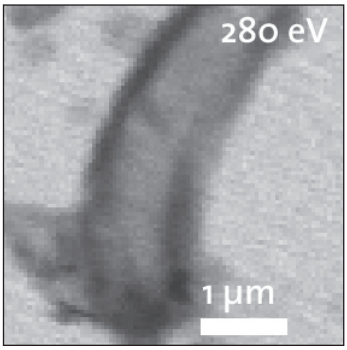

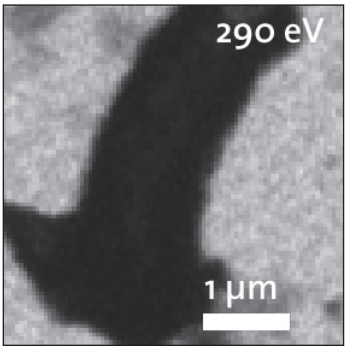

Unter-
Rickenzopfen

H-horizon

Stack 5

April
2001

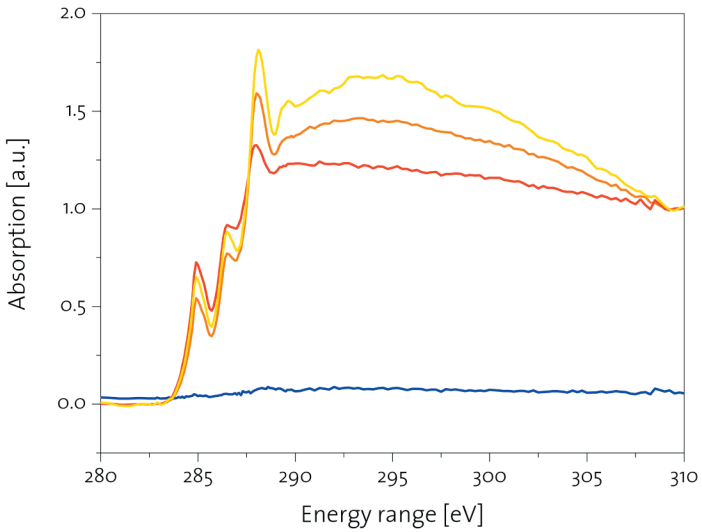

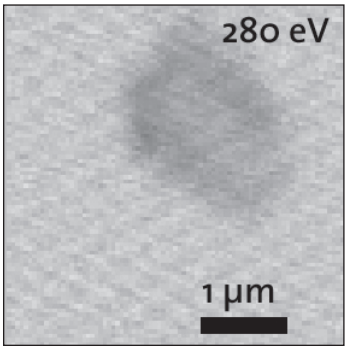

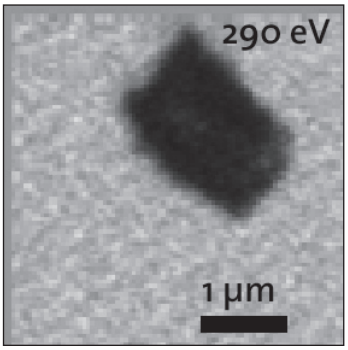

Unter-
Rickenzopfen

H-horizon

Stack 6

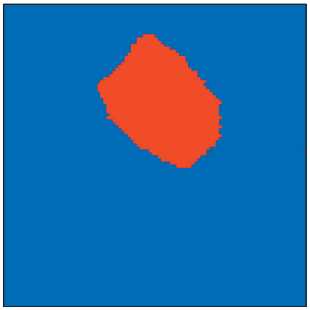

April
2001

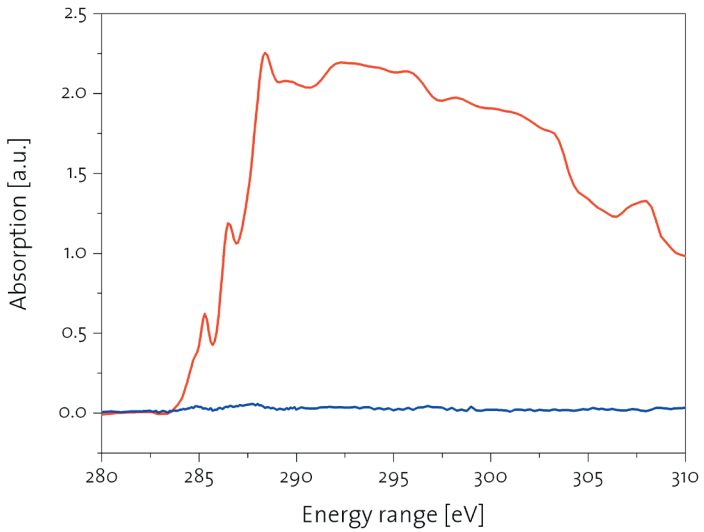

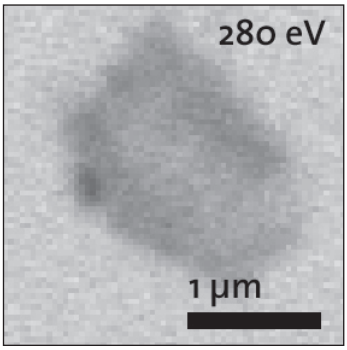

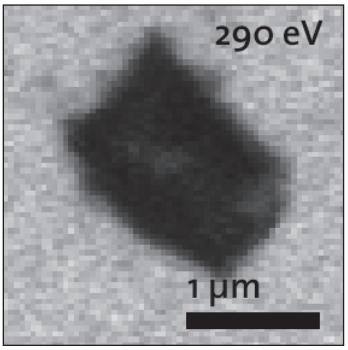

Unter-
Rickenzopfen

H-horizon

Stack 7

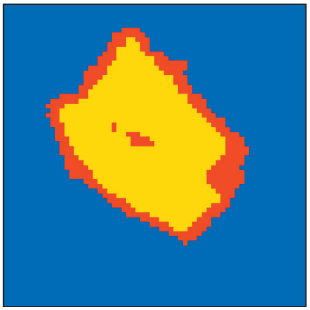

April
2001

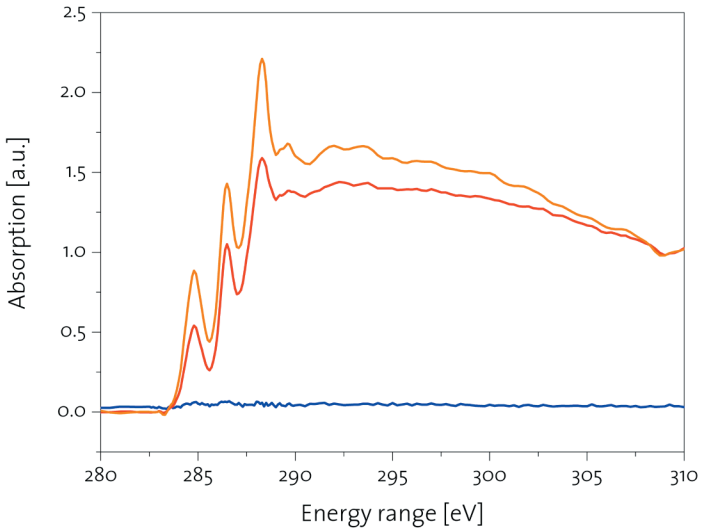

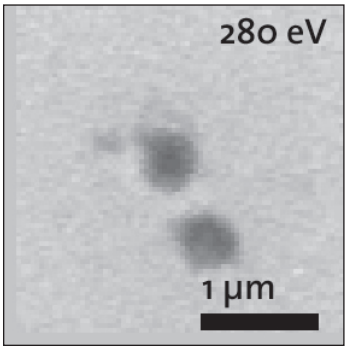

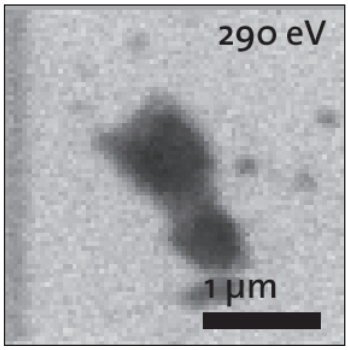

Unter-
Rickenzopfen

H-horizon

Stack 1

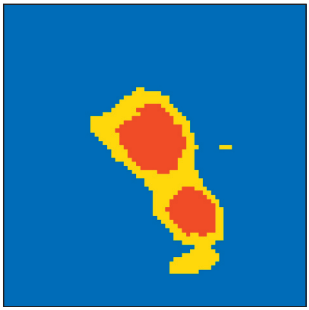

August
2001

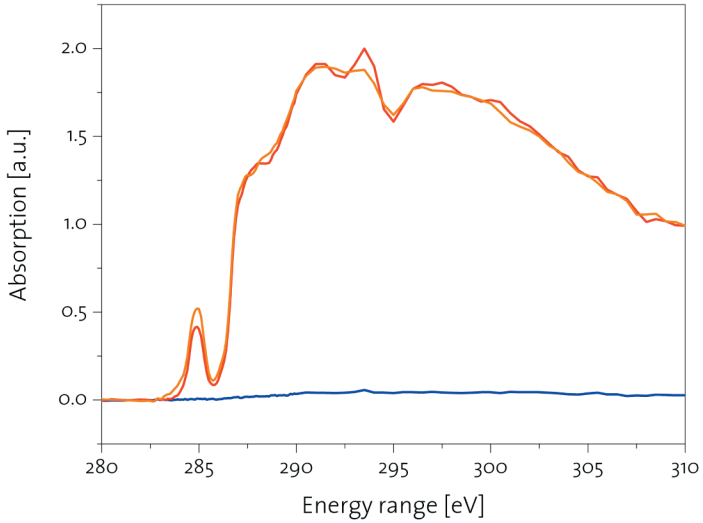

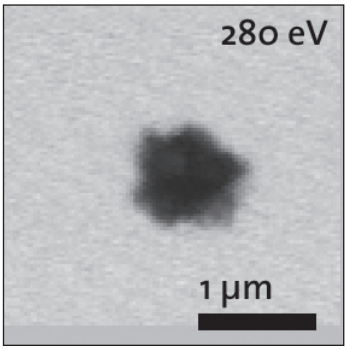

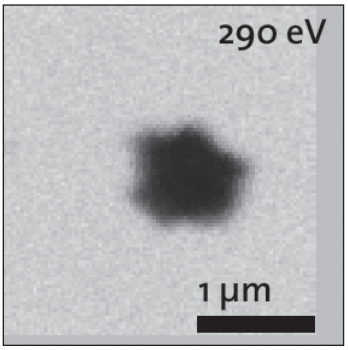

Unter-
Rickenzopfen

H-horizon

Stack 2

August
2001

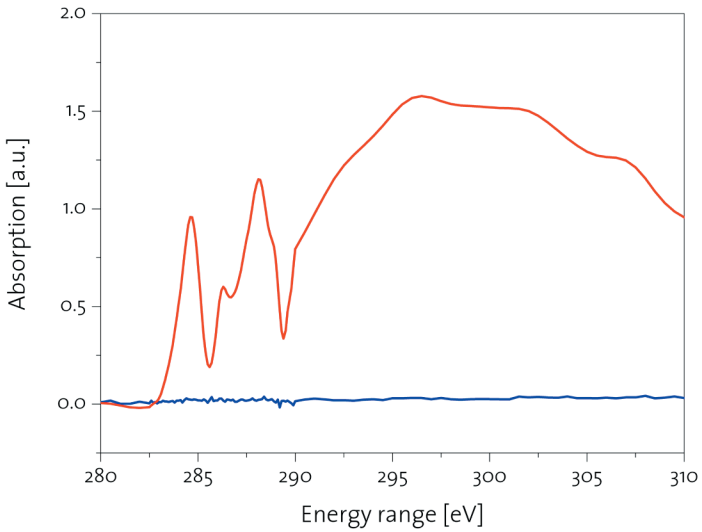

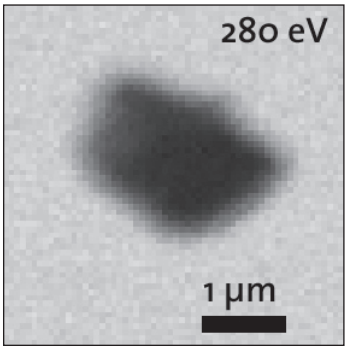

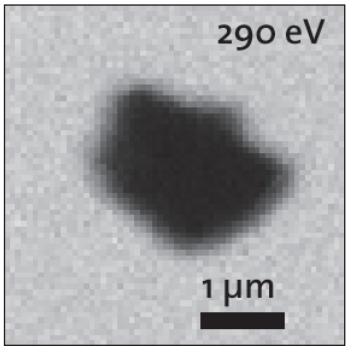

Unter-
Rickenzopfen

H-horizon

Stack 3

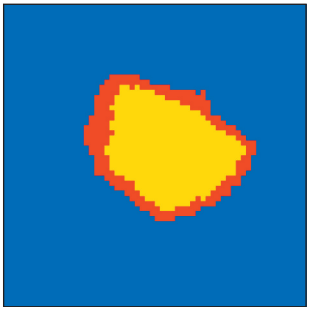

August
2001

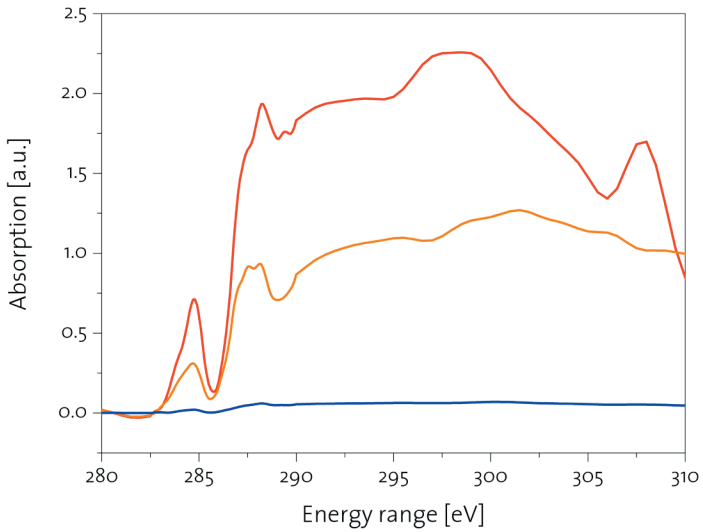

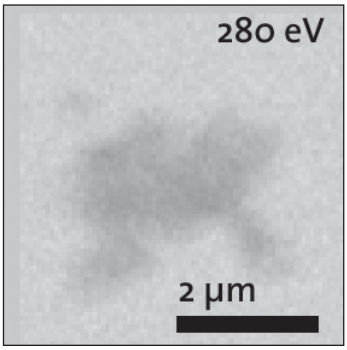

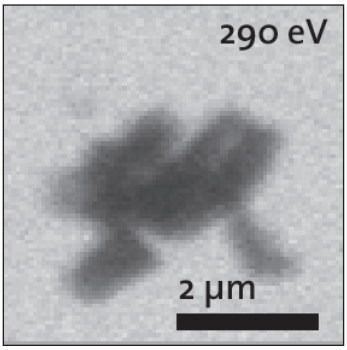

Unter-
Rickenzopfen

H-horizon

Stack 4

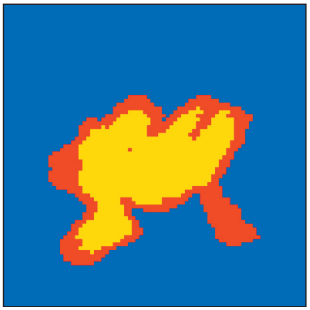

August
2001

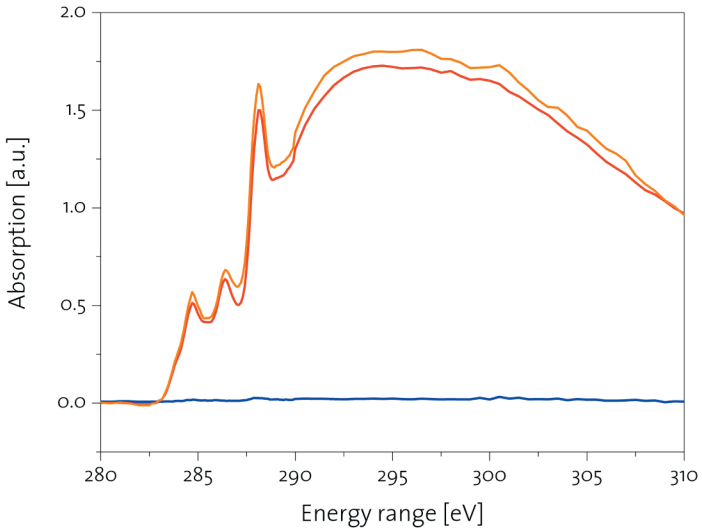

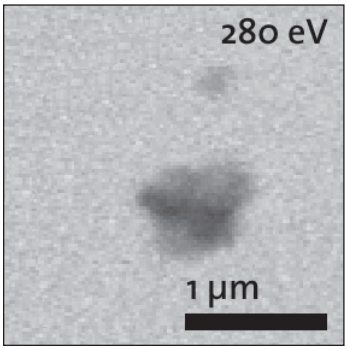

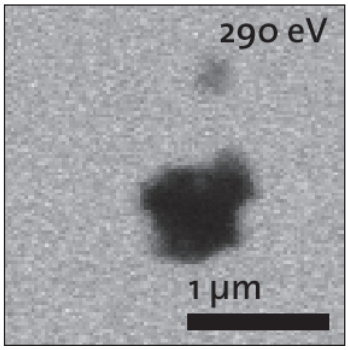

Unter-
Rickenzopfen

H-horizon

Stack 5

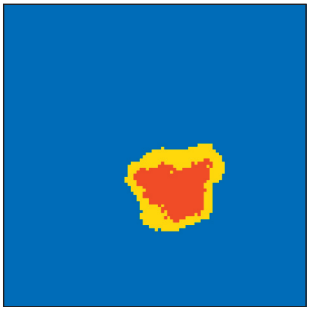

August
2001

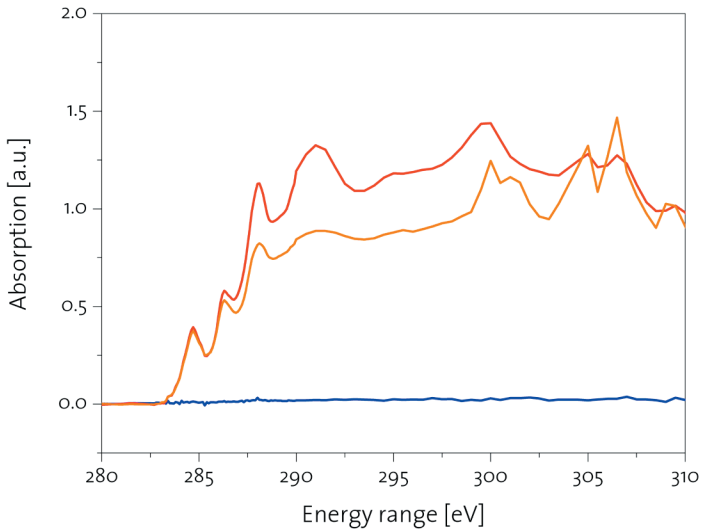

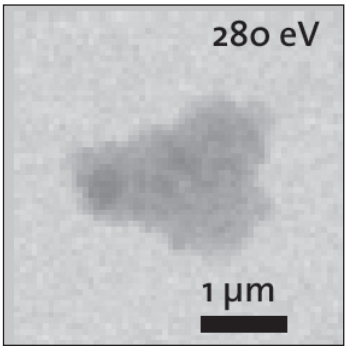

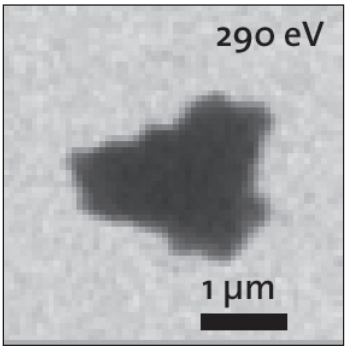

Unter-
Rickenzopfen

H-horizon

Stack 6

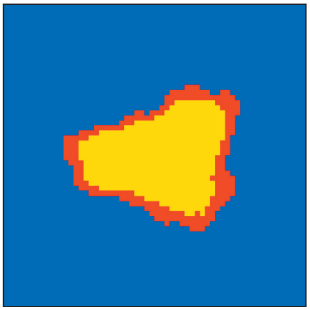

August
2001

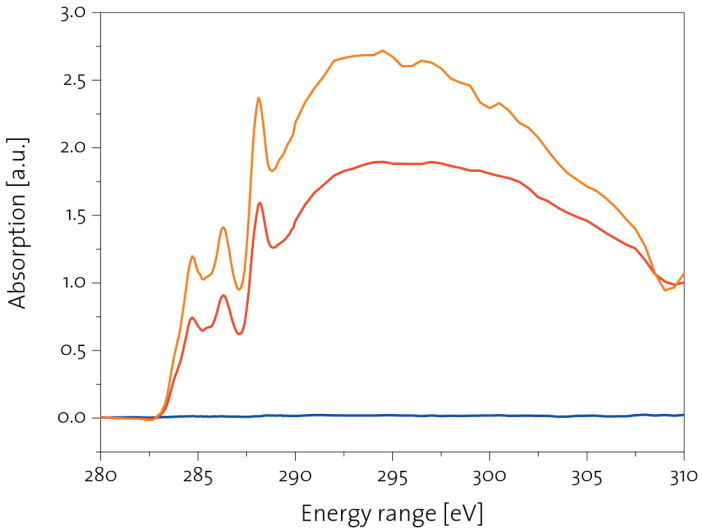

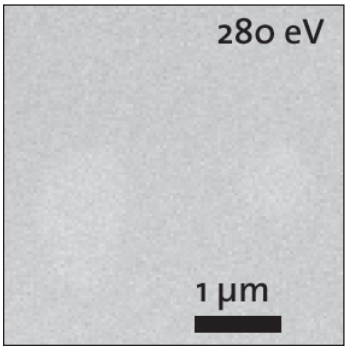

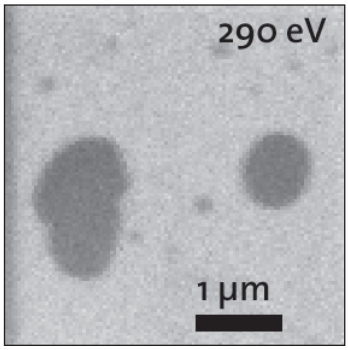

Unter-
Rickenzopfen

H-horizon

Stack 7

August
2001

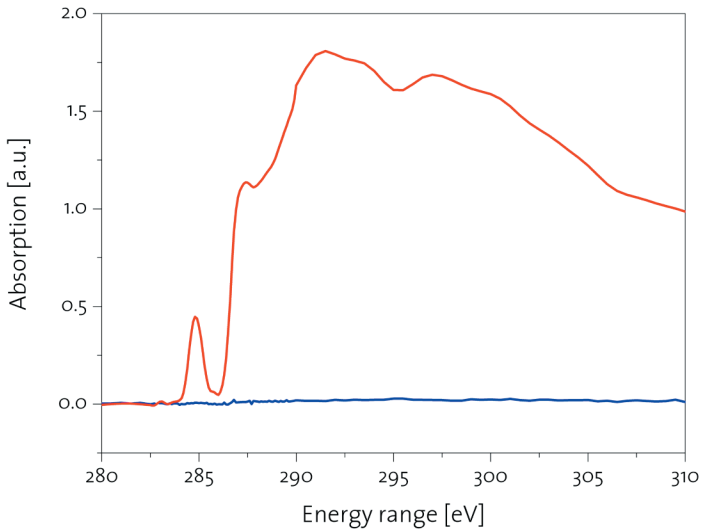

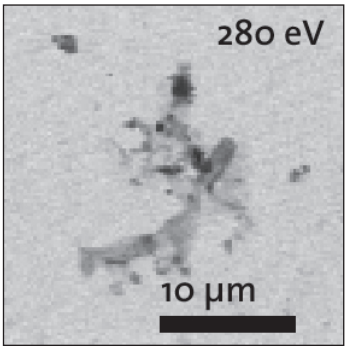

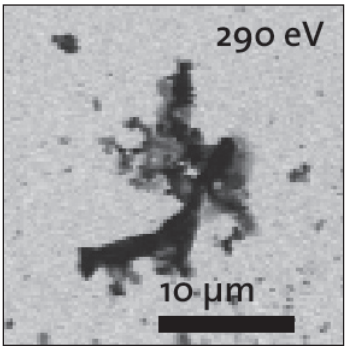

Unter-
Rickenzopfen

H-horizon

Stack 1

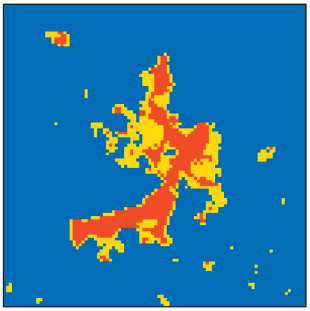

August
2002

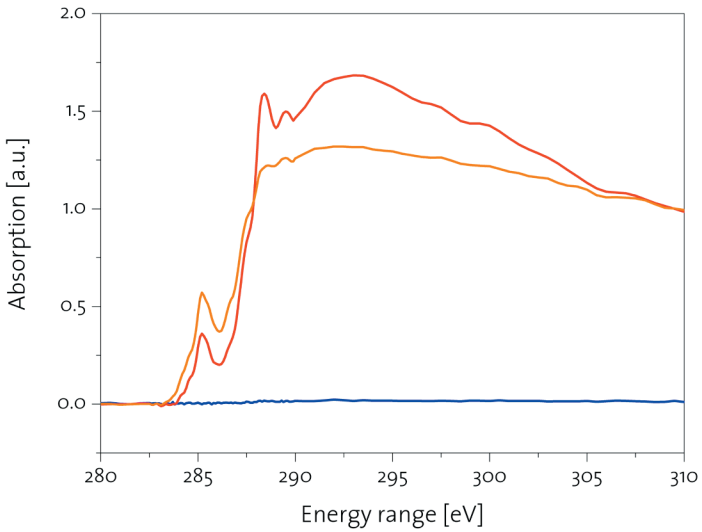

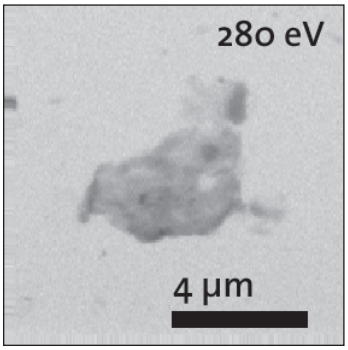

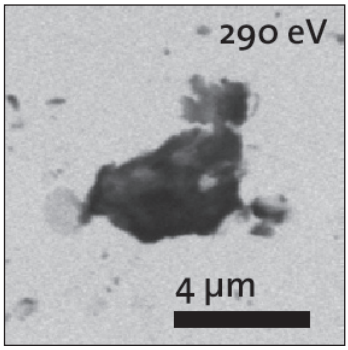

Unter-
Rickenzopfen

H-horizon

Stack 2

August
2002

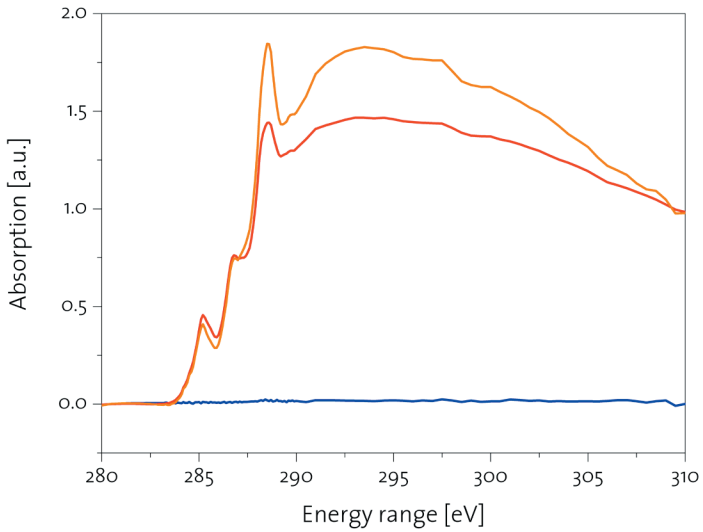

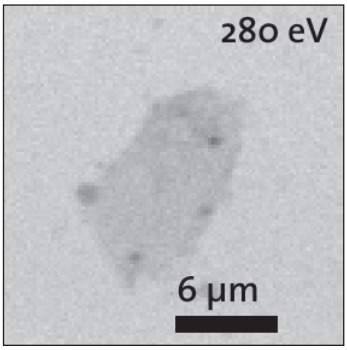

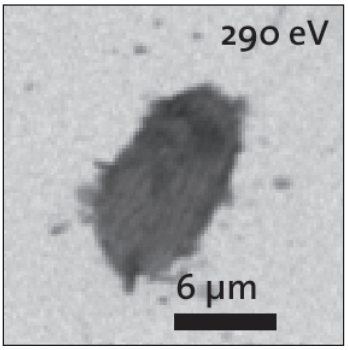

Unter-
Rickenzopfen

H-horizon

Stack 3

August
2002

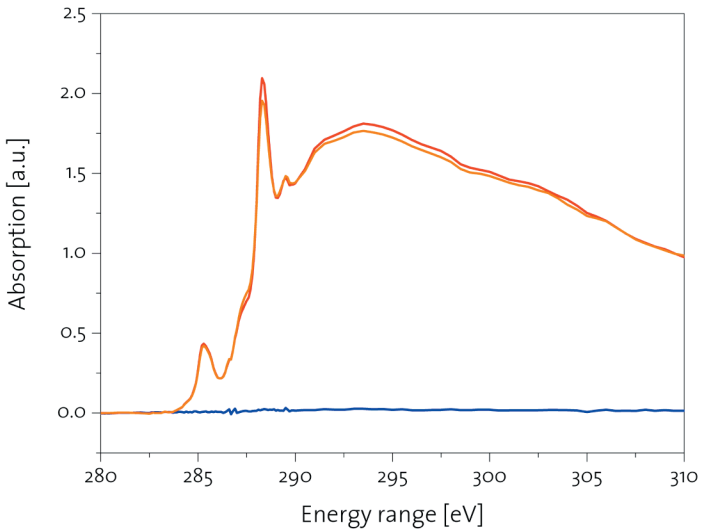

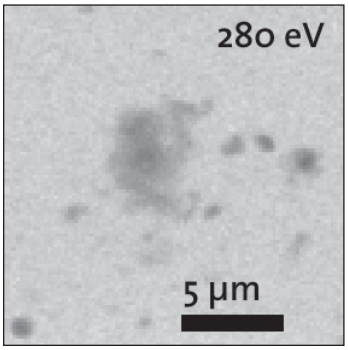

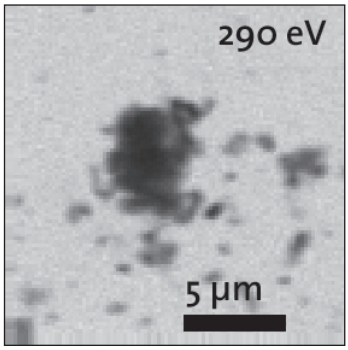

Unter-
Rickenzopfen

H-horizon

Stack 4

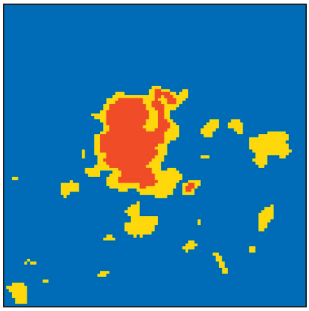

August
2002

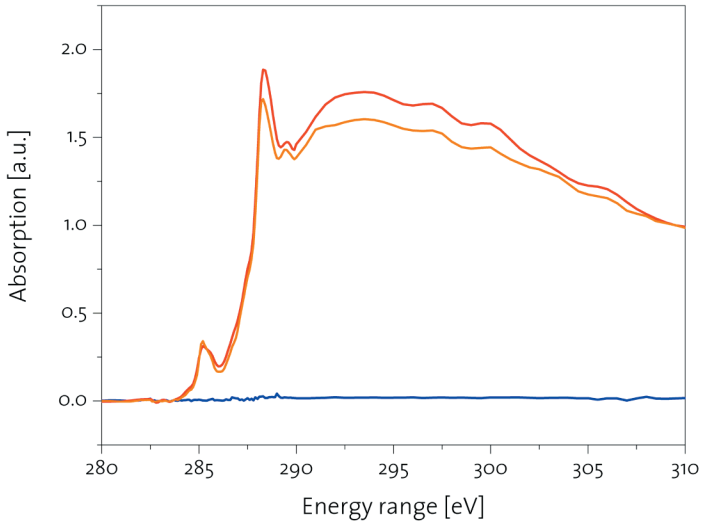

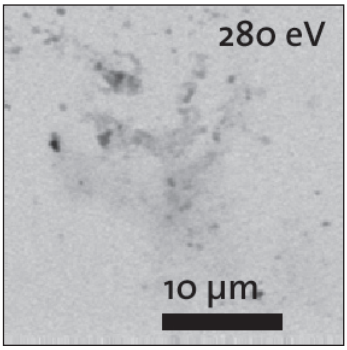

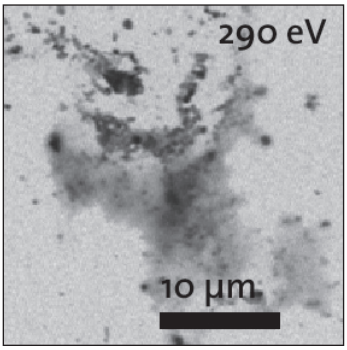

Unter-
Rickenzopfen

H-horizon

Stack 5

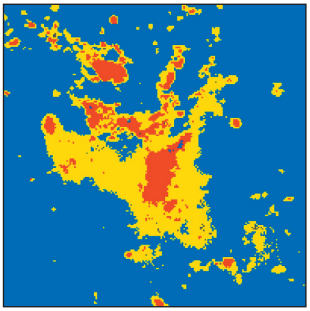

August
2002

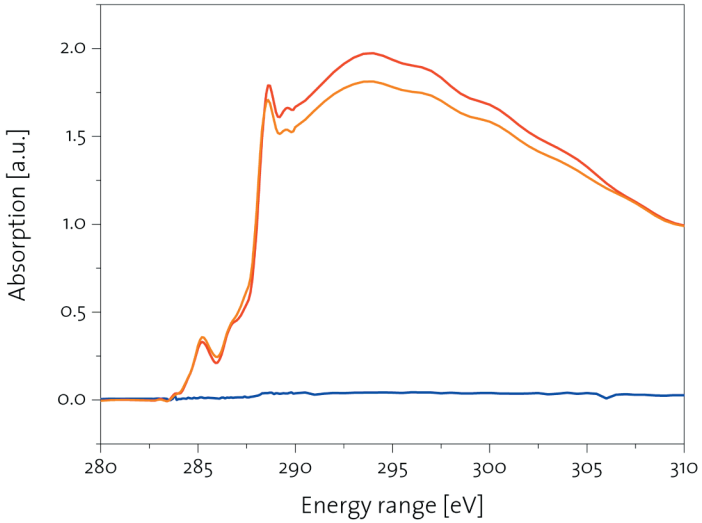

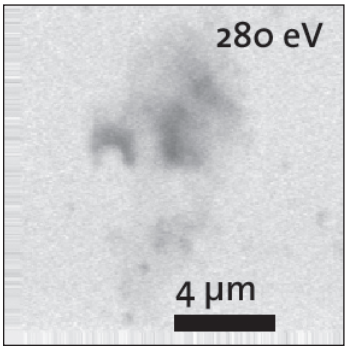

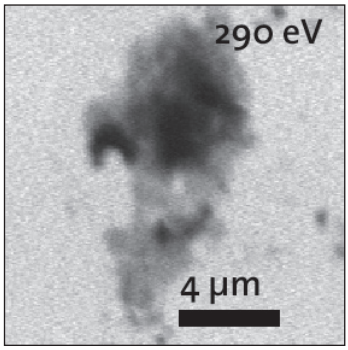

Unter-
Rickenzopfen

H-horizon

Stack 6

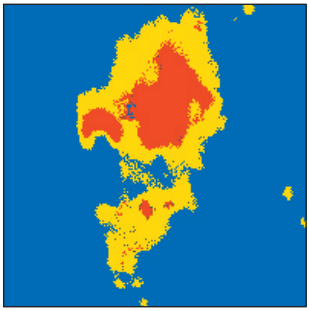

August
2002

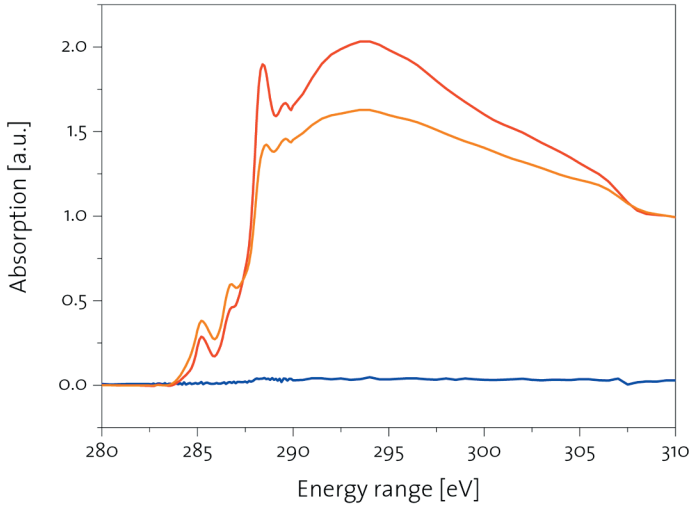

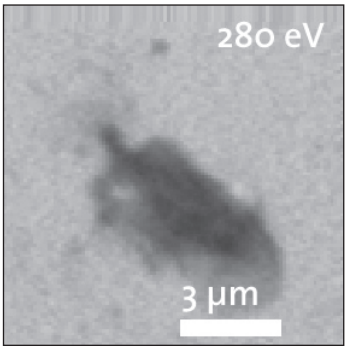

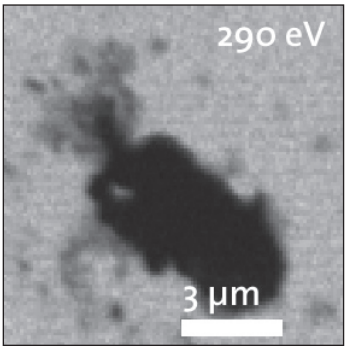

Unter-
Rickenzopfen

H-horizon

Stack 7

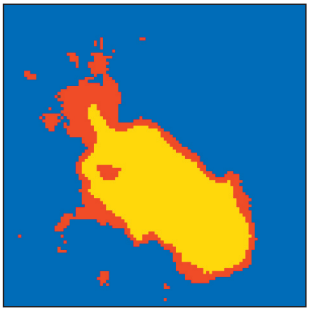

August
2002

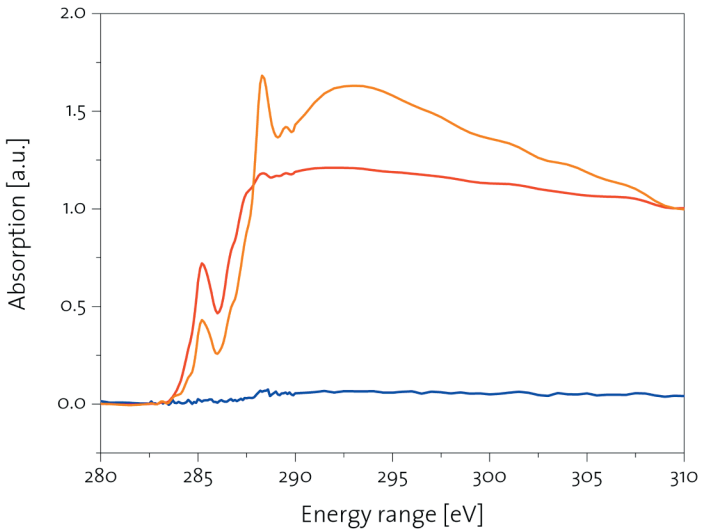

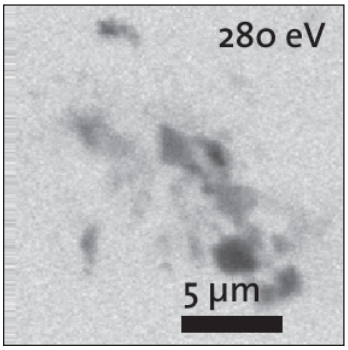

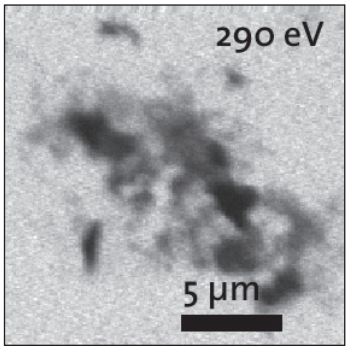

Unter-
Rickenzopfen

H-horizon

Stack 8

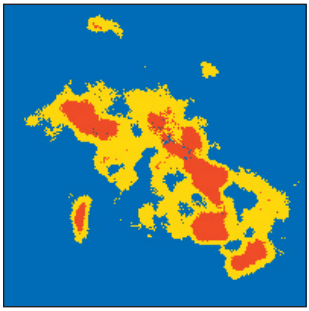

August
2002

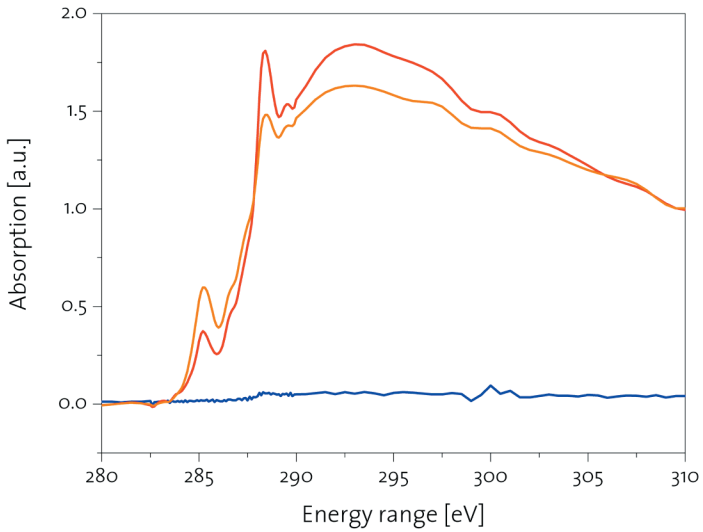

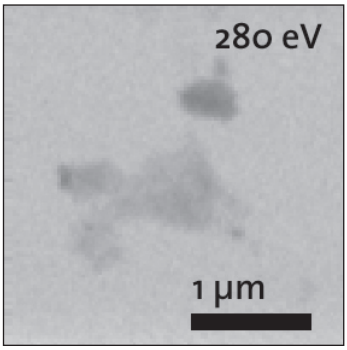

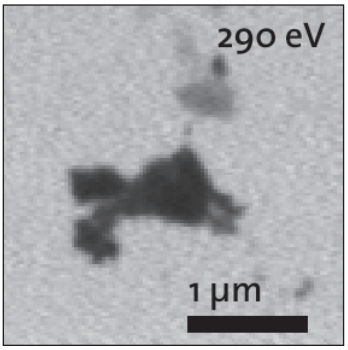

Unter-
Rickenzopfen

H-horizon

Stack 1

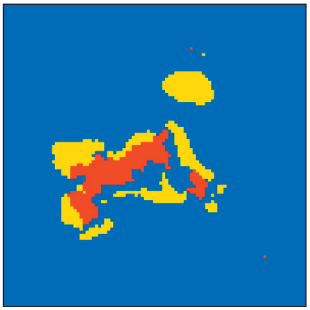

November
2002

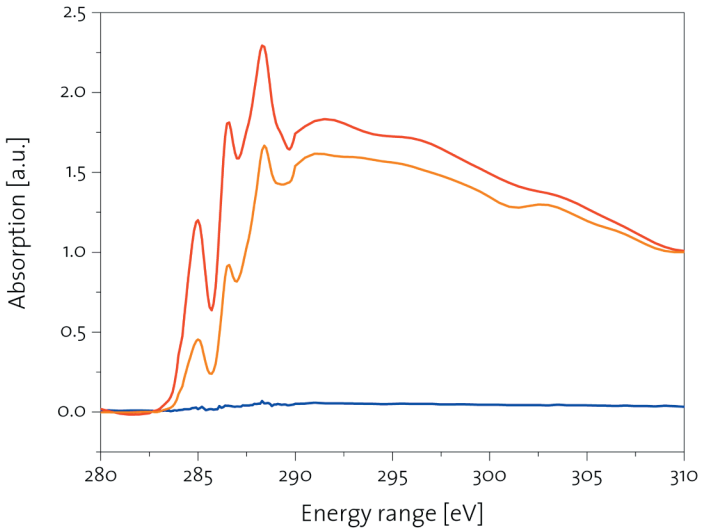

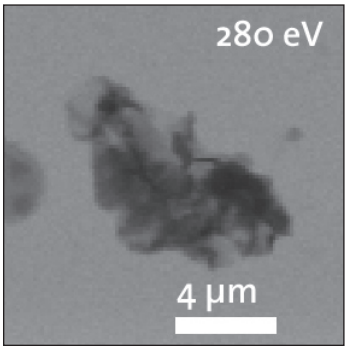

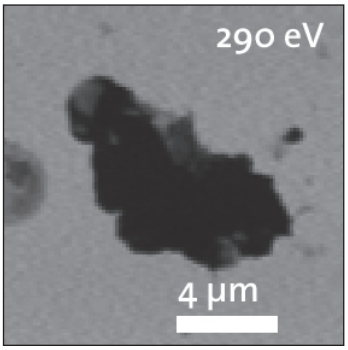

Unter-
Rickenzopfen

H-horizon

Stack 2

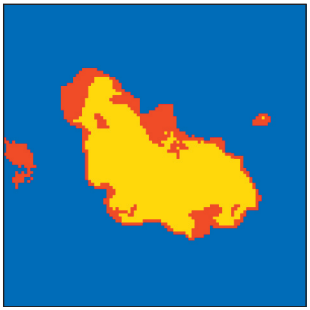

November
2002

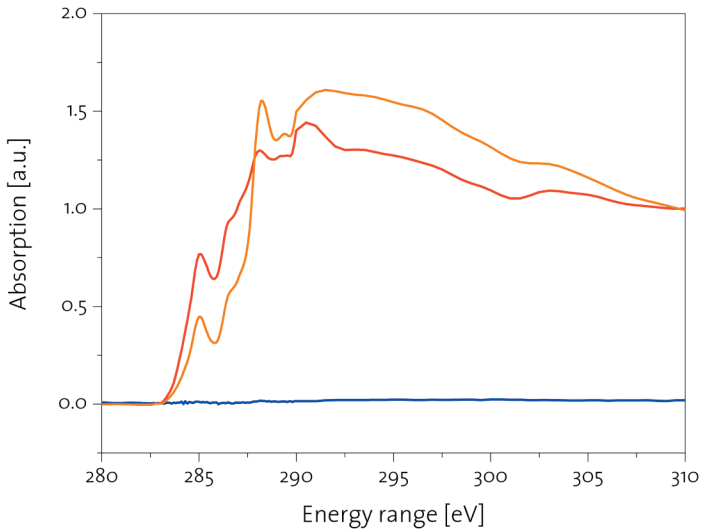

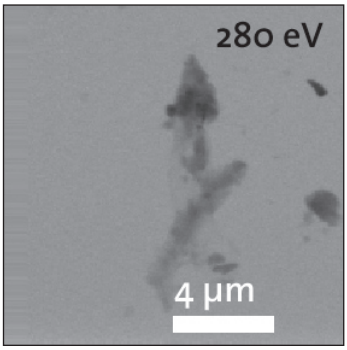

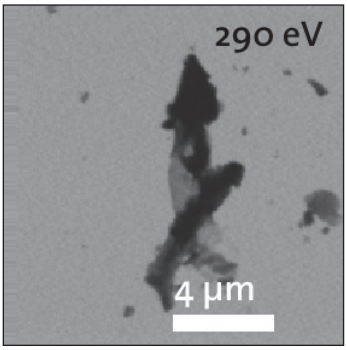

Unter-
Rickenzopfen

H-horizon

Stack 3

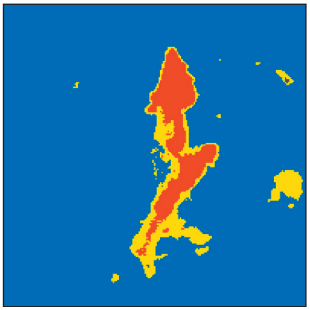

November
2002

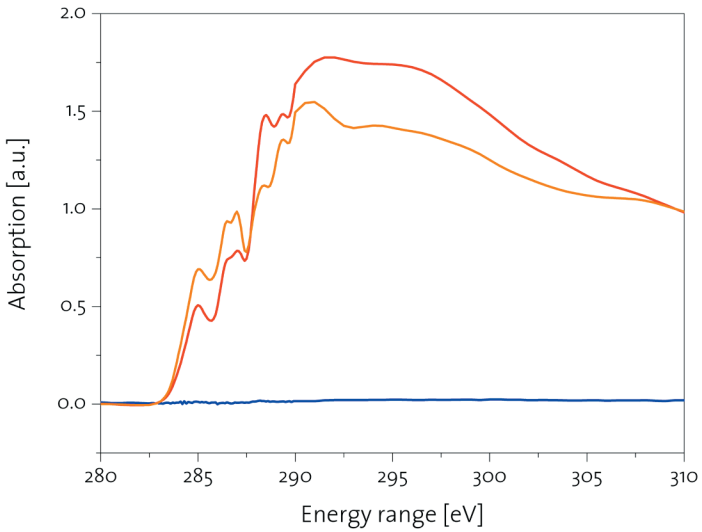

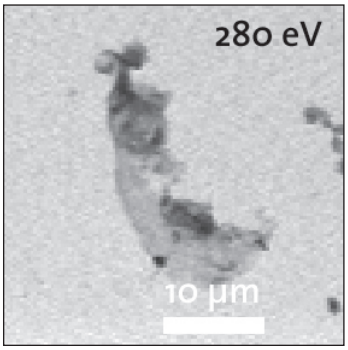

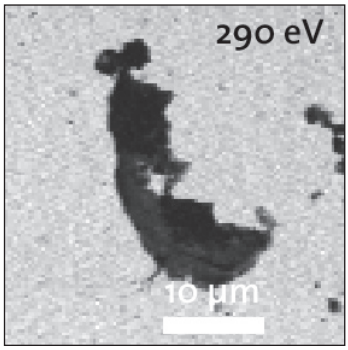

Unter-
Rickenzopfen

H-horizon

Stack 4

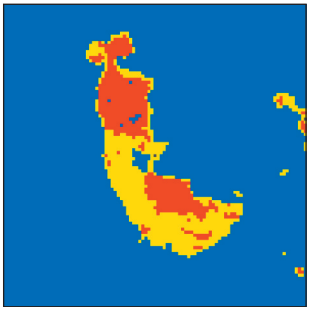

November
2002

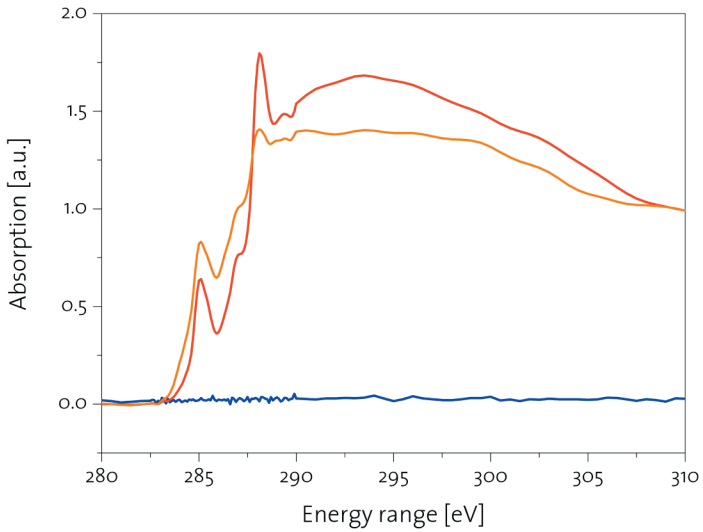

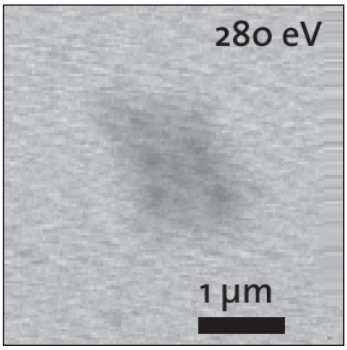

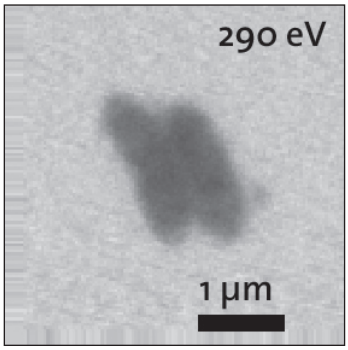

Unter-
Rickenzopfen

Ah-horizon

Stack 1

April
2002

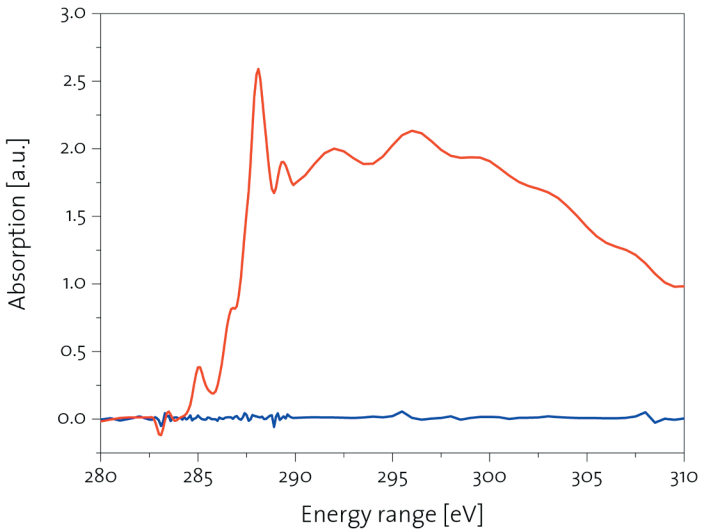

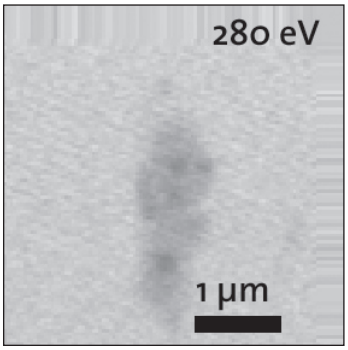

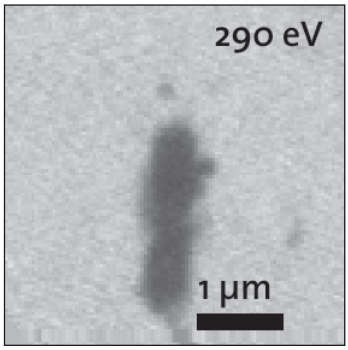

Unter-
Rickenzopfen

Ah-horizon

Stack 2

April
2002

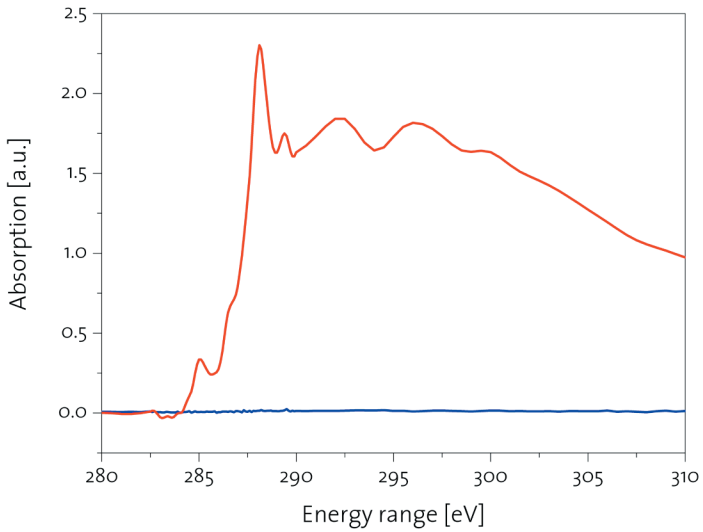

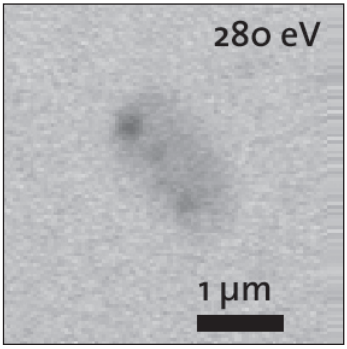

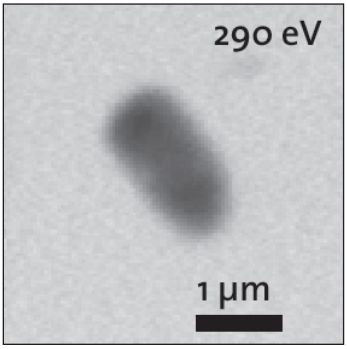

Unter-
Rickenzopfen

Ah-horizon

Stack 3

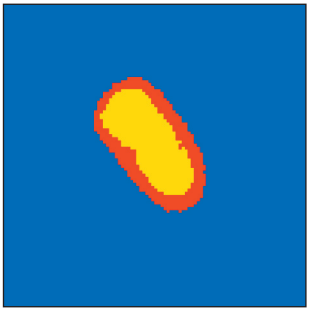

April
2002

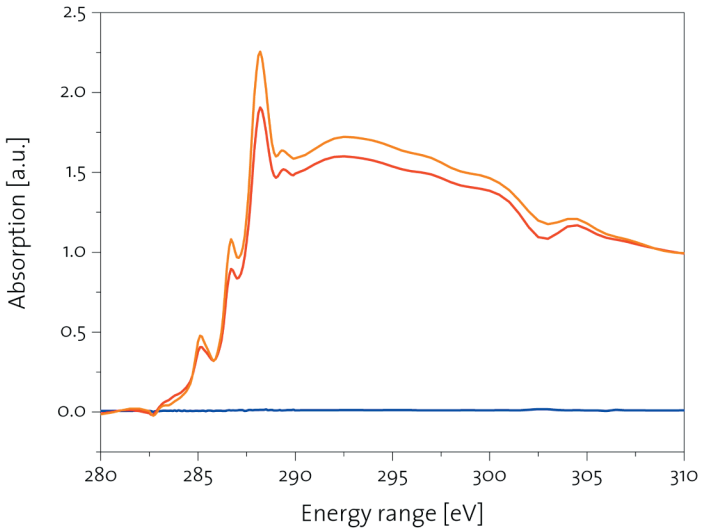

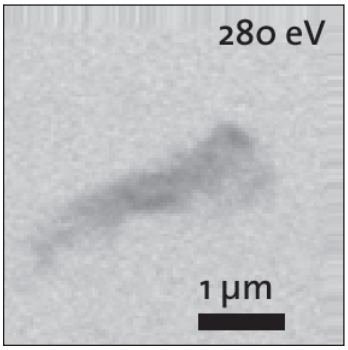

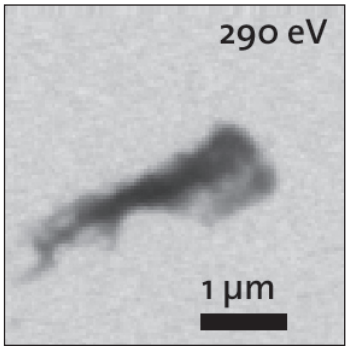

Unter-
Rickenzopfen

Ah-horizon

Stack 4

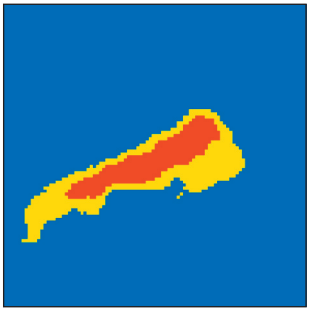

April
2002

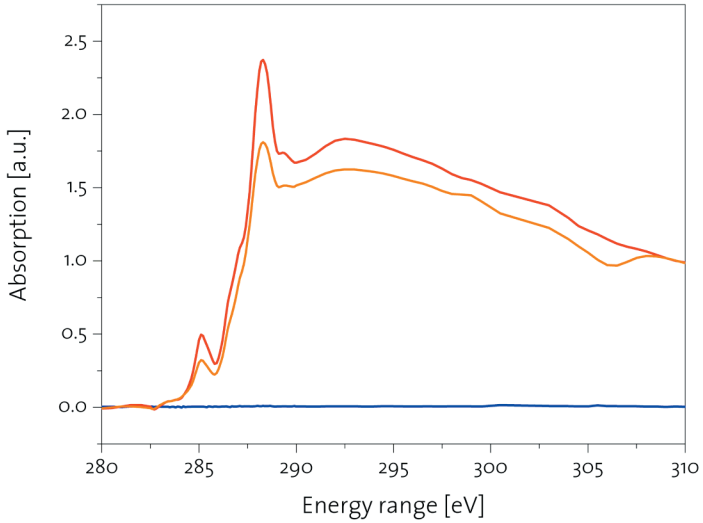

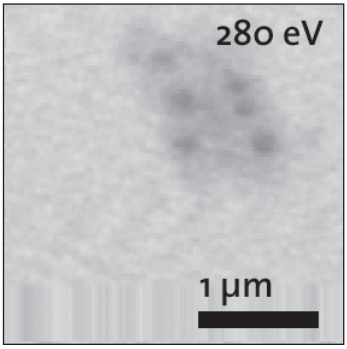

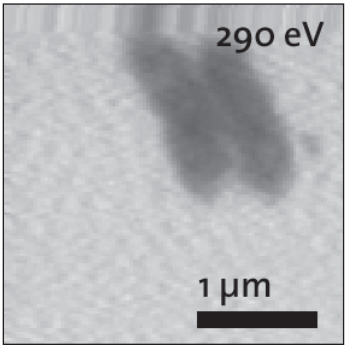

Unter-
Rickenzopfen

Ah-horizon

Stack 5

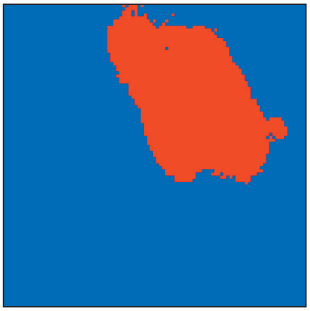

April
2002

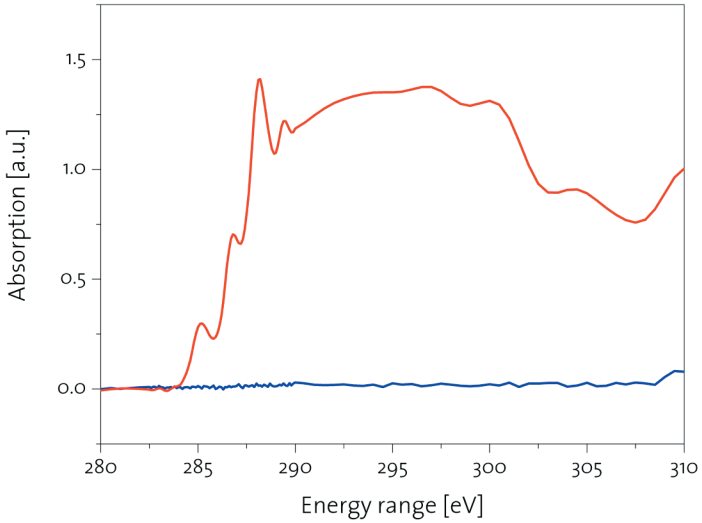

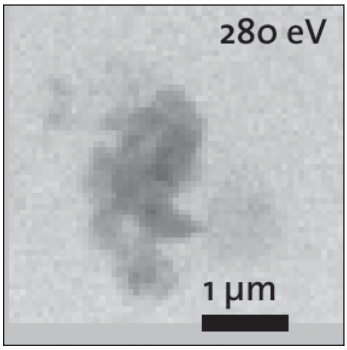

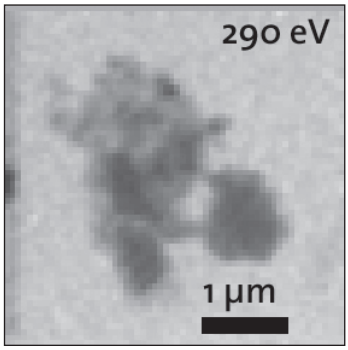

Unter-
Rickenzopfen

Ah-horizon

Stack 6

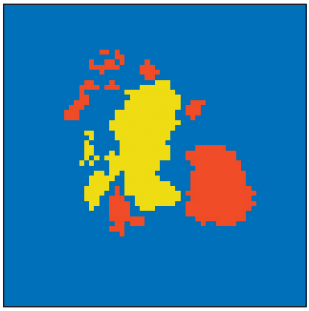

April
2002

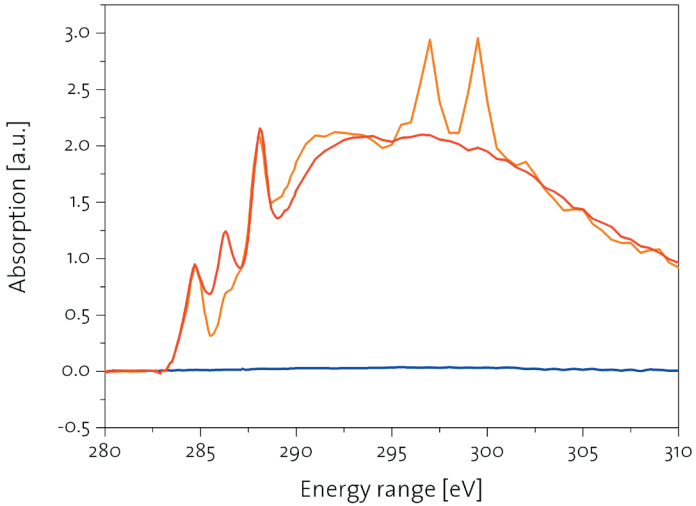

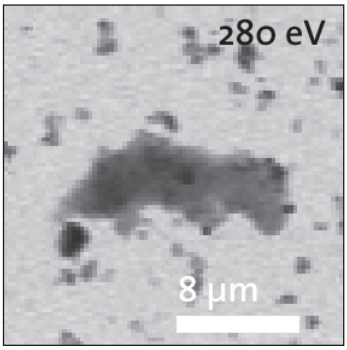

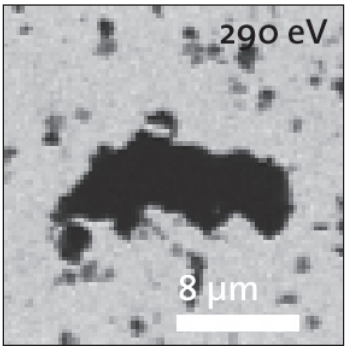

Unter-
Rickenzopfen

Ah-horizon

Stack 1

August
2002

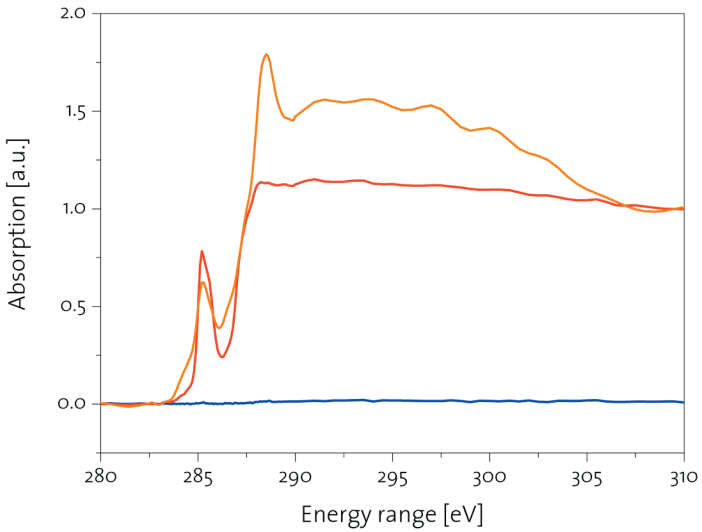

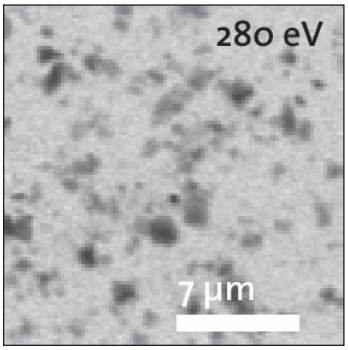

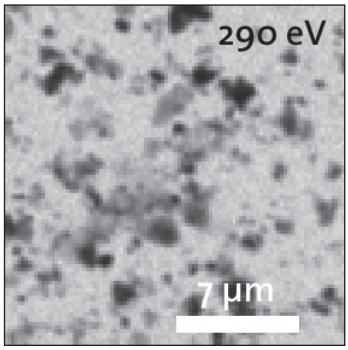

Unter-
Rickenzopfen

Ah-horizon

Stack 2

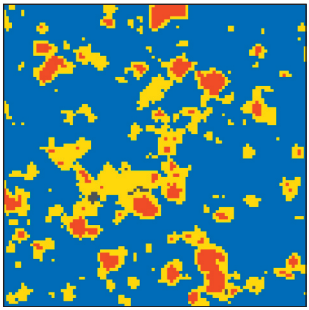

August
2002

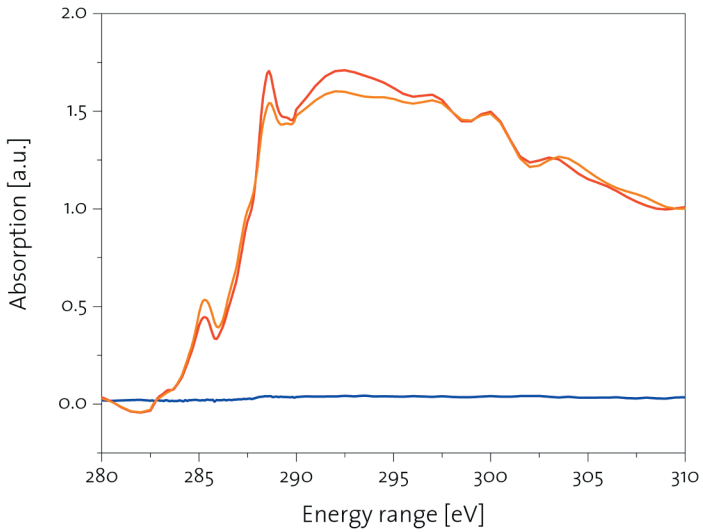

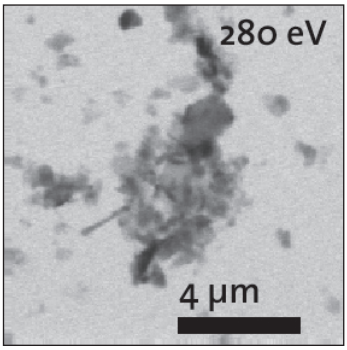

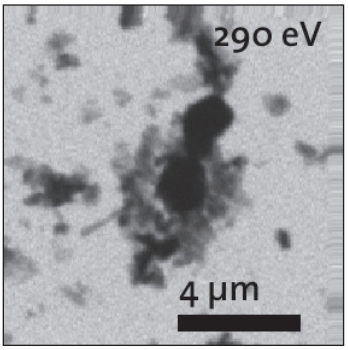

Unter-
Rickenzopfen

Ah-horizon

Stack 3

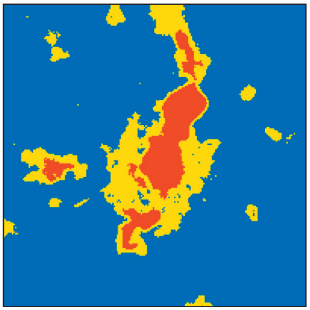

August
2002

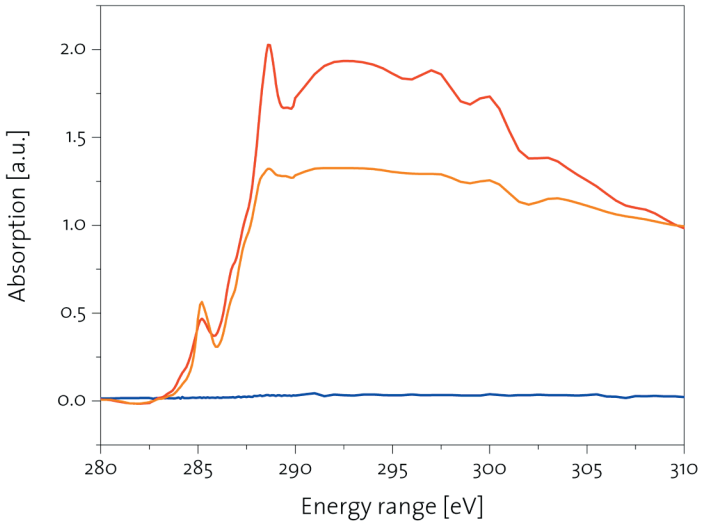

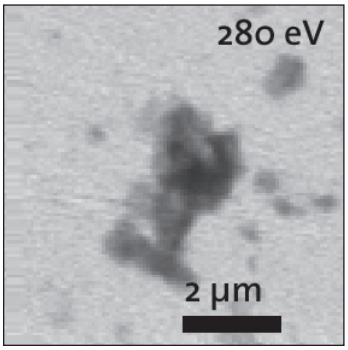

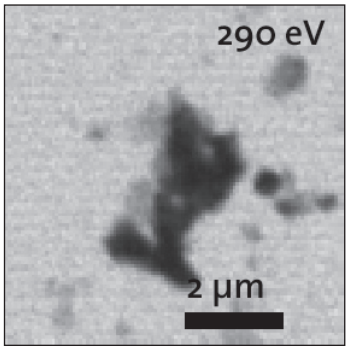

Unter-
Rickenzopfen

Ah-horizon

Stack 4

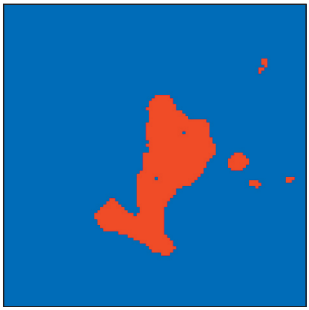

August
2002

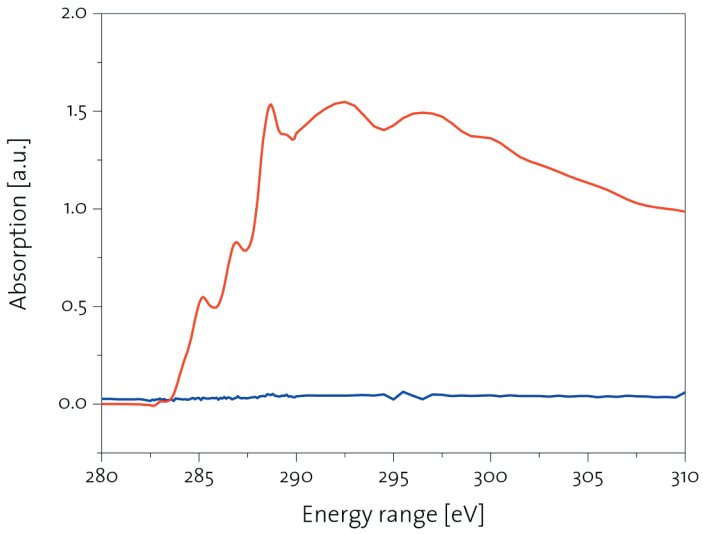

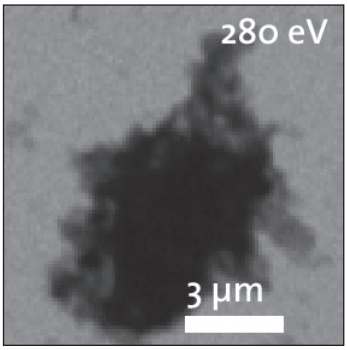

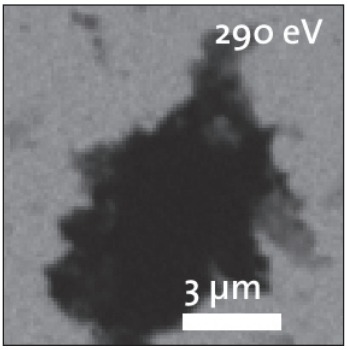

Unter-
Rickenzopfen

Ah-horizon

Stack 5

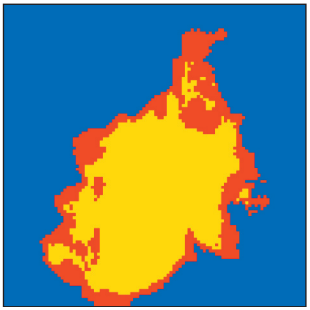

August
2002

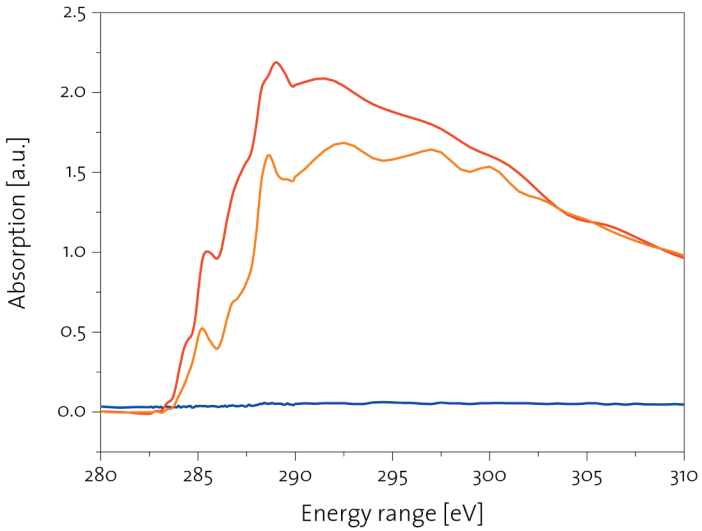

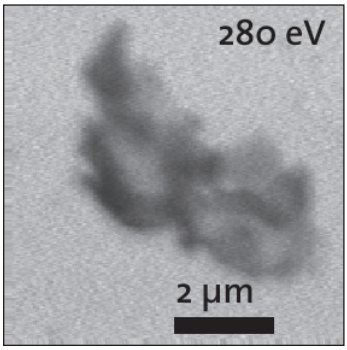

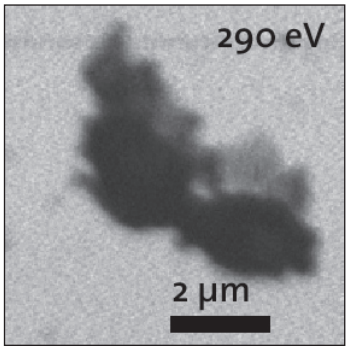

Unter-
Rickenzopfen

Ah-horizon

Stack 1

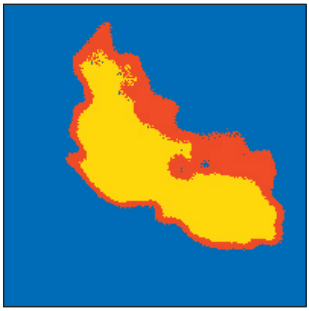

November
2002

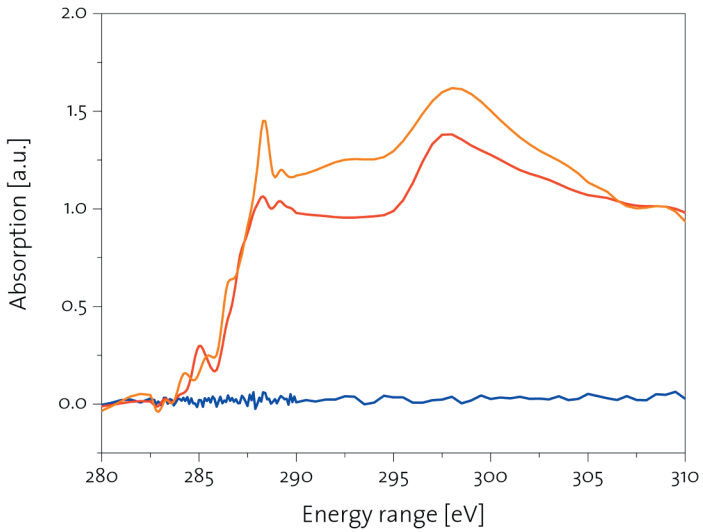

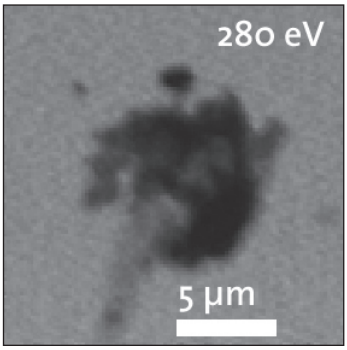

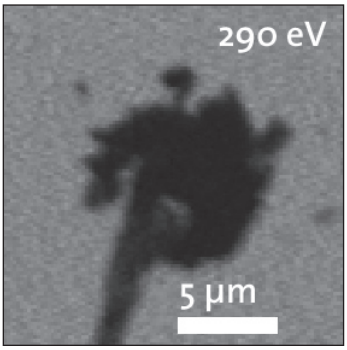

Unter-
Rickenzopfen

Ah-horizon

Stack 2

November
2002

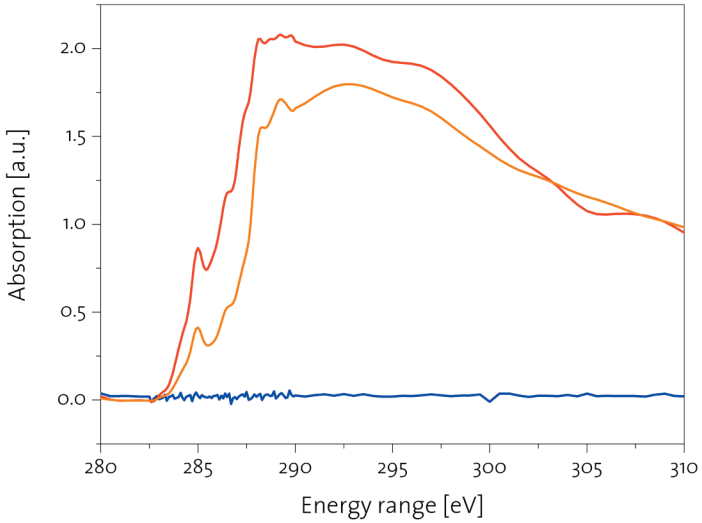

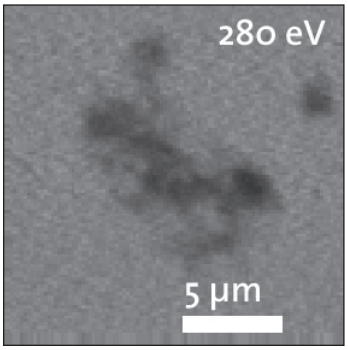

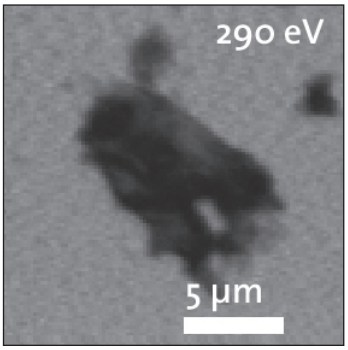

Unter-
Rickenzopfen

Ah-horizon

Stack 3

November
2002

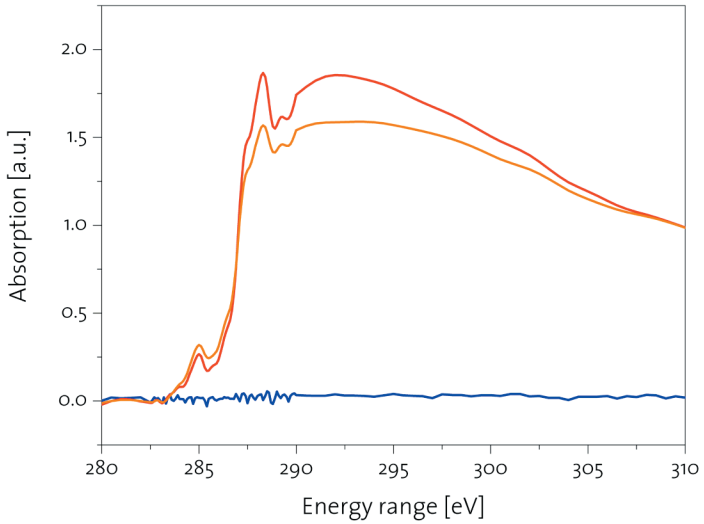

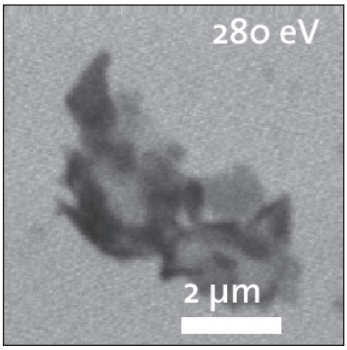

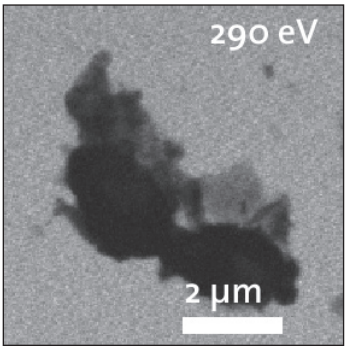

Unter-
Rickenzopfen

Ah-horizon

Stack 4

November
2002

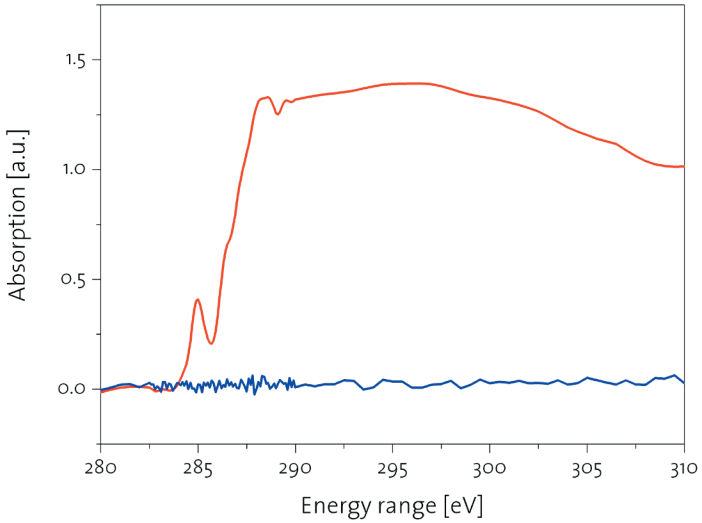

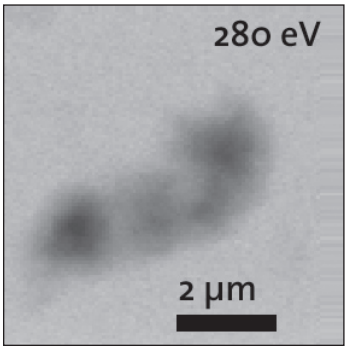

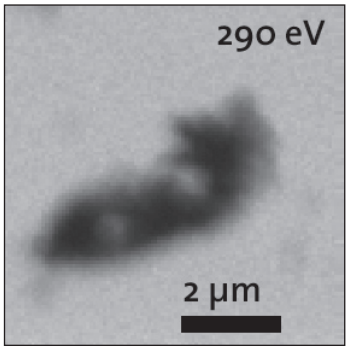

Unter-
Rickenzopfen

Ah-horizon

Stack 5

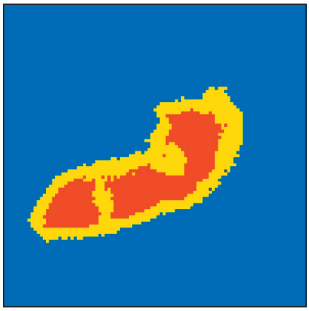

November
2002

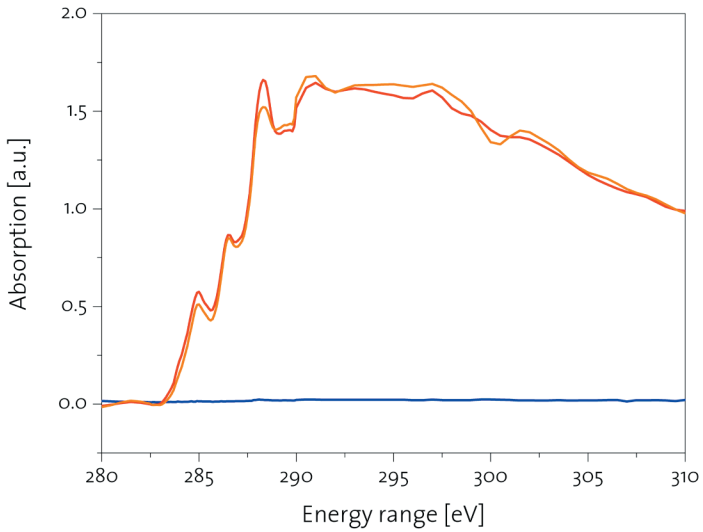

Acknowledgements

I am very grateful to Prof. Ruben Kretzschmar who gave me the opportunity to carry out this dissertation and supervised this work with sustained and constructive support.
I am indebted to Prof. Chris Jacobsen for his support, the review of this manuscript and for taking on the co-examiners position.
I would like to thank Dr. Iso Christl for the fast reviewing of the manuscripts, all the helpful and constructive advices and the motivating working atmosphere he created. I am indebted to Dr. Andreas C. Scheinost for the start of this project, his support and for giving me the possibility to work autonomously.

I would like to thank Prof. Rolf Vogt for providing the NOM samples and experimental data. Thanks to Kurt Barmettler for helping with numerous experiments and for hints regarding laboratory practice. I want to thank Sue Wirick for providing information and help during my beamtime at the National Synchrotron Light Source (NSLS) at the Brookhaven National Laboratory (BNL). I want to thank all the members of the X-ray optics group from Stony Brook University for their support, especially Dr. Tobi Beetz, Dr. Michael Feser, Holger Fleckenstein and Mirna Lerotic. Furthermore, I would like to acknowledge all the colleagues of the Soil Chemistry group and other members of ITO, especially Dr. Andreas Birkefeld, Olivier Jacquat, Charlotte Wüstholz and Dr. Petra Gulz.

I want to thank my family for their support and all my friends outside the Institute, especially Dr. Pascal Gerner, Dr. Rudolf Kocher and Raphael Köchli, with whom I shared good and bad times.

Last but not least I would like to thank my girlfriend Nadine Jordi for supporting my visions, her patience and her love. Without her enduring support, this work would have never been possible.

Curriculum vitae

Surname	Schumacher
Given names	Marc Michel
Date of birth	30.03.1976
Place of birth	Geneva, Switzerland
Citizenship	Swiss and German

School education

1982 – 1988	Primarschule, Schattdorf, UR
1988 – 1993	Kollegium Karl Borromäus, Altdorf, UR
1993 – 1995	Collège Sainte-Croix, Matura Type B, Fribourg, FR

Higher education

1996 – 2001	Studies of Earth Sciences, M.Sc., University of Berne, Switzerland
2001 – 2005	Ph.D. studies and work as research assistant at the Institute of Terrestrial Ecology, Soil Chemistry Group, Swiss Federal Institute of Technology (ETH) Zurich, Switzerland

Occupation

1999 – 2005	Environmental geologist and project leader at CSD Ingenieure & Geologen AG, Aarau, Switzerland

Berne, July 2005